Study on the Influence of Fiber Orientation to Flexural Performance of HPFRCC

Tetsuo Fukuhara

(Master's Program in Engineering Mechanics and Energy)

Advised by Toshiyuki Kanakubo

Submitted to the Graduate School of
Systems and Information Engineering
in Partial Fulfillment of the Requirements
for the Degree of Master of Engineering
at the
University of Tsukuba

March 2009

Study on the Influence of Fiber Orientation to Flexural Performance of HPFRCC

（HPFRCC の曲げ性状に及ぼす繊維配向性の影響）

CONTENTS

DISSERATION ABSTRACT······4

CHAPTER 1 INTRODUCTION······5

1.1. Research Background······5
1.2. Study Objective······7

CHAPTER 2 FOUR-POINT BENDING TEST······8

2.1. Introduction······8
2.2. Mix Proportion······8
2.3. Outline of Specimens······9
2.4. Specimen Identifications······10
2.5. Outline of Four-Point Bending Test······11
2.6. Experimental Result······12
2.6.1. Specimens with 1.5% volume fraction of fibers······13
2.6.1.1. Prepared Specimens······14
2.6.1.2. Coupons on X-direction······15
(1) Bending moment and curvature curve relationships
(2) Influence of mold surface
2.6.1.3. Coupons on Y-direction······20
2.6.2. Specimens with 2.0% volume fraction of fibers······22
2.6.2.1. Prepared Specimens······23
2.6.2.2. Coupons on X-direction······24
(1) Bending moment and curvature curve relationships
(2) Influence of mold surface
2.6.2.3. Coupons on Y-direction······29
2.7. Comparison and Discussion······31

CHAPTER 3 CROSS SECTION OBSERVATION ········ 32

3.1. Introduction ········ 32
3.2. Outline of Cross Section Observation ········ 32
3.3. Experimental Result ········ 34
3.3.1. Specimens with 1.5% volume fraction of fibers ········ 35
3.3.1.1. Prepared Specimens ········ 36
3.3.1.2. Coupons on X-direction ········ 36
(1) Influence of mold surface
(2) M_{max}, ϕ_{max} and number of PVA fiber relationships
3.3.1.3. Coupons on Y-direction ········ 39
3.3.2. Specimens with 2.0% volume fraction of fibers ········ 41
3.3.2.1. Prepared Specimens ········ 42
3.3.2.2. Coupons on X-direction ········ 42
(1) Influence of mold surface
(2) M_{max}, ϕ_{max} and number of PVA fiber relationships
3.3.2.3. Coupons on Y-direction ········ 45
3.4. Comparison and Discussion ········ 47

CHAPTER 4 THE INFLUENCE OF SURFACE ········ 48

4.1. Introduction ········ 48
4.2. Mix Proportion ········ 48
4.3. Outline of Specimens ········ 49
4.4. Specimen Identification ········ 51
4.5. Outline of Bending Test ········ 51
4.6. Experimental Result ········ 51
4.6.1. Bending moment-curvature curve relationships of specimens ········ 53
(1) Specimens with 1.5% volume fraction of fibers
(2) Specimens with 2.0% volume fraction of fibers
4.6.2. The thickness of polishing and the averaged data relationships ········ 56
(1) Specimens with 1.5% volume fraction of fibers
(2) Specimens with 2.0% volume fraction of fibers
4.7. Comparison and Discussion ········ 58

CHAPTER 5 SUMMARY FOR ALL CHPATERS ········ 59

5.1. Experimental result ········ 59
5.1.1. HPFRCC with 1.5% volume fraction of fibers ········ 60
5.1.2. HPFRCC with 2.0% volume fraction of fibers ········ 61

CHAPTER 6 CONCLUSION ········ 62

6.1. HPFRCC with 1.5% volume fractions of fibers ········ 62
6.2. HPFRCC with 2.0% volume fractions of fibers ········ 62
6.3. Recommendation ········ 62

REFERENCES ········ 63

APPENDIX ········ 64

ACKNOWLEDGMENTS ········ 83

DISSERATION ABSTRACT

High Performance Fiber Reinforced Cementitious Composites, HPFRCC has been expected as new material because the ductility on bending, tension, and shear behavior would be improved largely than ordinary concrete. However, to give an expected performance, it is important to know how the fiber will be orientated and distributed in the matrix. There are many indistinct point how fiber is oriented. This paper aims to present the influence of fiber orientation to the flexural performance of HPFRCC.

In this study, two large specimens of HPFRCC are prepared with 1.5% and 2.0% volume fraction of polyvinyl alcohol (PVA) fibers. Then two large specimens are cut to small coupons and the flexural performance of HPFRCC due to the influence of fiber is examined by using the bending test and observation of cross section by using mercury lamp. From the test result, number of fiber is related to the mechanical performance closely when coupon is cut on axial direction. The number of fiber is increasing as close to the mold surface. As increased the number of fiber, the bending performance increases. On the other hand, bending performance of coupon that is cut on perpendicular direction is not related to the position of the coupons and number of fibers directly in 1.5% volume fraction of fibers.

In addition, specimens with 1.5% and 2.0% volume fraction of PVA fibers are prepared as HPFRCC and polished surfaces of specimens to examine that the influence of polishing surfaces to flexural performance in HPFRCC. In the result, the influence of polishing surface is related to the flexural performance of HPFRCC with 1.5% volume fraction of fibers closely. For HPFRCC with 2.0% volume fraction of fibers, the influence of polishing is not related to the flexural performance directly.

CHAPTER 1 INTRODUCTION

1.1. *Research Background*

Recently, as the substitute of reinforced concrete, the research of High Performance Fiber Reinforced Cementitious Composites, HPFRCC has been carried out. HPFRCC is the composite material with mixing fiber in mortar, and fibers bear the tension in substitution for reinforcing bar. Many types of fiber, there are Steel, Polyvinyl alcohol (PVA), Polyethylene (PE), and polypropylene (PP) and so on.

For representative characteristic of HPFRCC, under the condition of uniaxial tensile stress or the bending stress, HPFRCC shows multiple cracks as described in Picture 1.1 for an example. Furthermore, it also shows that the stress increases after the first cracking, which is called as strain hardening in case of tensile stress or deflection hardening in case of bending stress. Therefore, HPFRCC is expected as new materials, because the ductility of bending, tension, and shear behavior would be improved largely than ordinary reinforced concrete as the seismic members.

Hence, HPFRCC has been applied as maintenance and repair method for control the cracks and prevent corrosion of reinforcement bar in the field of civil engineering. [1.1] In addition, Engineered Cementitious Composite, ECC, investigated by Dr. Li, [1.2] has been used for a part of high-rise building such as coupling beams in the field of building engineering. The guide for design and construction of HPFRCC has been published by Japan Society for Civil Engineers recently. [1.3]

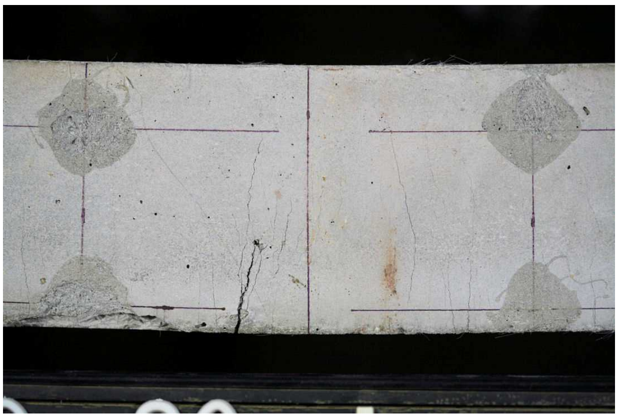

Picture 1.1 The multiple cracks

The distribution and orientation of fibers is one of the important factors in terms of flexural performance of the composite. In other words, the large difference of mechanical performance is observed when fibers are oriented by axial and perpendicular direction of loading.

The research of HPFRCC has been developed well in the past decade. For example, the difference of casting direction is achieved results that casting at horizontally toward the long direction of mold shows higher mechanical performance than that at vertically long direction of mold. [1.4]

The portion of the specimen that locates more near to the casting or mold surface shows higher at tensile performance because the fibers will be orientated at axial direction on loading at casting or mold surface, that is called as wall-effect. [1.5]

However, it is very difficult to confirm clearly the wall-effect. The wall-effect is controlled strongly by bridging law of fibers in case of having direction of crack surface.

1.2. Study Objective

The aim of this research is to clarify the influence of the fiber orientation and distribution to the flexural performance of HPFRCC.

In chapter 2, two large specimens are prepared as HPFRCC with 1.5% and 2.0% volume fraction of PVA fibers and cut to small coupons, and then four-point bending test is applied to examine the influence of cast, mold direction and cutout surface to the flexural performance of HPFRCC.

In chapter 3, a specimen for cross section observation is cut around the largest crack occurred by bending test and observation of cross section is applied by used mercury lamp to examine how fibers are distributed and orientated in matrix.

In chapter 4, specimens are prepared as HPFRCC with 1.5% and 2.0% volume fraction of fibers. Then, those are polished and cutout by grinder machine, and then four-point bending test is applied to examine the influence to the flexural performance and compare the result of chapter 2 and 3.

CHAPTER 2 FOUR-POINT BENDING TEST

2.1. Introduction

Because the distribution and orientation of fibers is an important factor in terms of flexural performance of the composite, it is important to know how the fiber will be orientated and distributed in the matrix. In this chapter 2, two same large specimens of HPFRCC are prepared with polyvinyl alcohol (PVA) fiber with the fiber volume fraction of 1.5% and 2.0%. Then two same large specimens are cut to small coupons and the flexural performance of HPFRCC due to the influence of fiber is examined by using the bending test.

2.2. Mix Proportion

The mechanical characteristic of PVA fiber is shown in Table2.1. For HPFRCC with 1.5% volume fraction of fibers, the mix proportion of HPFRCC that is shown in Table2.2 is used and unit quantity of PVA fiber is 19.50 kg/m^3. For HPFRCC with 2.0% volume fraction of fibers, specimen is prepared as Engineered Cementitious Composite (ECC). [1.2] Two large same specimens are cured by stream at first day, and after that the specimens were left in atmospheric curing, then the cast surface will be polished before bending test is applied.

Detailed information of manufacturer and brand name of materials for HPFRCC with 1.5% volume fraction of fibers is shown in Appendix: A.

Table2.1 The mechanical characteristic of PVA fiber

Type of fiber	Length (mm)	Diameter (μm)	Tensile strength (MPa)	Elastic modulus (GPa)
PVA	12	40	1600	40

Table2.2 The mix proportion of HPFRCC

	Unit quantity (kg/m^3)		Unit quantity (kg/m^3)
Water	380	Cement	576
Fine aggregate	484	Fly ash	291
Expansion agent	101.7	Shrinkage-reducing admixture	20
Thickening agent	1.91	High performance AE water reducing agent	5.78

2.3. *Outline of Specimens*

A large size specimen with 140mm in depth, 780mm in width and 1675mm in length and five prepared small specimens that cross section is 60mm x 60mm and length is 350mm is prepared.

Overall view of cutting for a large specimen is shown in Figure 2.1. To compare the influence of the cast direction, a large specimen is cut to three parts such as A, B and C by using the diamond cuter. Then, to compare the influence of cast, mold and cutout surface, part A and C is cut to 14 coupons in each part. The detailed view of cutting in part A and C is shown in Figure 2.2. 4 coupons on axial direction (X-direction) and 3 coupons on perpendicular direction (Y-direction) are cut from both upper and lower section. Part B is cut to 9 coupons. The detailed view of cutting in part B is shown in Figure 2.2 also. 5 coupons on X-direction and 4 coupons on Y-direction are cut from middle section. Therefore, the total number of coupons is 37 for each large size specimen. The size of coupons is same as five small prepared specimens that cross section is 60mm x 60mm and length is 350mm.

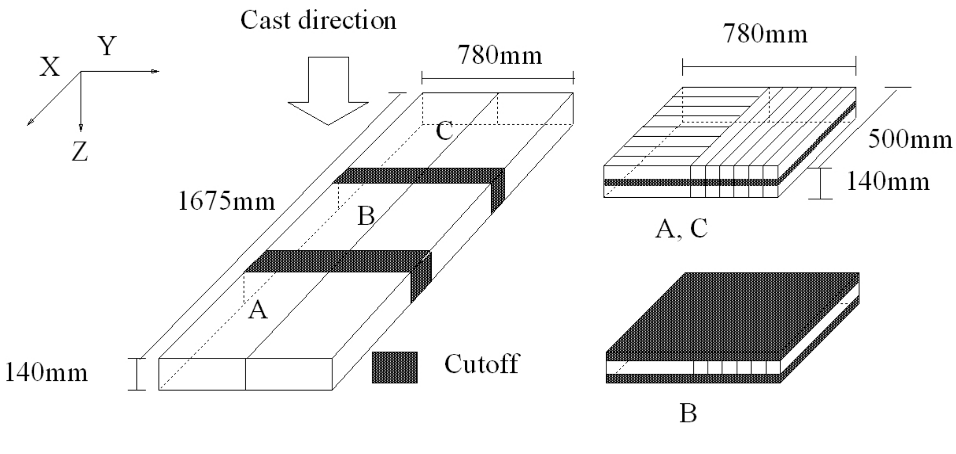

Figure 2.1 Overall view of cutting

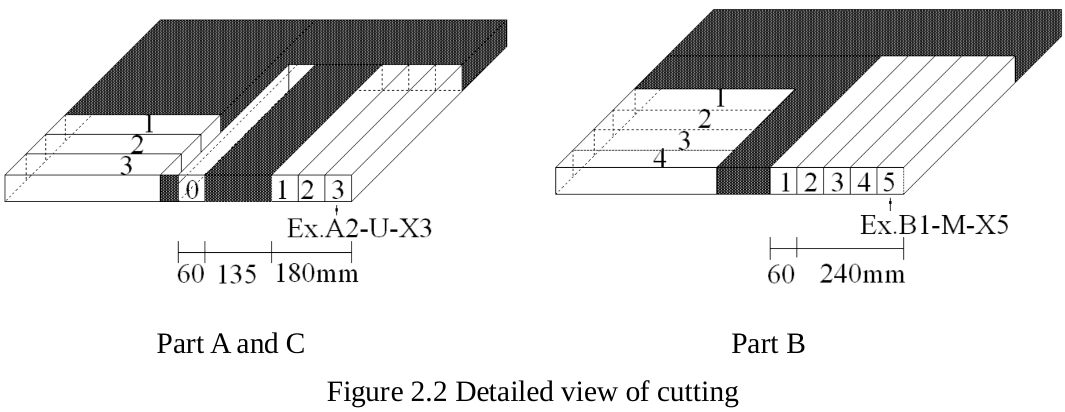

Figure 2.2 Detailed view of cutting

2.4. *Specimen Identifications*

The identification of coupon with 1.5% volume fraction of fibers is shown in Figure 2.3 and the identification of coupon with 2.0% volume fraction of fibers is shown in Figure 2.4. Cutting part is A, B and C that is shown in Figure 2.1. Cutting section is that upper section as U, middle section as M and lower section as L. Cutting direction is on X-direction and Y-direction from Figure 2.1. The position number is shown in Figure 2.2. Also, an example of specimens' identification is shown in Figure 2.2.

In addition, the identification of five prepared specimens is as 1.5-1 to 1.5-5 for 1.5% volume fraction of fibers and as 2.0-1 to 2.0-5 for 2.0% volume fraction of fibers.

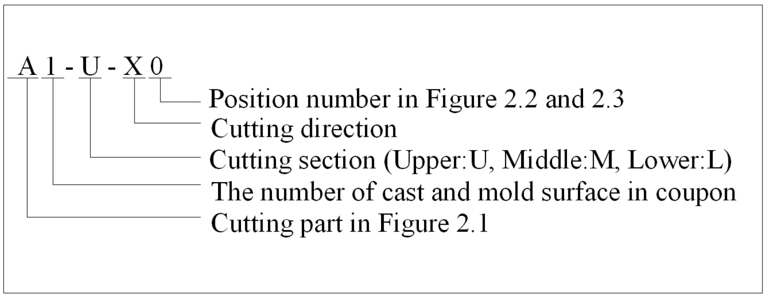

Figure 2.3 Identification of coupon with 1.5% volume fraction of fibers

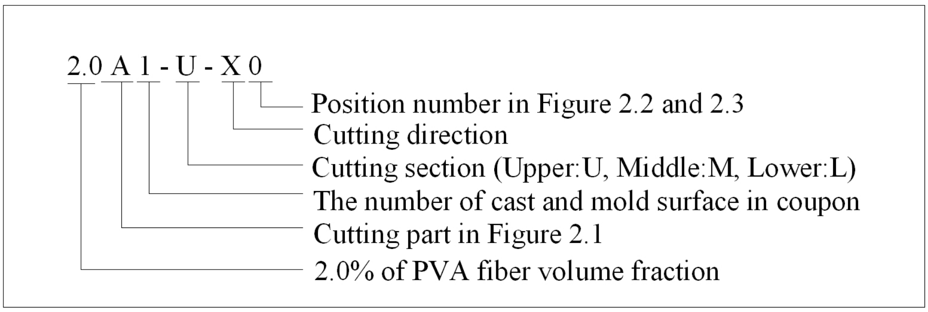

Figure 2.4 Identification of coupon with 2.0% volume fraction of fibers

2.5. *Outline of Four-Point Bending Test*

Four-point bending test based on Method of Test for Bending Moment-Curvature Curve of Fiber-Reinforced Cementitious Composites (JCI-S-003-2007) in Japan Concrete Institute (JCI) Standard is performed by using 2MN universal testing machine.

Therefore, specimen size is used as 60mm in depth, 60mm in width and 350mm in length instead of 100mm in depth, 100mm in width and 400mm in length. Outline of four-point bending test is shown in Figure 2.5. The specimen is applied the load continuously without shock at a constant rate of 0.5mm per minute.

To compare the influence of cast, mold and cutout surface, the cast surface is placed as tension side for coupons from upper section, the cutout surface for coupons from middle section, and then the mold surface is as tension side for coupons from lower section.

The bending moment and curvature is calculated by using the following equation (2.1) and (2.2) to obtain the bending moment-curvature curve.

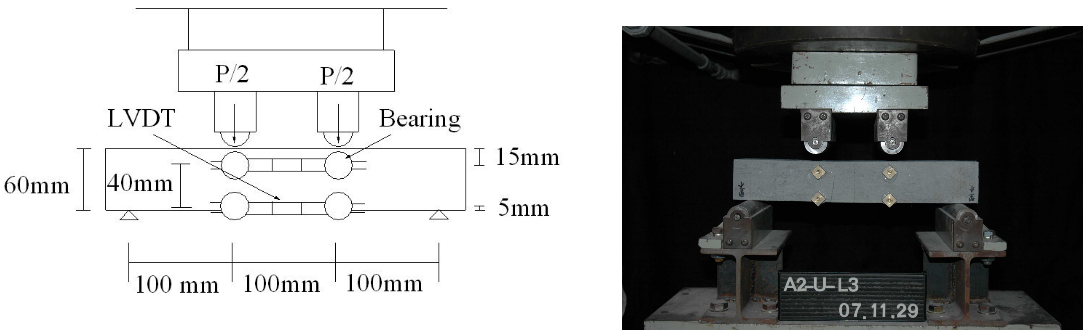

Figure 2.5 Four-point bending test

$$M = \frac{P}{2} \cdot \frac{l}{3} \tag{2.1}$$

$$\phi = \frac{\varepsilon_2 - \varepsilon_1}{d_0} \tag{2.2}$$

M	:Bending moment (kN・mm)
P	:Applied load (kN)
l	:Span (= 300mm)
ϕ	:Curvature (1/mm)
$\varepsilon 1$, $\varepsilon 2$	:Strains calculated by dividing the measured displacements of upper and lower LVDTs by contact length (mm) (elongation is defined as positive)
d_0	:Distance between two LVDTs (= 40mm)

2.6. *Experimental Result*

An example of the bending moment and curvature curve relationships is shown in Figure 2.6.

From the figure of bending moment and curvature curve relationships, M_{max} is defined as the maximum bending moment at maximum load and ϕ_{max} is the curvature at the maximum bending moment. M_u is defined as the ultimate bending moment where the deflection hardening behavior is stopped to fracture and ϕ_u is the curvature at the ultimate bending moment.

In addition, σ_{max} and ε_{max} is calculated from M_{max} and ϕ_{max} by using equations of Evaluation Method for Tensile Strength and Ultimate Tensile Strain of Fiber-reinforced Cementitious Composite (JCI-S-003-2007) in Japan Concrete Institute (JCI) Standard. [2.1]
σ_u and ε_u is calculated by same calculation to evaluate M_u and ϕ_u as same as σ_{max} and ε_{max}.

To obtain tensile strain and tensile strength, static modulus of elasticity (E) has been used. E is evaluated from modulus of 1/3 secant by compressive test. From this test result, 17.07 GPa is used for coupon with 1.5% volume fraction of fibers and 15.34 GPa is used for coupon with 2.0% volume fraction of fibers. The detailed experimental result of compressive test is shown in Appendix: B.

In addition, the detailed data of coupons is shown in Appendix: C and the detailed view of bending moment-curvature curve relationship of coupons is shown in Appendix: D.
In the Appendix: C, if the largest crack occurs outside of pure bending span on coupons, it is marked as X in the column of Fracture position. The other is that the largest crack occurs in the pure bending span.

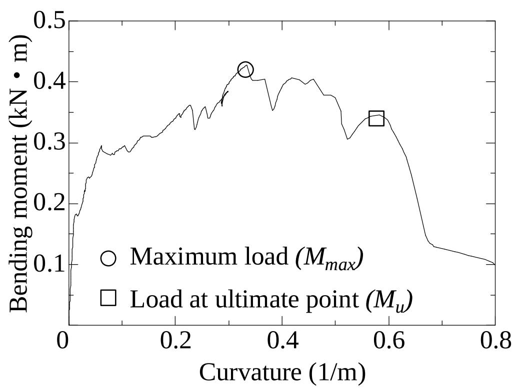

Figure 2.6 An example of test result

2.6.1. Specimens with 1.5% volume fraction of fibers

The list of experimental result of prepared specimens and coupons with 1.5% volume fraction of fibers is shown in Table 2.3.

Table 2.3 Experimental Result of specimens and coupons with 1.5% of fiber volume of fraction

ID	M_{max} (kN•m)	M_u (kN•m)	ϕ_{max} (1/m)	ϕ_u (1/m)	σ_{max} (N/mm^2)	σ_u (N/mm^2)	ε_{max} (%)	ε_u (%)
1.5-1	0.327	0.327	0.390	0.390	3.26	3.26	2.06	2.06
1.5-2	0.445	0.440	0.142	0.153	4.89	4.79	0.66	0.72
1.5-3	0.412	0.412	0.280	0.280	4.10	4.10	1.44	1.44
1.5-4	0.440	0.440	0.242	0.242	4.57	4.57	1.21	1.21
1.5-5	0.400	0.400	0.171	0.171	4.30	4.30	0.82	0.82
A1-U-X0	0.126	0.115	0.008	0.082	2.09	1.25	0.02	0.41
A1-U-X1	0.159	0.140	0.011	0.087	2.50	1.51	0.03	0.43
A1-U-X2	0.218	0.218	0.100	0.100	2.31	2.31	0.49	0.49
A2-U-X3	0.391	0.391	0.288	0.288	4.05	4.05	1.47	1.47
A1-U-Y1	0.247	0.247	0.132	0.132	2.90	2.90	0.63	0.63
A1-U-Y2	0.276	0.264	0.124	0.188	3.09	2.85	0.59	0.93
A2-U-Y3	0.194	0.174	0.011	0.085	3.09	1.82	0.03	0.42
A1-L-X0	0.250	0.250	0.126	0.126	2.68	2.68	0.62	0.62
A1-L-X1	0.300	0.300	0.237	0.237	3.16	3.16	1.21	1.21
A1-L-X2	0.347	0.347	0.228	0.228	3.70	3.70	1.13	1.13
A2-L-X3	0.381	0.381	0.246	0.246	3.98	3.98	1.24	1.24
A1-L-Y1	0.112	0.107	0.040	0.053	1.38	1.27	0.18	0.25
A1-L-Y2	0.142	0.142	0.162	0.162	1.40	1.40	0.87	0.87
A2-L-Y3	0.245	0.223	0.045	0.157	3.12	2.45	0.18	0.78
B0-M-X1	0.162	No Data						
B0-M-X2	0.221	0.221	0.089	0.089	2.40	2.40	0.42	0.42
B0-M-X3	0.318	0.318	0.232	0.232	3.40	3.40	1.16	1.16
B0-M-X4	0.378	0.378	0.166	0.166	4.16	4.16	0.80	0.80
B1-M-X5	0.355	0.355	0.212	0.212	3.78	3.78	1.06	1.06
B0-M-Y1	0.073	0.073	0.065	0.065	0.75	0.75	0.34	0.34
B0-M-Y2	0.083	0.083	0.004	0.004	1.44	1.44	0.01	0.01
B0-M-Y3	0.072	0.059	0.077	0.244	0.74	0.58	0.40	1.37
B0-M-Y4	0.062	0.062	0.096	0.096	0.64	0.64	0.51	0.51
C1-U-X0	0.164	0.164	0.086	0.086	1.84	1.84	0.41	0.41
C1-U-X1	0.110	0.074	0.007	0.111	1.85	0.78	0.02	0.58
C1-U-X2	0.185	0.126	0.056	0.139	2.09	1.29	0.26	0.73
C2-U-X3	0.258	0.258	0.083	0.083	3.03	3.03	0.38	0.38
C1-U-Y1	0.216	0.216	0.130	0.130	2.28	2.28	0.66	0.66
C1-U-Y2	0.084	0.084	0.027	0.027	1.03	1.03	0.12	0.12
C2-U-Y3	0.270	0.270	0.203	0.203	2.97	2.97	1.01	1.01
C1-L-X0	0.272	0.272	0.245	0.245	2.83	2.83	1.27	1.27
C1-L-X1	0.292	0.292	0.242	0.242	3.11	3.11	1.23	1.23
C1-L-X2	0.319	0.285	0.151	0.181	3.67	3.20	0.72	0.89
C2-L-X3	0.427	0.405	0.334	0.460	4.38	4.07	1.71	2.42
C1-L-Y1	0.299	0.299	0.180	0.180	3.19	3.19	0.90	0.90
C1-L-Y2	0.361	0.356	0.230	0.246	3.96	3.88	1.13	1.22
C2-L-Y3	0.284	0.284	0.079	0.079	3.22	3.22	0.36	0.36

2.6.1.1. Prepared Specimens

The bending moment and curvature curve relationships of five prepared specimens is shown in Figure 2.7. The average of five prepared specimens' M_{max} is 0.405 kN·m, and ϕ_{max} is 0.245 1/m. In addition, the standard deviation of M_{max} is 0.042 kN·m and standard deviation of ϕ_{max} is 0.088 1/m. From Figure 2.7, the deflection hardening behavior is recognized well.

According to Figure 2.7, the result of M_{max} of each prepared specimen are almost similar, however, the result of ϕ_{max} has varied greatly. The reason why ϕ_{max} has varied greatly can be recognized that the largest crack to rupture may occur differently. For example, in 1.5-5 of prepared specimen, the largest crack to rupture occurs outside of the pure bending span so that ϕ_{max} has been measured smaller than it occurs in the pure bending span such as 1.5-1.

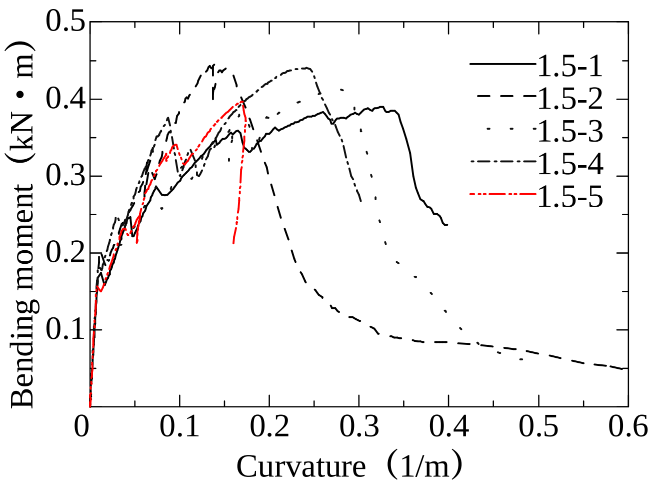

Figure 2.7 Bending moment – curvature curve relationships of prepared specimens

2.6.1.2. Coupons on X-direction

(1) Bending moment and curvature curve relationships

The relationships between bending moment and curvature curve of coupon on X-direction in Part A, B and C are shown in Figure 2.8.

From the result of Figure 2.8, the deflection hardening behavior is observed well at lower section of Part A and C. However, the deflection hardening behavior is little observed at upper section of Part A and C. Therefore, coupons at upper section are shown lower strength than those at lower section in both Part A and C. Therefore, the maximum moment of coupons at upper section is lower than the maximum moment of coupons at lower section.

In addition, according to the result of Table 2.3 and Figure 2.8, the maximum moment of Part A at upper section is similar to Part C at upper section in the same position number of Figure 2.2. Therefore, assuming that the distribution and orientation of fiber is related to flexural performance closely, it is said that the fiber will be distributed and orientated similarly and symmetrically from the center line of the large specimen. Moreover, the bending strength increases with increase the position number of coupons in generally.

In other hand, the deflection hardening behavior is little observed in coupons at middle section in Part B, however, the bending strength increases with increases of the position number of coupons as same as in Part A and C.

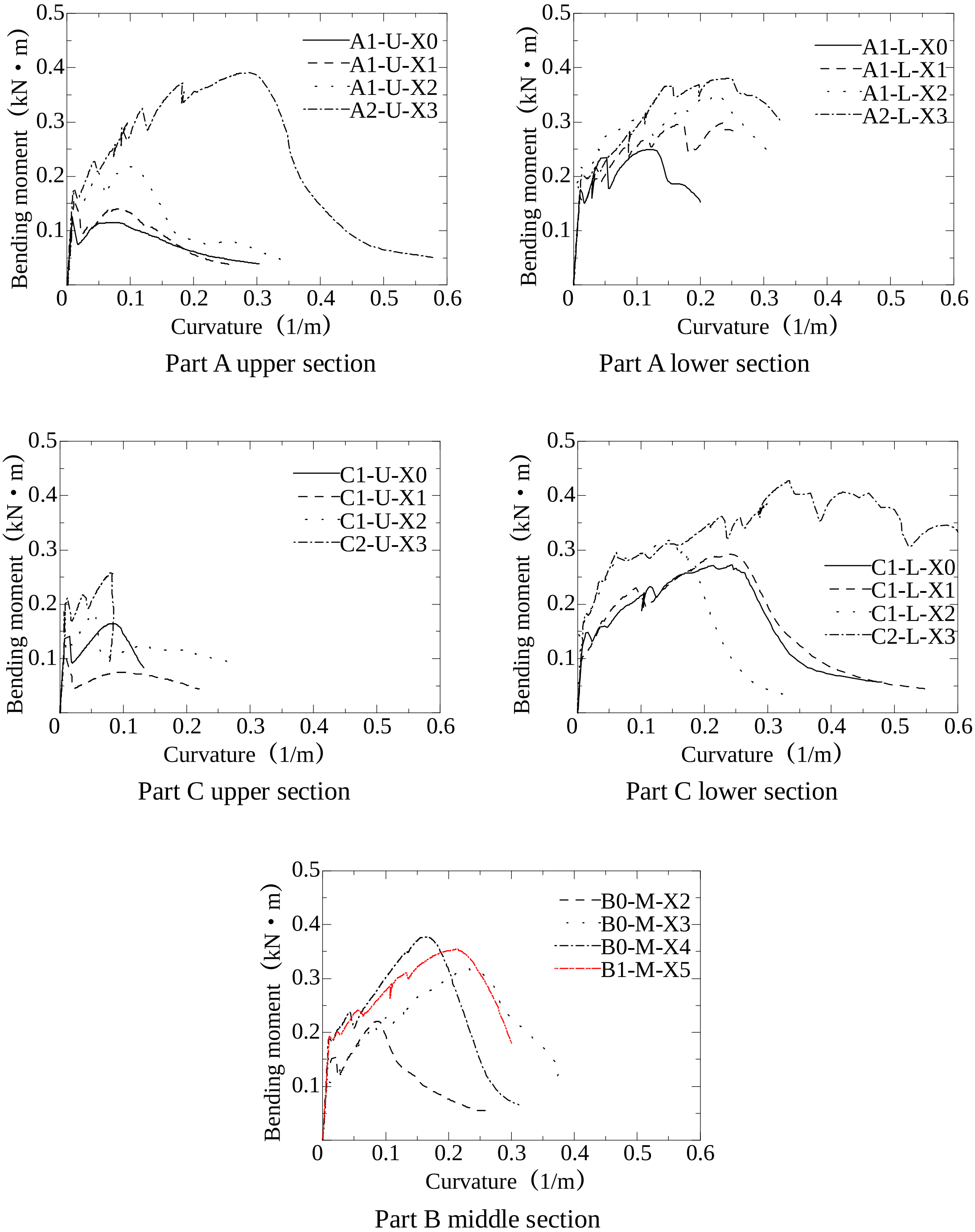

Figure 2.8 Bending moment-curvature curve relationships of coupons on X-direction

(2) Influence of mold surface

The distance from mold surfaces to the center of each coupon and M_{max} or M_u relationship in Part A, B and C is shown in Figure 2.9 and the distance from mold surfaces to the center of each coupon and ϕ_{max} or ϕ_u relationship in Part A, B and C is shown in Figure 2.10. The distance from mold surface to center is calculated from each center of coupons.

According to Figure 2.9, M_{max} of coupons at lower section is larger than M_{max} of coupons at upper section on Part A and C. Therefore, it can be recognized that the flexural performance is depending on whether the deflection hardening behavior is occurred or not because coupons at lower section, which the deflection hardening behavior is recognized well, is higher strength than coupons at upper section, which the deflection hardening behavior is little recognized.

M_{max} of coupon decreases with increase of the distance from the mold surface to center of each coupon at Part A and C. However, in Part B, M_{max} of coupon increases around 100mm from mold surface once, and then decreases with increases of the distance. Therefore, it can be recognized that the influence of mold surface is larger than cast surface to flexural performance for HPFRCC with 1.5% volume fraction of fibers and the reason why maximum moment increases as the mold surface comes to a close can be said that PVA fiber will be concentrated around mold surface and orientated as parallel to mold surface, called as wall-effect. M_u and distance from mold surface relationships has same tendency described in Figure 2.9.

The test result of ϕ_{max} or ϕ_u and distance from mold surface relationships is also same tendency as the test result of M_{max} described in Figure 2.10 so that the influence of surface on coupons is also related to curvature closely.

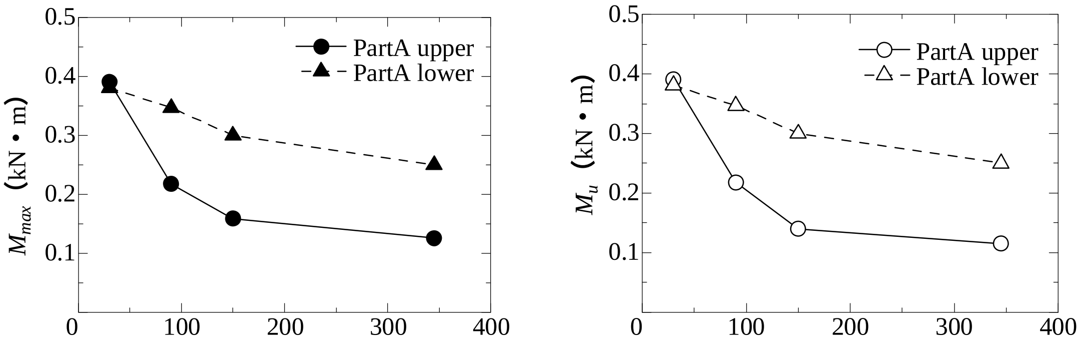

Distance from mold surface to center of each coupon (mm)

Part A upper and lower section

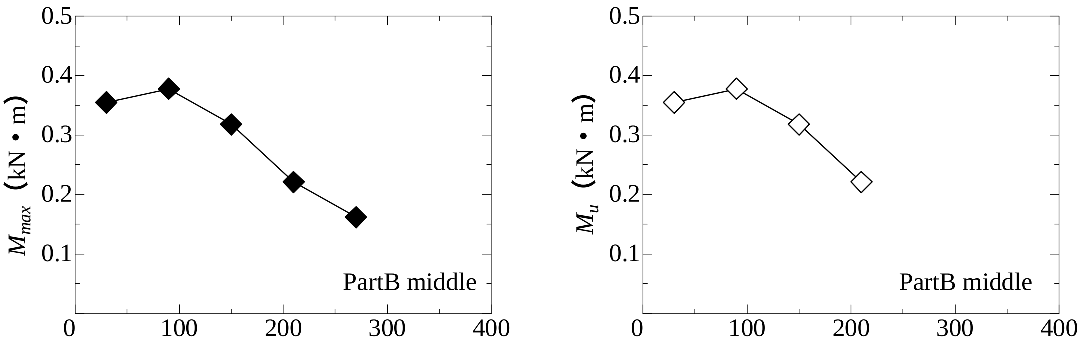

Distance from mold surface to center of each coupon (mm)

Part B middle section

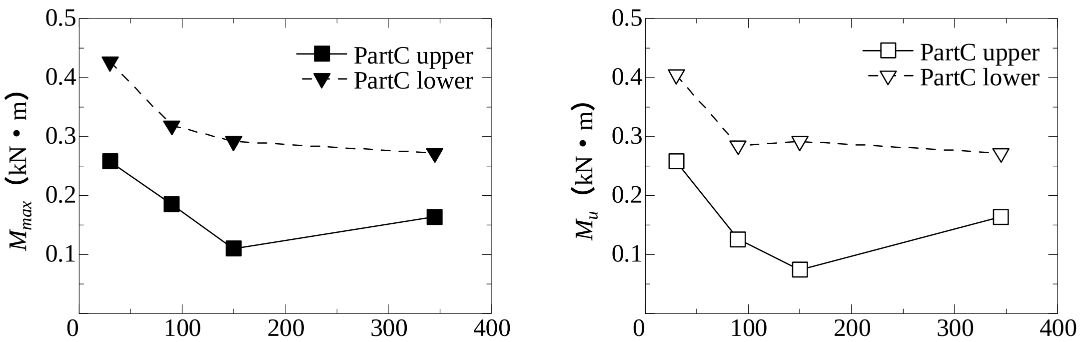

Distance from mold surface to center of each coupon (mm)

Part C upper and lower section

Figure 2.9 M_{max} or M_u and distance from mold surface relationships

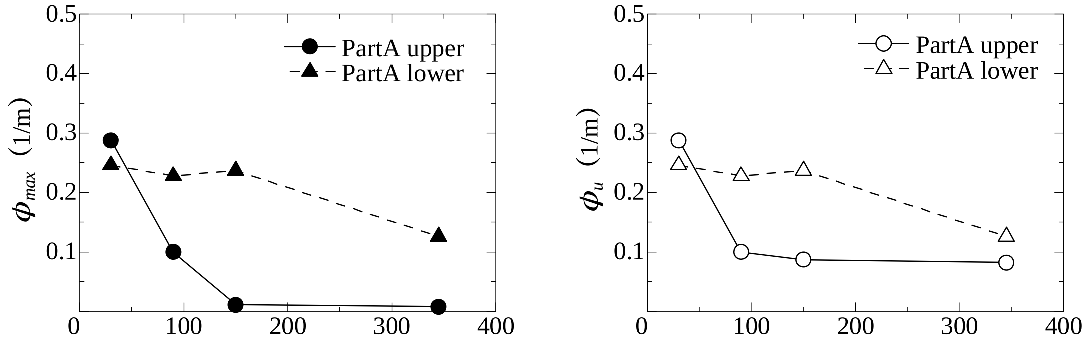

Distance from mold surface to center of each coupon (mm)

Part A upper and lower section

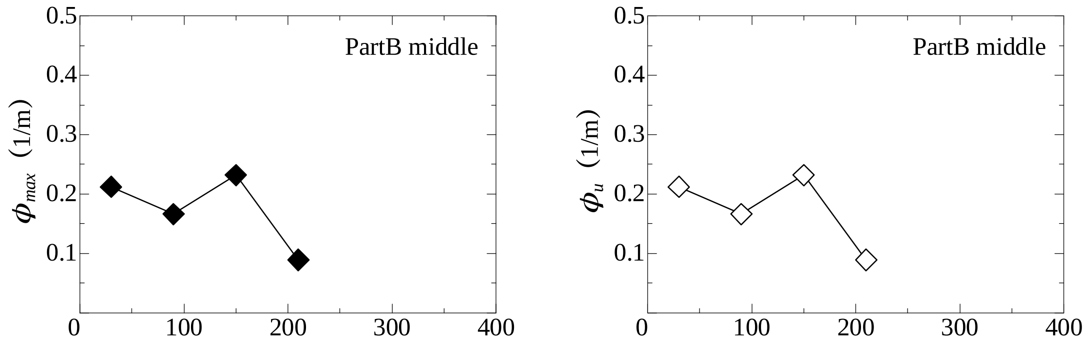

Distance from mold surface to center of each coupon (mm)

Part B middle section

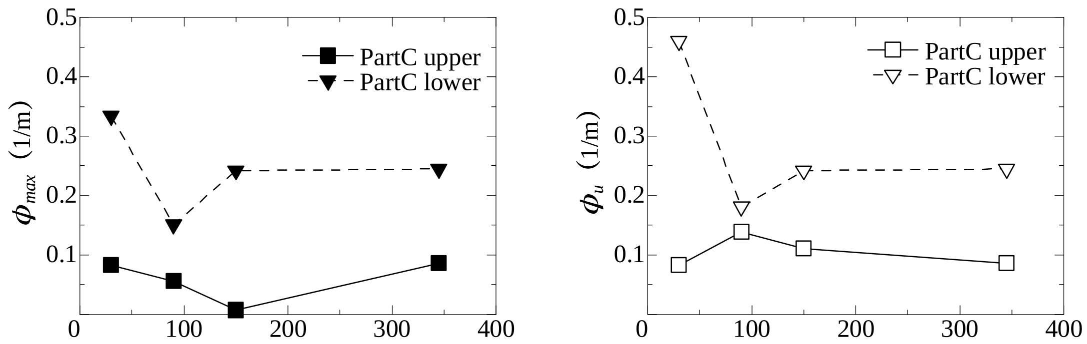

Distance from mold surface to center of each coupon (mm)

Part C upper and lower section

Figure 2.10 ϕ_{max} or ϕ_u and distance from mold surface relationships

2.6.1.3. Coupons on Y-direction

The bending moment and curvature curve relationships of coupon in Part A, B and C on Y-direction is shown in Figure 2.11.

The deflection hardening behavior on coupon at Y-direction is little observed so that the result of bending strength such as M_{max} is lower than coupons on X-direction in general. In addition, M_{max} on coupon at upper section is lower than those at lower section by compared at same position number. This result shows same trend as the result of coupon on X-direction.

From Table 2.3, the result of ϕ_{max} of coupon on Y-direction is smaller than those on X-direction in general also. In addition, position number is not related as the result of the maximum moment or curvature and the result of coupon on Y-direction is varying widely. The reason can be recognized that PVA fiber has tendency to be orientated as parallel at the cross section of coupon on Y-direction. PVA fiber of the coupon on X-direction is not related to flexural performance for Y-direction coupons directly.

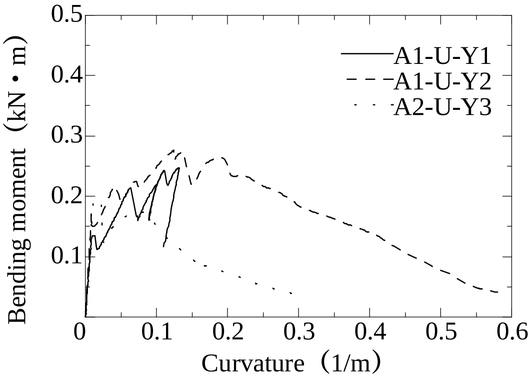

Part A upper section

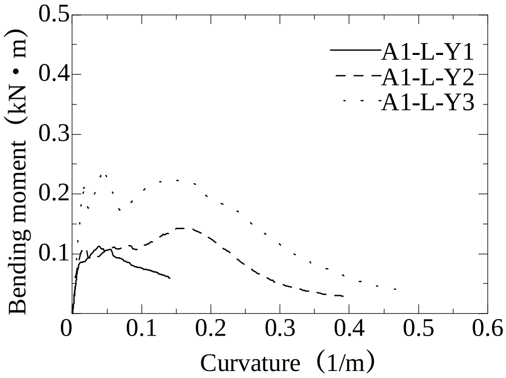

Part A lower section

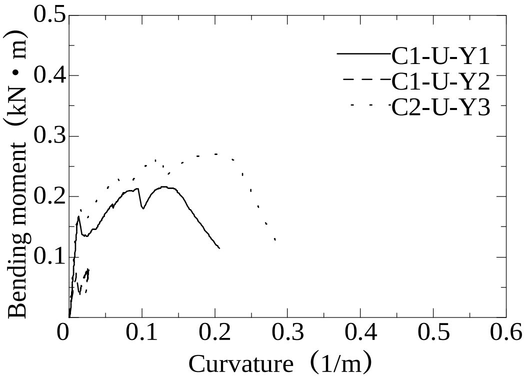

Part C upper section

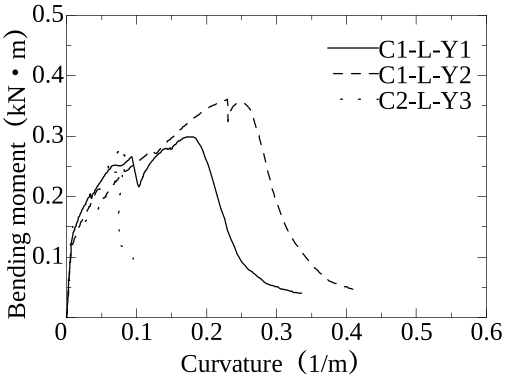

Part C lower section

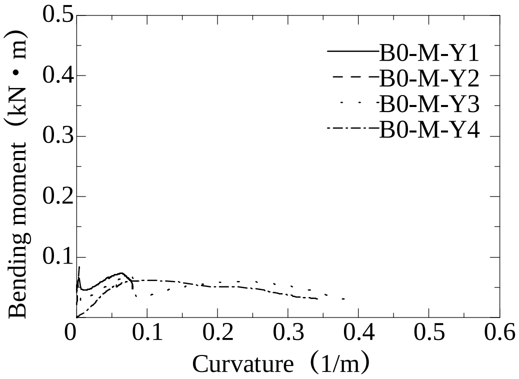

Part B middle section

Figure 2.11 Bending moment-curvature curve relationships on Y-direction

2.6.2. Specimens with 2.0% volume fraction of fibers

The list of experimental result of prepared specimens and coupons with 2.0% volume fraction of fibers is shown in Table 2.4.

Table 2.4 Experimental Result of specimens and coupons with 2.0% of fiber volume of fraction

ID	M_{max} (kN・m)	M_u (kN・m)	ϕ_{max} (1/m)	ϕ_u (1/m)	σ_{max} (N/mm^2)	σ_u (N/mm^2)	ε_{max} (%)	ε_u (%)
2.0-1	0.446	0.446	0.256	0.256	5.27	5.27	1.18	1.18
2.0-2	0.404	0.375	0.186	0.218	4.23	3.85	0.89	1.08
2.0-3	0.473	0.473	0.340	0.340	4.54	4.54	1.79	1.79
2.0-4	0.380	0.366	0.221	0.297	3.86	3.64	1.11	1.53
2.0-5	0.407	0.407	0.284	0.284	4.09	4.09	1.43	1.43
2.0A1-U-X0	0.155	0.151	0.030	0.097	1.91	1.62	0.12	0.48
2.0A1-U-X1	0.154	0.154	0.170	0.170	1.71	1.71	0.85	0.85
2.0A1-U-X2	0.294	0.294	0.118	0.118	3.29	3.29	0.55	0.55
2.0A2-U-X3	0.342	0.342	0.246	0.246	3.83	3.83	1.20	1.20
2.0A1-U-Y1	0.275	0.275	0.187	0.187	2.91	2.91	0.93	0.93
2.0A1-U-Y2	0.355	0.308	0.336	0.326	3.74	3.22	1.71	1.67
2.0A2-U-Y3	0.316	0.316	0.319	0.319	3.34	3.34	1.63	1.63
2.0A1-L-X0	0.245	0.245	0.098	0.098	2.92	2.92	0.45	0.45
2.0A1-L-X1	0.265	0.265	0.300	0.300	2.89	2.89	1.52	1.52
2.0A1-L-X2	0.323	0.316	0.323	0.336	3.30	3.21	1.66	1.74
2.0A2-L-X3	0.332	0.320	0.184	0.220	3.68	3.49	0.88	1.08
2.0A1-L-Y1	0.140	0.140	0.172	0.172	1.45	1.45	0.90	0.90
2.0A1-L-Y2	0.365	0.350	0.303	0.334	3.85	3.66	1.54	1.72
2.0A2-L-Y3	0.421	0.327	0.452	0.704	4.29	3.23	2.35	3.83
2.0B0-M-X1	0.278	0.136	0.305	0.863	3.01	1.38	1.55	4.80
2.0B0-M-X2	0.268	0.266	0.103	0.170	3.18	3.01	0.47	0.82
2.0B0-M-X3	0.374	0.364	0.221	0.228	4.05	3.92	1.08	1.12
2.0B0-M-X4	0.359	0.332	0.197	0.214	3.92	3.58	0.95	1.05
2.0B1-M-X5	0.375	0.352	0.312	0.382	4.02	3.71	1.57	1.96
2.0B0-M-Y1	0.087	0.078	0.014	0.053	1.22	0.91	0.05	0.26
2.0B0-M-Y2	0.136	0.136	0.170	0.170	1.38	1.38	0.89	0.89
2.0B0-M-Y3	0.090	0.086	0.004	0.020	1.93	1.06	0.01	0.08
2.0B0-M-Y4	0.080	0.066	0.005	0.128	1.43	0.69	0.01	0.68
2.0C1-U-X0	0.148	0.100	0.026	0.119	1.86	1.04	0.10	0.62
2.0C1-U-X1	0.194	0.115	0.076	0.284	2.22	1.18	0.35	1.55
2.0C1-U-X2	0.326	0.326	0.206	0.206	3.56	3.56	1.00	1.00
2.0C2-U-X3	0.311	0.235	0.355	0.529	3.24	2.38	1.83	2.85
2.0C1-U-Y1	0.284	0.280	0.163	0.171	2.85	2.80	0.82	0.86
2.0C1-U-Y2	0.339	0.292	0.292	0.349	3.53	2.99	1.49	1.82
2.0C2-U-Y3	0.340	0.338	0.269	0.328	3.65	3.58	1.34	1.66
2.0C1-L-X0	0.226	0.223	0.255	0.265	2.49	2.45	1.28	1.33
2.0C1-L-X1	0.249	0.249	0.269	0.269	2.96	2.96	1.32	1.32
2.0C1-L-X2	0.298	0.288	0.132	0.263	3.33	3.04	0.62	1.34
2.0C2-L-X3	0.350	0.314	0.311	0.365	3.69	3.26	1.57	1.89
2.0C1-L-Y1	0.268	0.268	0.199	0.199	2.94	2.94	0.98	0.98
2.0C1-L-Y2	0.249	0.249	0.270	0.270	2.92	2.92	1.32	1.32
2.0C2-L-Y3	0.366	0.335	0.260	0.366	3.88	3.46	1.30	1.90

2.6.2.1. Prepared Specimens

The bending moment and curvature curve relationships of five prepared specimens is shown in Figure 2.12. The average of five prepared specimens' M_{max} is 0.422 kN・m, and ϕ_{max} is 0.257 1/m. In addition, the standard deviation of M_{max} is 0.033 kN·m and standard deviation of ϕ_{max} is 0.053 1/m. From Figure 2.12, the deflection hardening behavior is recognized well.

According to Figure 2.12, the results of M_{max} of each prepared specimen are almost similar. At 2.0-2 of prepared specimen, the largest crack to rupture occurred outside of the pure bending span so that ϕ_{max} has been measured smaller than other prepared specimens, which the largest crack is occurred in the pure bending span.

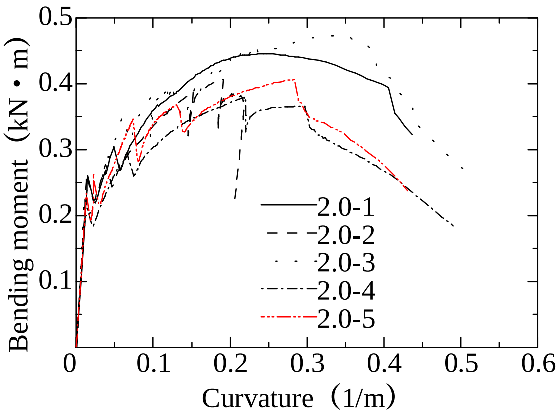

Figure 2.12 Bending moment – curvature curve relationships of prepared specimens

2.6.2.2. Coupons on X-direction

(1) Bending moment and curvature curve relationships

The relationship between bending moment and curvature curve of coupon on X-direction in Part A, B and C with 2.0% volume fraction of fibers are shown in Figure 2.13.

From Figure 2.13, the deflection hardening behavior is observed well at both lower and upper section in Part A and C. In addition, according to Table 2.4 and Figure 2.13, M_{max} of coupons on Part A at upper section is similar to those on Part C at upper section in the same position number. M_{max} of coupons on Part A at lower section is similar to those on Part C at lower section in the same position number also. Therefore, assuming that the distribution and orientation of fiber is related to flexural performance closely, it is said that the fiber will be distributed and orientated similarly and symmetrically from the center line of specimen.

Coupons at middle section in Part B, the deflection hardening behavior is observed well as same as Part A and C. In addition, the strength increases with increase of the position number of coupons as same as in Part A and C.

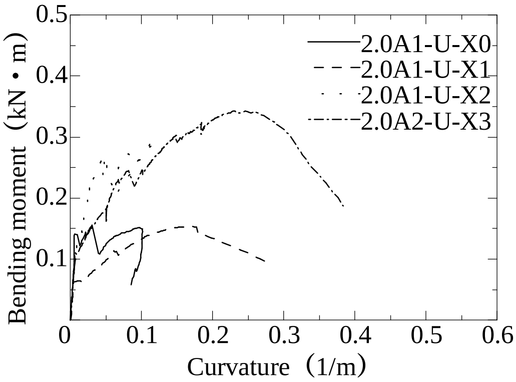

Part A upper section

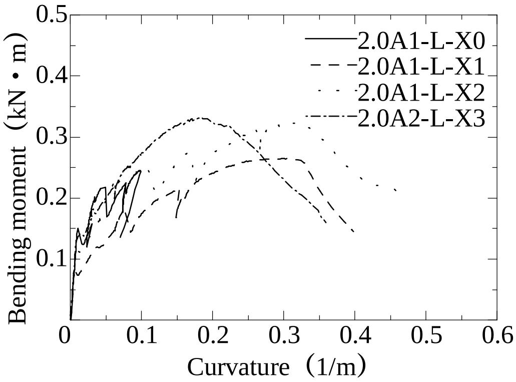

Part A lower section

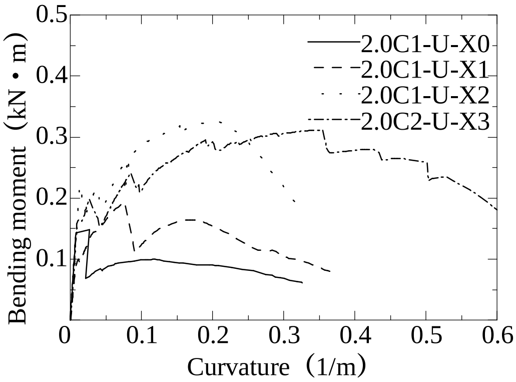

Part C upper section

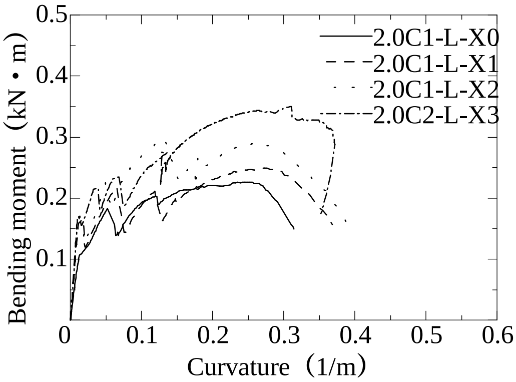

Part C lower section

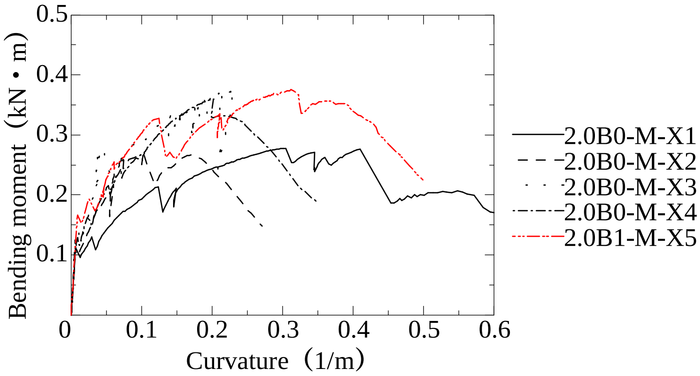

Part B middle section

Figure 2.13 Bending moment-curvature curve of coupons on Y-direction

(2) Influence of mold surface

The distance from mold surfaces to the center of each coupon and M_{max} or M_u relationship in Part A, B and C is shown in Figure 2.14 and the distance from mold surfaces to the center of each coupon and ϕ_{max} or ϕ_u relationship in Part A, B and C is shown in Figure 2.15. The distance from mold surface to center is calculated from each center of coupons.

According to Figure 2.14, M_{max} of coupons at lower section is larger than M_{max} of coupons at upper section on Part A and C even if the deflection hardening behavior is recognized at both upper and lower section. In addition, the maximum moment of coupon decreases with increase of the distance from the mold surface to center of each coupon at Part A and C. Coupons at middle section in Part B, M_{max} of coupon also decreases with increase of the distance from the mold surface to center of each coupon.

Therefore, it is said that coupon in lower section's PVA fiber is more distributed and orientated on axial direction of loading than those in upper sections because of wall-effect and the influence of mold surface is related to the bending strength closely.

The test result of ϕ_{max} or ϕ_u and distance from mold surface relationships is also same tendency as the test result of M_{max} described in Figure 2.10 so that the influence of surface on coupons is related to curvature closely too.

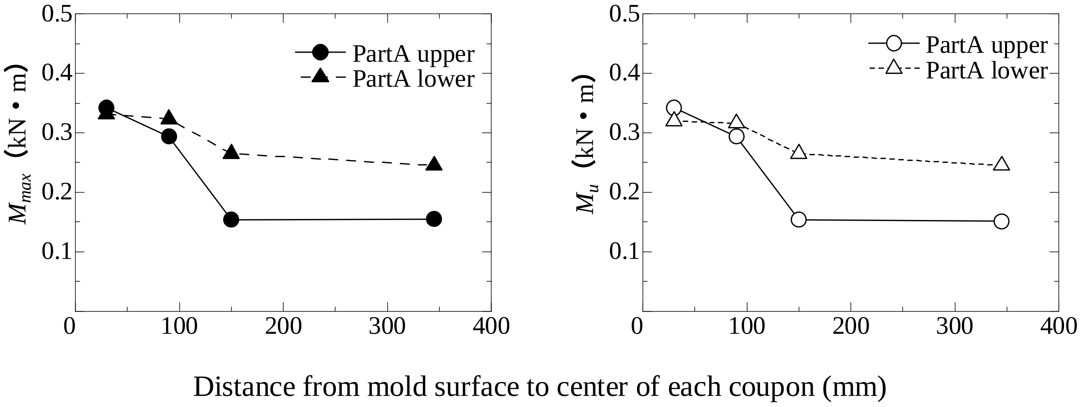

Part A upper and lower section

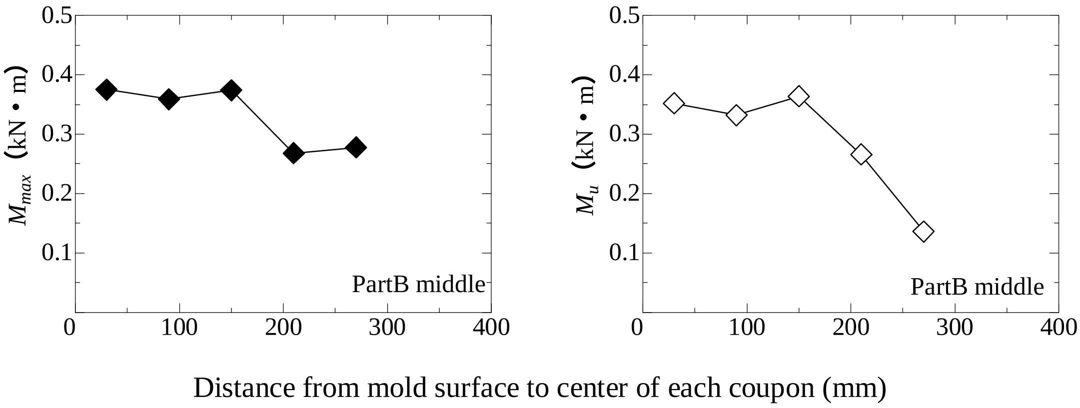

Part B middle section

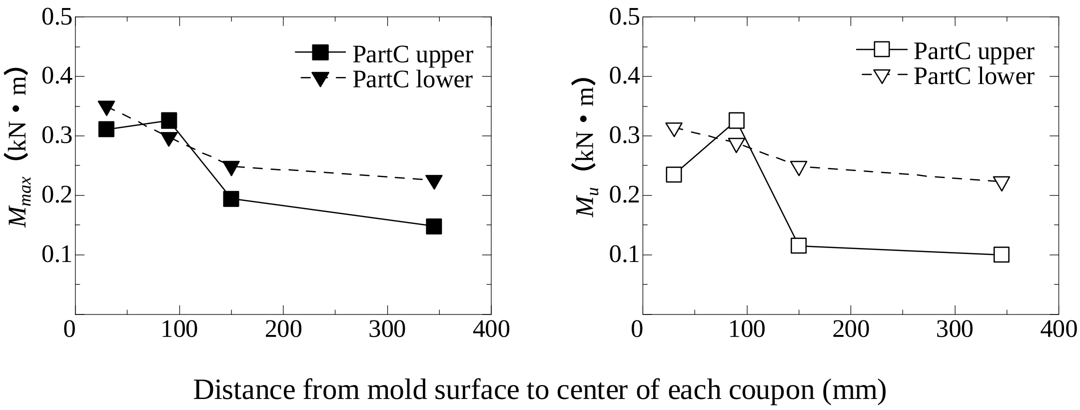

Part C upper and lower section

Figure 2.14 M_{max} or M_u and distance from mold surface relationships

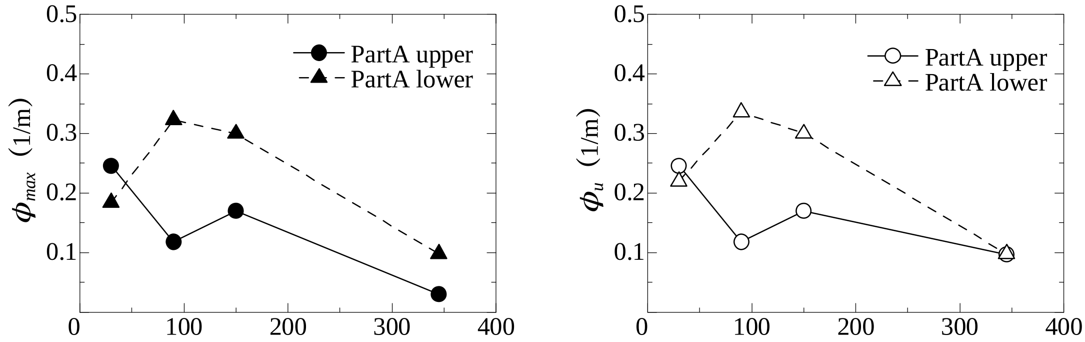

Distance from mold surface to center of each coupon (mm)

Part A upper and lower section

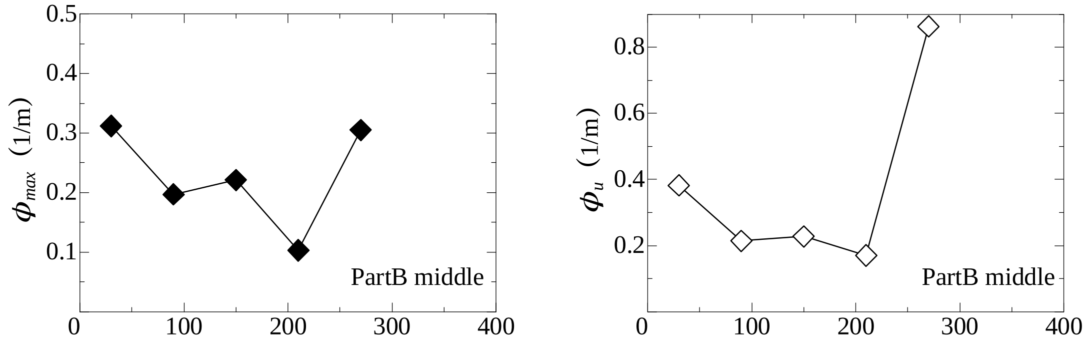

Distance from mold surface to center of each coupon (mm)

Part B middle section

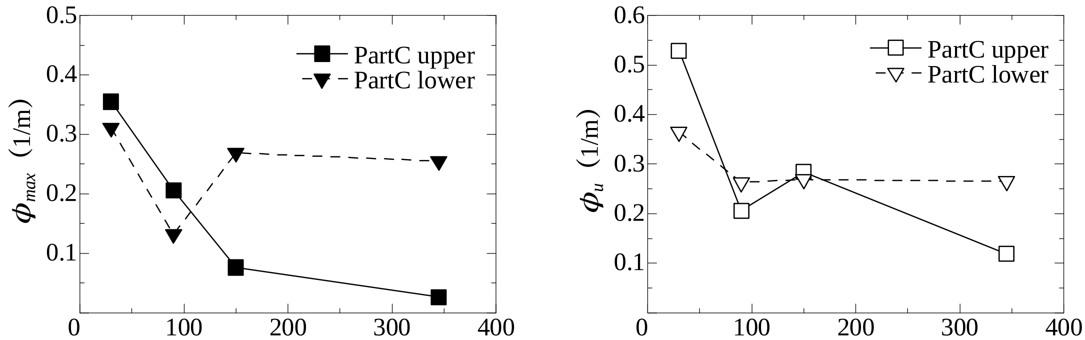

Distance from mold surface to center of each coupon (mm)

Part C upper and lower section

Figure 2.15 ϕ_{max} or ϕ_u and distance from mold surface relationships

2.6.2.3. Coupons on Y-direction

The bending moment and curvature curve relationships of coupon in Part A, B and C on Y-direction is shown in Figure 2.16. Coupon at Part A and C, the deflection hardening behavior is recognized as those on X-direction. Maximum bending moment on coupon in both upper and lower section is almost same at same position number in Part C. In addition, the strength of bending increases with increase of the position number. Therefore, it is same tendency as those on X-direction. However, the deflection hardening behavior is not seen clearly at middle section in Part B.

In these result, it is said that PVA fiber is distributed and orientated well not only on axial direction but also on perpendicular direction on loading in Part A and C with 2.0% volume fraction of fibers so that the deflection hardening behavior could be realized well in coupon on Y-direction and wall-effect is an important factor to flexural performance for HPFRCC.

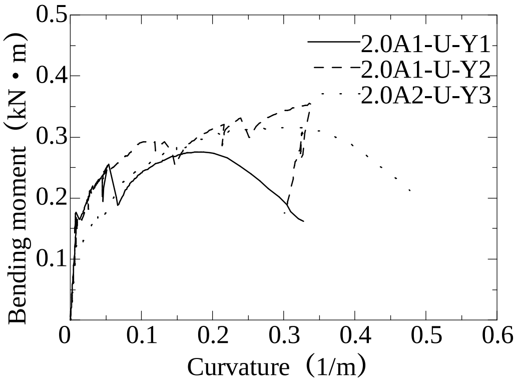

Part A upper section

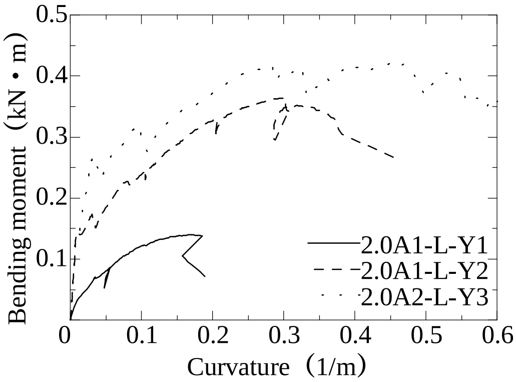

Part A lower section

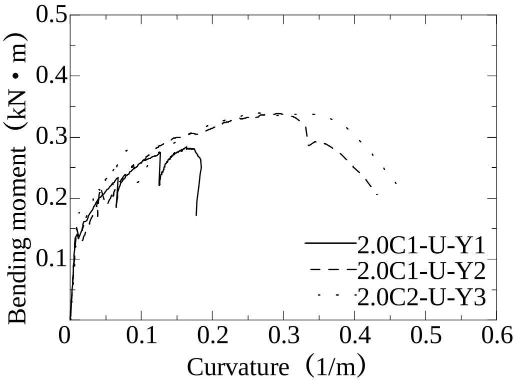

Part C upper section

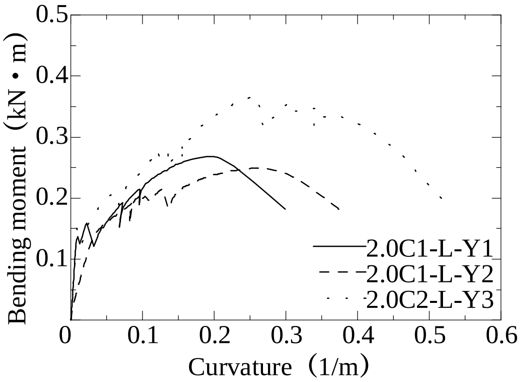

Part C lower section

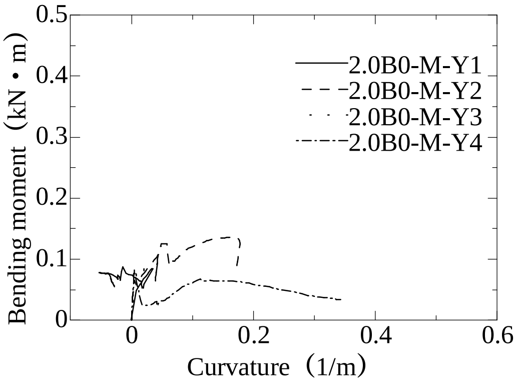

Part B middle section

Figure 2.16 Bending moment-curvature curve relationships on Y-direction

2.7. Comparison and Discussion

In this chapter 2, two large specimens, which is prepared as HPFRCC with 1.5% and 2.0% volume fraction of PVA fibers, are cut to small coupons and the flexural performance of HPFRCC due to the influence of fiber and surface such as cast, mold and cutout surface is examined by using four-point bending test.

In this result, the flexural performance of coupons is lower than same size of prepared specimens and the flexural performance decreases with increase of the distance from the mold surface in generally. In addition, the coupon at lower section shows higher ductility than those at upper section.

The results is achieved that the influence of cast, mold and cutout surface is related to the flexural performance of HPFRCC closely.

To compare the result of coupon between 1.5% and 2.0% volume fraction of fibers, the result of maximum bending moment and curvature on prepared specimens with 2.0% volume fraction of fibers is higher than those with 1.5% volume fraction of fibers. Moreover, the decreasing rate of flexural performance with increase of the distance from mold surface to center on coupon with 2.0% volume fraction of fibers is smaller than those with 1.5% volume fraction of fibers.

In addition, the deflection hardening behavior is observed on the coupon with 2.0% volume fraction of fibers on Y-direction is recognized even if the deflection hardening behavior is observed little at 1.5% volume fraction of fibers.

In these result, volume fraction of fibers in HPFRCC is also a factor to the flexural performance because the fibers will bear the tension more if volume fraction of fibers increases in the matrix.

CHAPTER 3 CROSS SECTION OBSERVATION

3.1. Introduction

In chapter 2, four-point bending test has been examined to achieve how mold, cast and cutout surface affect to the flexural performance for HPFRCC. In this chapter, to know how the fiber will be orientated and distributed in the matrix, cross section observation is applied by using mercury lamp.

3.2. Outline of Cross Section Observation

It is known that materials which have a particular chemical structure absorb an electromagnetic wave with a particular wave length. For PVA fiber, PVA fiber absorbs the ultraviolet radiation and emits fluorescence. [3.1] Based on this principle, mercury lamp is used to observe PVA fiber.

Outline of the cross section of coupon is shown in Figure 3.1. The cross section is cut around close to the largest crack which occurred by four-point bending test, then, the number of PVA fiber on the cross section, which is close to the largest crack, is defined as A. The number of PVA fiber on the opposite side of cross section A is defined as B. In addition, the size of observation specimen is 60mm in width, 60mm in depth and 60mm in length.

The number of PVA fiber of cross section A and B is counted and the number of PVA fiber is defined as $N_{f\text{-}A}$ and $N_{f\text{-}B}$, respectively. Then, it is taken the average of both cross sections. The average of $N_{f\text{-}A}$ and $N_{f\text{-}B}$ is defined as $N_{f\text{-}ave}$ as the number of PVA fiber in each coupons.

Outline of cross section observation is shown in Figure 3.2. The image of cross section's coupons is captured with a digital camera through a microscope by using mercury lamp. The yellow cellophane sheet is used with mercury lamp to let PVA fiber emphasize the emission of light more.

The captured image of cross section is analyzed and mapped as two valued color that PVA fiber is to black dots and cement is to white color by using image analysis software. Finally, the block dots are counted as the number of fibers by using image analysis software.

The picture of experimental equipment is shown in Picture 3.1. The outside of mercury lamp's diameter is 200mm and the peak wavelength is 351nm. The specimen is set on the table and the image is captured over the mercury lamp by a digital camera.

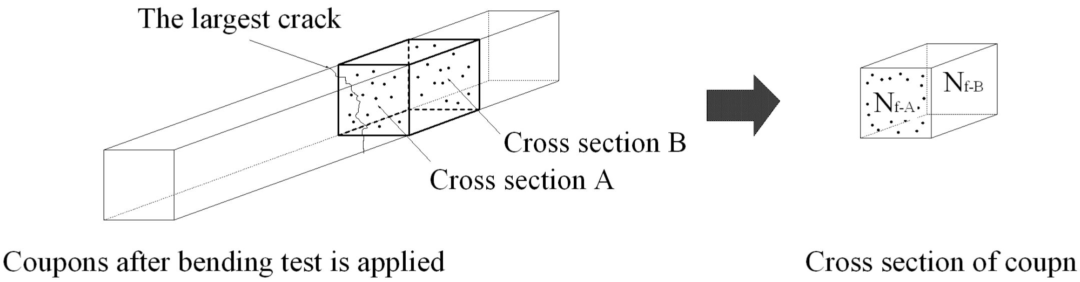

Figure 3.1 Outline of cross section of coupon

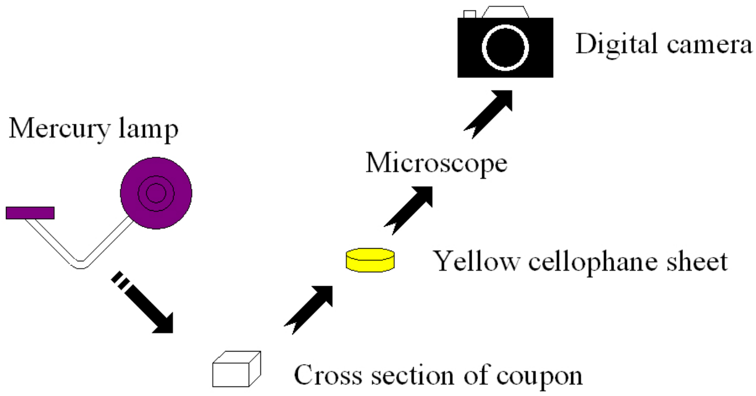

Figure 3.2 Outline of cross section observation

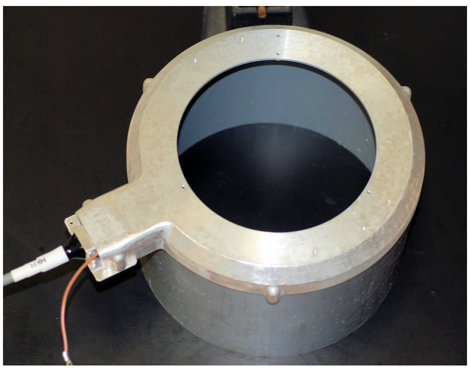

Picture 3.1 Experimental equipment

3.3. Experimental Result

The average of five prepared specimens' M_{max} and ϕ_{max} is defined as $M_{max,w}$ and $\phi_{max,w}$, respectively. In addition, the average of five prepared specimens' number of PVA fiber is defined as $N_{f,w}$.

The pictures of cross section A after mapped with two values such as black for PVA fiber and white for cement, is shown in Appendix: E.

3.3.1. *Specimens with 1.5% volume fraction of fibers*

The list of experimental result of specimens and coupon with 1.5% volume fraction of fibers is shown in Table 3.1.

Table 3.1 Experimental Result of specimens and coupons with 1.5% volume fraction of fibers

ID	$N_{f\text{-}A}$	$N_{f\text{-}B}$	$N_{f\text{-}ave}$	$N_{f\text{-}ave}$ / $N_{f,w}$	M_{max} / $M_{max,w}$	ϕ_{max} / $\phi_{max,w}$
1.5-1	6486	12743	9615	$N_{f,w}$ = 9638	$M_{max,w}$ = 0.405 kN•m	$\phi_{max,w}$ = 0.245 1/m
1.5-2	10345	11767	11056			
1.5-3	7721	12518	10120			
1.5-4	6293	11700	8997			
1.5-5	8855	7950	8403			
A1-U-X0	8388	8041	8215	0.852	0.311	0.033
A1-U-X1	6219	8344	7282	0.756	0.393	0.045
A1-U-X2	6824	11958	9391	0.974	0.538	0.408
A2-U-X3	10737	11838	11288	1.171	0.965	1.176
A1-U-Y1	6747	8010	7379	0.766	0.610	0.539
A1-U-Y2	6566	10607	8587	0.891	0.681	0.506
A2-U-Y3	5827	11846	8837	0.917	0.479	0.045
A1-L-X0	7918	8901	8410	0.873	0.617	0.514
A1-L-X1	5801	9788	7795	0.809	0.741	0.967
A1-L-X2	10046	12094	11070	1.149	0.857	0.931
A2-L-X3	9463	8983	9223	0.957	0.941	1.004
A1-L-Y1	5407	8600	7004	0.727	0.277	0.163
A1-L-Y2	7045	11628	9337	0.969	0.351	0.661
A2-L-Y3	4943	12437	8690	0.902	0.605	0.184
B0-M-X1	10992	9602	10297	1.068	0.400	No Data
B0-M-X2	7346	10186	8766	0.910	0.546	0.363
B0-M-X3	10057	11237	10647	1.105	0.785	0.947
B0-M-X4	11038	13559	12299	1.276	0.933	0.678
B1-M-X5	12784	13842	13313	1.381	0.877	0.865
B0-M-Y1	4352	6306	5329	0.553	0.180	0.265
B0-M-Y2	5882	6466	6174	0.641	0.205	0.016
B0-M-Y3	6622	4753	5688	0.590	0.178	0.314
B0-M-Y4	4979	8371	6675	0.693	0.153	0.392
C1-U-X0	8427	10000	9214	0.956	0.405	0.351
C1-U-X1	6934	7584	7259	0.753	0.272	0.029
C1-U-X2	7088	10417	8753	0.908	0.457	0.229
C2-U-X3	9856	7949	8903	0.924	0.637	0.339
C1-U-Y1	5795	5006	5401	0.560	0.533	0.531
C1-U-Y2	6334	8933	7634	0.792	0.207	0.110
C2-U-Y3	5975	12889	9432	0.979	0.667	0.829
C1-L-X0	9223	10582	9903	1.027	0.672	1.000
C1-L-X1	9699	9710	9705	1.007	0.721	0.988
C1-L-X2	11184	12015	11600	1.204	0.788	0.616
C2-L-X3	9348	12342	10845	1.125	1.054	1.363
C1-L-Y1	6303	10738	8521	0.884	0.738	0.735
C1-L-Y2	4823	12214	8519	0.884	0.891	0.939
C2-L-Y3	3368	12535	7952	0.825	0.701	0.322

3.3.1.1. Prepared Specimens

The average number of PVA fiber of five prepared specimens' $N_{f\text{-}ave}$ is 9638. In addition, the standard deviation of $N_{f\text{-}ave}$ is 914.30 and the coefficient of variation of $N_{f\text{-}ave}$ is 0.095. The result of $N_{f\text{-}ave}$ has varied greatly.

3.3.1.2. Coupons on X-direction

(1) Influence of mold surface

The distance from mold surface to center of each coupon and number of PVA fiber ($N_{f\text{-}ave}$) relationship in Part A, B and C is shown in Figure 3.3.

The number of PVA fiber decreases with increase of the distance from mold surface. This result has same tendency described in Figure 2.9. Especially in Part C, the maximum moment increases after the distance from mold surface is around 150mm, as same as number of PVA fiber in Figure 3.3. Therefore, it can be recognized that the number of PVA fiber is related closely with the maximum moment for each coupon.

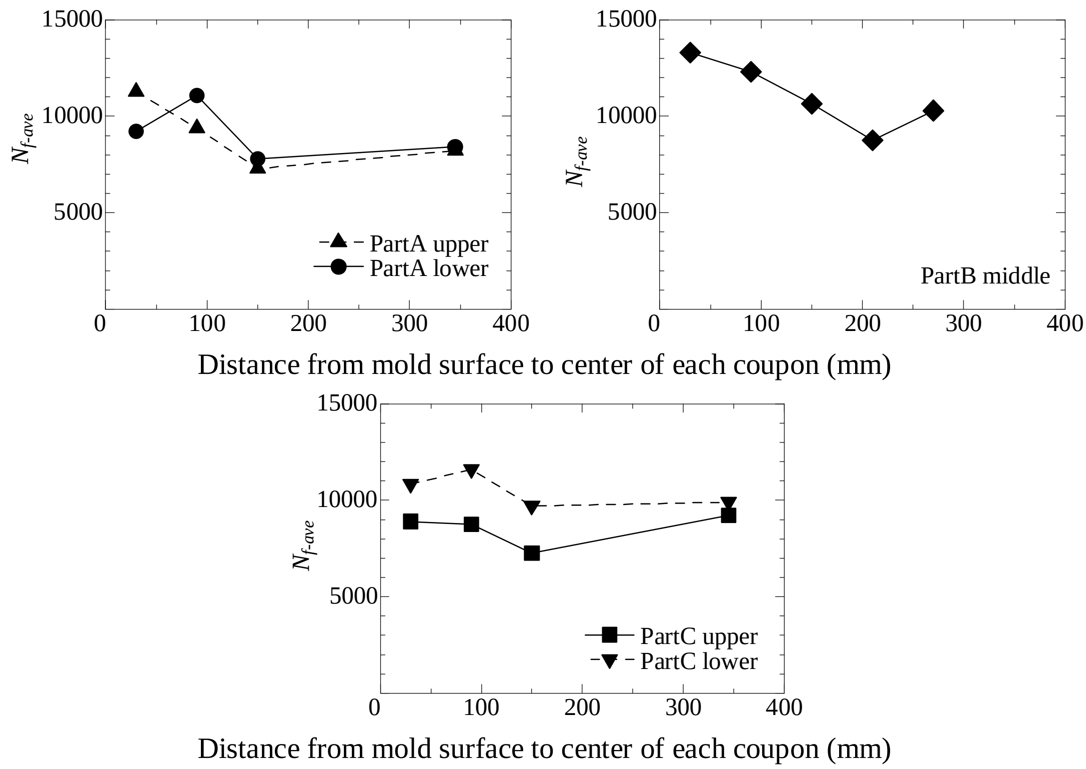

Figure 3.3 Number of PVA fiber ($N_{f,\text{-}ave}$) and distance from mold surface relationships

(2)　M_{max}, ϕ_{max} and number of PVA fiber relationships

The ratio of maximum moment (M_{max} / $M_{max,w}$), the ratio of curvature (ϕ_{max} / $\phi_{max,w}$) and the ratio of number of PVA fiber ($N_{f\text{-}ave}$ / $N_{f,w}$) relationships in Part A, B and C is shown in Figure 3.4.

The ratio is defined as that the maximum moment or curvature of each coupon is standardized by $M_{max,w}$ or $\phi_{max,w}$. The ratio of number of PVA fiber is same calculation as the ratio of maximum moment or curvature.

From Figure 3.4, higher ratio of maximum moment or curvature has higher ratio of number of PVA fiber basically. However, some results show that even if higher ratio of number of PVA fiber, the ratio of maximum moment or curvature has lower ratio at upper section in Part A and C especially in curvature. Furthermore, the ratio of maximum moment and curvature in upper section is lower than those in lower section at same position number. This result can be recognized that the influence of polishing and cleaning on cast surface in upper section is very large.

In Part B, the ratio of number of PVA fiber is larger than those in Part A and C in generally. It is said that Part B is the closest location to the cast place than another location such as Part A and C. Therefore, the PVA fiber will be concentrated around the center line of large specimens. In other hand, the ratio of maximum moment and curvature is little lower than the ratio in Part A and C even if the ratio of number of PVA fiber in Part B is higher than in Part A and C. It can be said that the influence of cutout surface affects the flexural performance also.

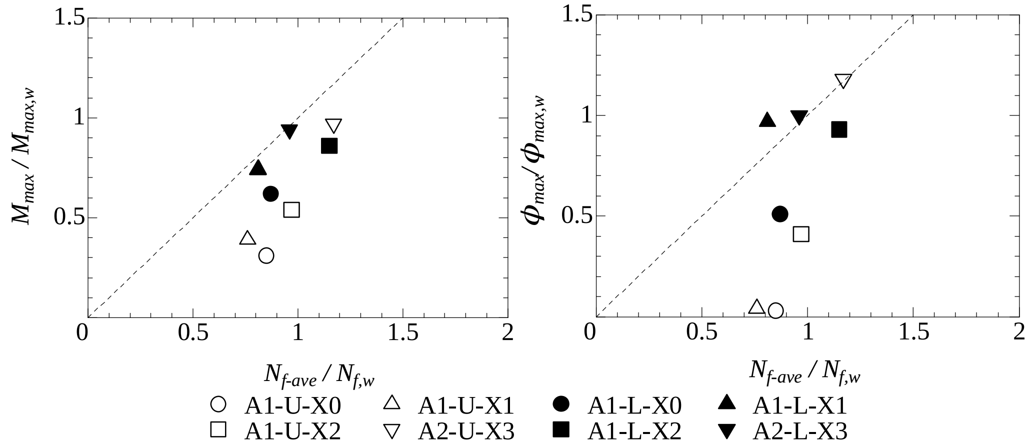

The ratio of M_{max} and $N_{f\text{-}ave}$ in Part A The ratio of ϕ_{max} and $N_{f\text{-}ave}$ in Part A

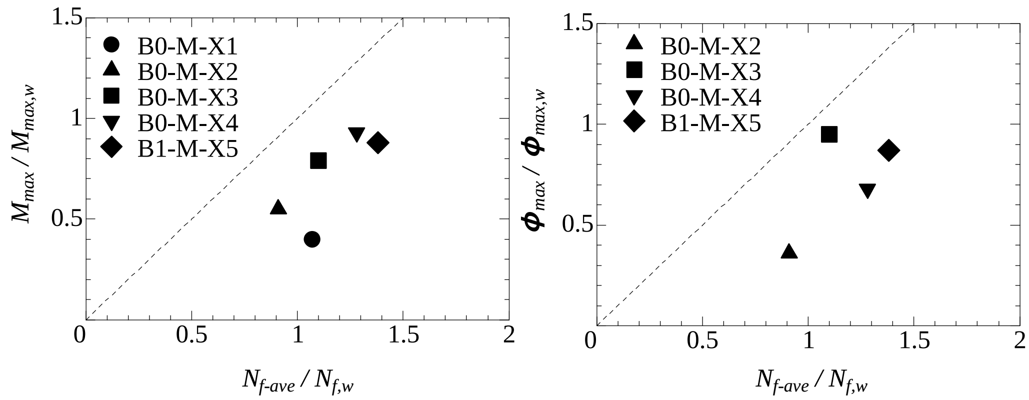

The ratio of M_{max} and $N_{f\text{-}ave}$ in Part B The ratio of ϕ_{max} and $N_{f\text{-}ave}$ in Part B

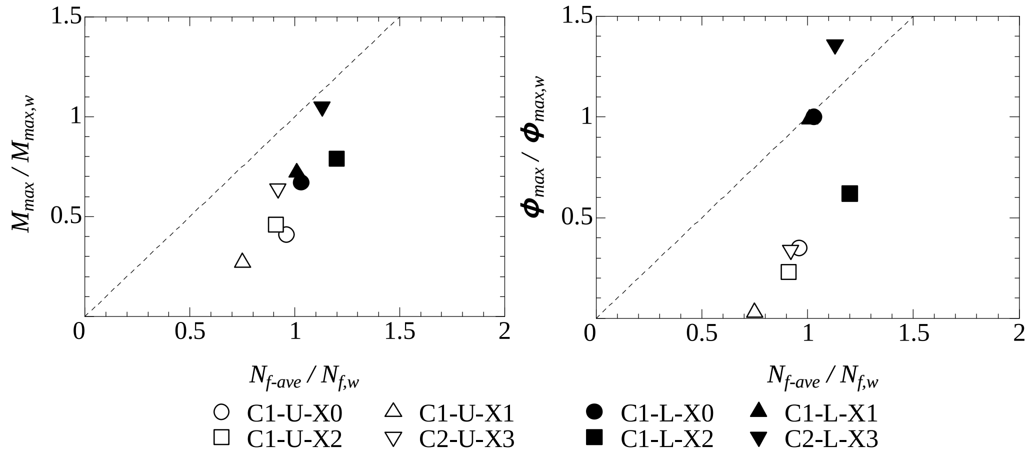

The ratio of M_{max} and $N_{f\text{-}ave}$ in Part C The ratio of ϕ_{max} and $N_{f\text{-}ave}$ in Part C

Figure 3.4 M_{max}, ϕ_{max} and $N_{f\text{-}ave}$ relationships on X-direction

3.3.1.3. Coupons on Y-direction

The ratio of maximum moment ($M_{max}/ M_{max,w}$), the ratio of curvature ($\phi_{max}/ \phi_{max,w}$) and the ratio of number of PVA fiber ($N_f/ N_{f,w}$) relationships on Y-direction in Part A, B and C is shown in Figure 3.5.

The number of PVA fiber of coupon on Y-direction is almost 2/3 of the average number of PVA fiber on prepared specimens and coupon on X-direction and the ratio of the maximum moment and curvature is lower than the ratio of the number of PVA fiber in general.

In Part A and C, the ratio of maximum moment and curvature on coupon in Part C is higher than that in Part A at same position number even if the ratio of number of PVA fiber is almost same in both Part A and C. Therefore, the influence of mold surface affects more than cast surface to flexural performance of HPFRCC.

In Part B, the ratio of maximum moment and curvature is too low so that PVA fiber is not bore the bending, therefore, it does not affect flexural performance on coupons at Part B directly.

In these result, it is said that the PVA fiber is orientated at axial direction more than at perpendicular direction of loading in coupons on Y-direction.

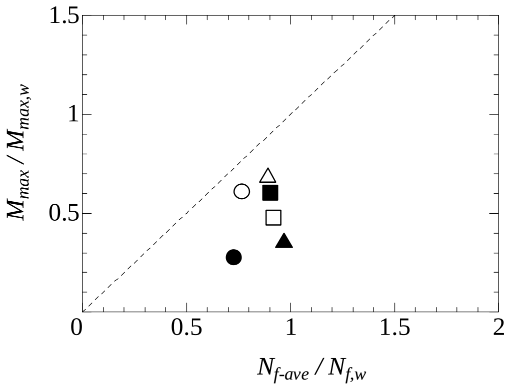

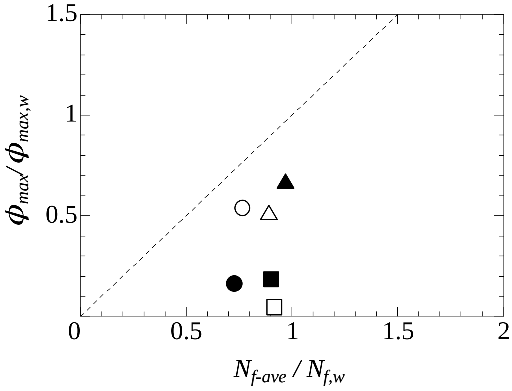

○ A1-U-Y1 △ A1-U-Y2 □ A2-U-Y3 ● A1-L-Y1 ▲ A1-L-Y2 ■ A2-L-Y3

The ratio of M_{max} and $N_{f\text{-}ave}$ in Part A

The ratio of ϕ_{max} and $N_{f\text{-}ave}$ in Part A

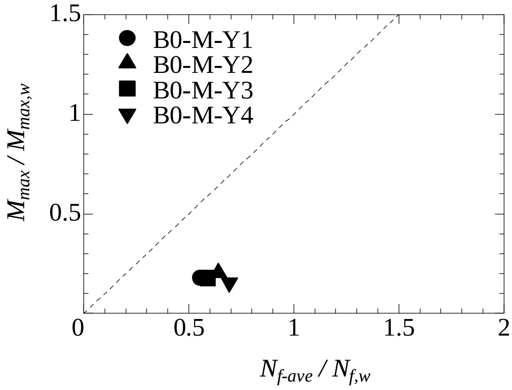

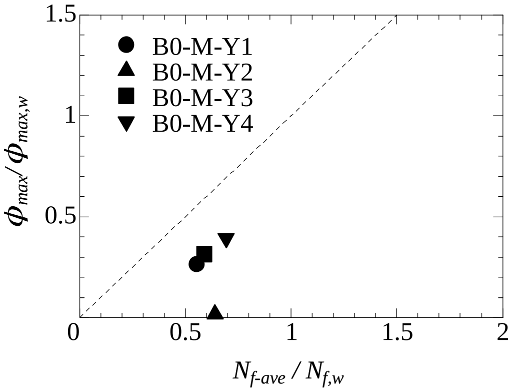

The ratio of M_{max} and $N_{f\text{-}ave}$ in Part B

The ratio of ϕ_{max} and $N_{f\text{-}ave}$ in Part B

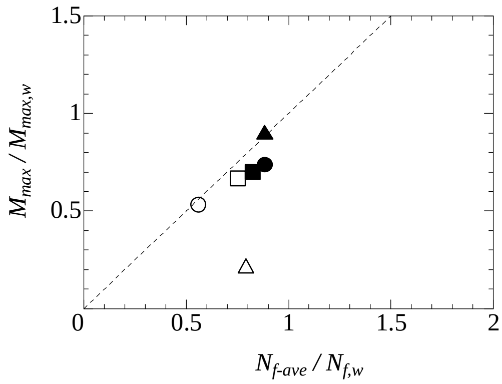

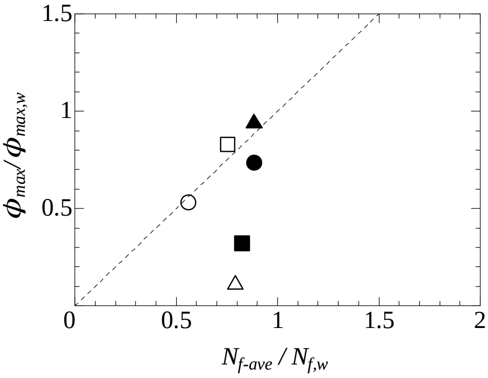

○ C1-U-Y1 △ C1-U-Y2 □ C2-U-Y3 ● C1-L-Y1 ▲ C1-L-Y2 ■ C2-L-Y3

The ratio of M_{max} and $N_{f\text{-}ave}$ in Part C

The ratio of ϕ_{max} and $N_{f\text{-}ave}$ in Part C

Figure 3.5 M_{max}, ϕ_{max} and $N_{f\text{-}ave}$ relationships on Y-direction

3.3.2. *Specimens with 2.0% volume fraction of fibers*

The list of experimental result of specimens and coupons with 2.0% volume fraction of fibers is shown in Table 3.2.

Table 3.2 Experimental Result of specimens and coupons with 2.0% volume fraction of fibers

ID	$N_{f\text{-}A}$	$N_{f\text{-}B}$	$N_{f\text{-}ave}$	$N_{f\text{-}ave}$ / $N_{f,w}$	M_{max} / $M_{max,w}$	ϕ_{max} / $\phi_{max,w}$
2.0-1	10614	11238	10926	$N_{f,w}$ = 10678	$M_{max,w}$ = 0.422 kN•m	$\phi_{max,w}$ = 0.257 1/m
2.0-2	9884	8224	9054			
2.0-3	9899	8600	9250			
2.0-4	10156	12768	11462			
2.0-5	13377	12019	12698			
2.0A1-U-X0	6036	4262	5149	0.482	0.367	0.117
2.0A1-U-X1	6858	9017	7938	0.743	0.365	0.661
2.0A1-U-X2	9205	7825	8515	0.797	0.697	0.459
2.0A2-U-X3	9174	9019	9097	0.852	0.810	0.957
2.0A1-U-Y1	7576	11127	9352	0.876	0.652	0.728
2.0A1-U-Y2	10103	8268	9186	0.860	0.841	1.307
2.0A2-U-Y3	8859	9705	9282	0.869	0.749	1.241
2.0A1-L-X0	11105	8692	9899	0.927	0.581	0.381
2.0A1-L-X1	10386	8773	9580	0.897	0.628	1.167
2.0A1-L-X2	9418	7942	8680	0.813	0.765	1.257
2.0A2-L-X3	10576	8430	9503	0.890	0.787	0.716
2.0A1-L-Y1	12370	12115	12243	1.147	0.332	0.669
2.0A1-L-Y2	9584	10964	10274	0.962	0.865	1.179
2.0A2-L-Y3	7289	9732	8511	0.797	0.998	1.759
2.0B0-M-X1	9886	12053	10970	1.027	0.659	1.187
2.0B0-M-X2	9712	9127	9420	0.882	0.635	0.401
2.0B0-M-X3	10497	9728	10113	0.947	0.886	0.860
2.0B0-M-X4	11451	11050	11251	1.054	0.851	0.767
2.0B1-M-X5	9407	10551	9979	0.935	0.889	1.214
2.0B0-M-Y1	9557	10943	10250	0.960	0.206	0.054
2.0B0-M-Y2	7202	8877	8040	0.753	0.322	0.661
2.0B0-M-Y3	5959	5145	5552	0.520	0.213	0.016
2.0B0-M-Y4	5497	9069	7283	0.682	0.190	0.019
2.0C1-U-X0	7685	7909	7797	0.730	0.351	0.101
2.0C1-U-X1	8745	9036	8891	0.833	0.460	0.296
2.0C1-U-X2	8188	11612	9900	0.927	0.773	0.802
2.0C2-U-X3	10434	8089	9262	0.867	0.737	1.381
2.0C1-U-Y1	9079	8486	8783	0.822	0.673	0.634
2.0C1-U-Y2	10593	10473	10533	0.986	0.803	1.136
2.0C2-U-Y3	12321	10815	11568	1.083	0.806	1.047
2.0C1-L-X0	7582	7998	7790	0.730	0.536	0.992
2.0C1-L-X1	10254	6886	8570	0.803	0.590	1.047
2.0C1-L-X2	9360	12029	10695	1.002	0.706	0.514
2.0C2-L-X3	9181	9427	9304	0.871	0.829	1.210
2.0C1-L-Y1	6302	11225	8764	0.821	0.635	0.774
2.0C1-L-Y2	7363	8395	7879	0.738	0.590	1.051
2.0C2-L-Y3	9892	8113	9003	0.843	0.867	1.012

3.3.2.1. Prepared Specimens

The average number of PVA fiber of five prepared specimens' $N_{f\text{-}ave}$ is 10678. In addition, the standard deviation of $N_{f\text{-}ave}$ is 1373.54 and the coefficient of variation is 0.129. The result of $N_{f\text{-}ave}$ has varied greatly.

3.3.2.2. Coupons on X-direction

(1) Influence of mold surface

The distance from mold surface to center of each coupon and number of PVA fiber ($N_{f\text{-}ave}$) relationship in Part A, B and C is shown in Figure 3.6.

In Part A, the number of PVA fiber decrease with increase of the distance from mold surface at upper section, meanwhile, the number of PVA fiber is almost same at lower section. In addition, the number of PVA fiber on coupon at lower section is larger than those in upper section.

In Part B and C, the number of PVA fiber in coupon at upper section is almost equal to those at lower section and the average number of PVA fiber of five prepared specimens, 10678.

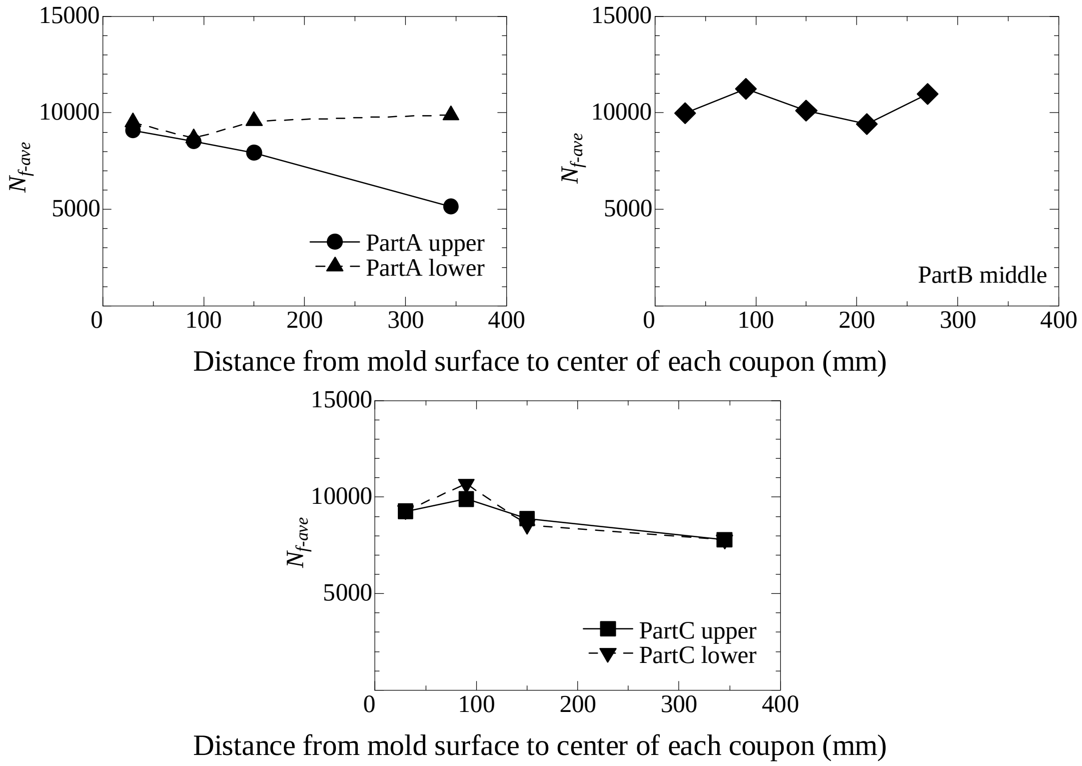

Figure 3.6 Number of PVA fiber ($N_{f,\text{-}ave}$) and distance from mold surface relationships

(2) M_{max}, ϕ_{max} and number of PVA fiber relationships

The ratio of maximum moment (M_{max}/ $M_{max,w}$), the ratio of curvature (ϕ_{max}/ $\phi_{max,w}$) and the ratio of number of PVA fiber ($N_{f\text{-}ave}$/ $N_{f,w}$) relationships on X-direction in Part A, B and C is shown in Figure 3.7.

In Part A, the ratio of maximum moment is almost same as the ratio of number of PVA fiber. In addition, the ratio of maximum moment and curvature on coupon in lower section is higher than those in upper section on same position number. It is same tendency as coupons with 1.5% volume fraction of fibers.

In Part B, the ratio of maximum moment on coupon increases with increase of the position number even if the ratio of number of PVA fiber is almost same. The result of ratio of curvature has varied greatly even if the ratio of number of PVA fiber is almost same.

In Part C, the ratio of maximum moment and curvature of coupon at upper section is lower than those at lower section at same position number. Especially in the result of rate of curvature and number of PVA fiber relationships, coupons in lower section, the ratio of curvature has high rate.

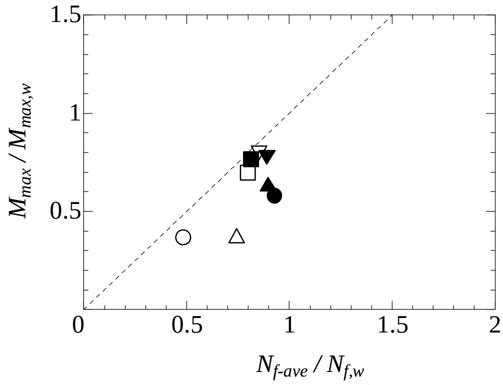

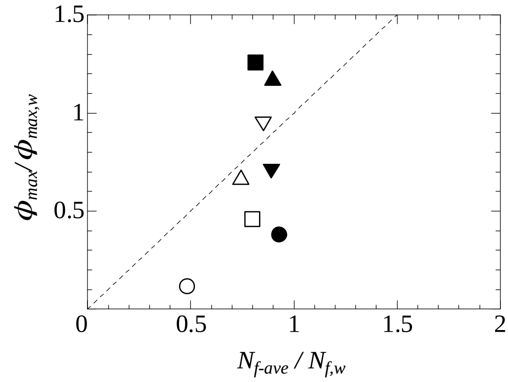

○ 2.0A1-U-X0 △ 2.0A1-U-X1 ● 2.0A1-L-X0 ▲ 2.0A1-L-X1
□ 2.0A1-U-X2 ▽ 2.0A2-U-X3 ■ 2.0A1-L-X2 ▼ 2.0A2-L-X3

The ratio of M_{max} and $N_{f\text{-}ave}$ in Part A The ratio of ϕ_{max} and $N_{f\text{-}ave}$ in Part A

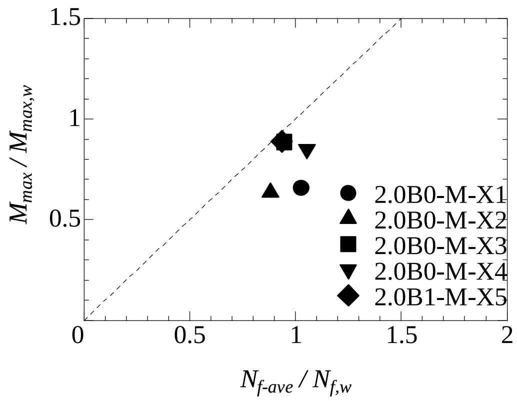

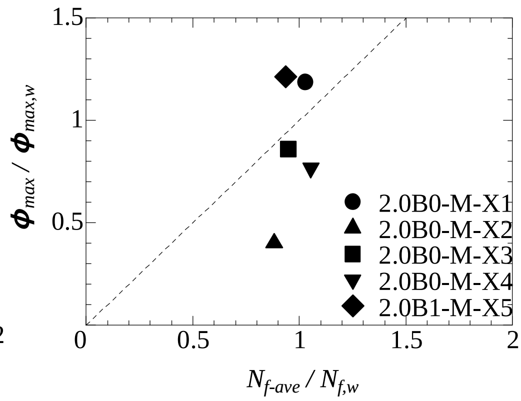

The ratio of M_{max} and $N_{f\text{-}ave}$ in Part B The ratio of ϕ_{max} and $N_{f\text{-}ave}$ in Part B

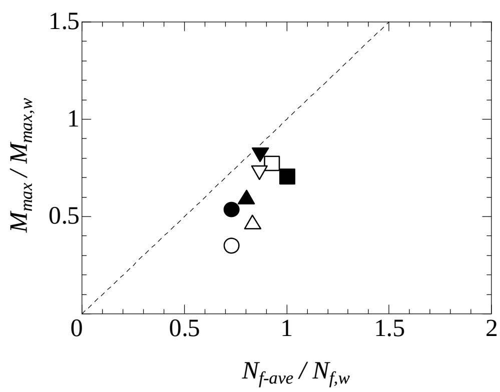

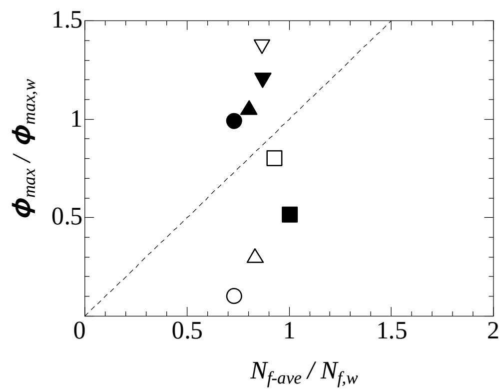

○ 2.0C1-U-X0 △ 2.0C1-U-X1 ● 2.0C1-L-X0 ▲ 2.0C1-L-X1
□ 2.0C1-U-X2 ▽ 2.0C2-U-X3 ■ 2.0C1-L-X2 ▼ 2.0C2-L-X3

The ratio of M_{max} and $N_{f\text{-}ave}$ in Part C The ratio of ϕ_{max} and $N_{f\text{-}ave}$ in Part C

Figure 3.7 M_{max}, ϕ_{max} and $N_{f\text{-}ave}$ relationships on X-direction

3.3.2.3. Coupons on Y-direction

The ratio of maximum moment (M_{max}/ $M_{max,w}$), the ratio of curvature (ϕ_{max}/ $\phi_{max,w}$) and the ratio of number of PVA fiber ($N_{f\text{-}ave}$/ $N_{f,w}$) relationships on Y-direction in Part A, B and C is shown in Figure 3.8.

In Part A, the result of the ratio of curvature has varied widely even if the ratio of number of PVA fiber is almost same.

In Part B, the result of the ratio of maximum moment and curvature are too low. The reason why ratios are too low is that the deflection hardening behavior did not occur so that the flexural performance of coupon is too low. Therefore, it is considered that PVA fiber in coupons is oriented and distributed more on axial direction than on perpendicular direction on loading.

In Part C, the ratio of number of PVA fiber in upper section is higher than those in lower section even if the ratio of maximum moment and curvature is same in generally. Therefore, PVA fiber is distributed at upper section is more than those at lower section; however, it does not affect the flexural performance on Y-direction directly.

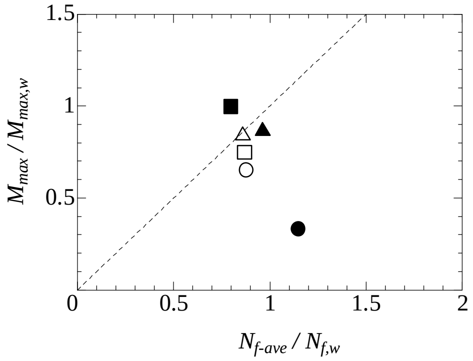

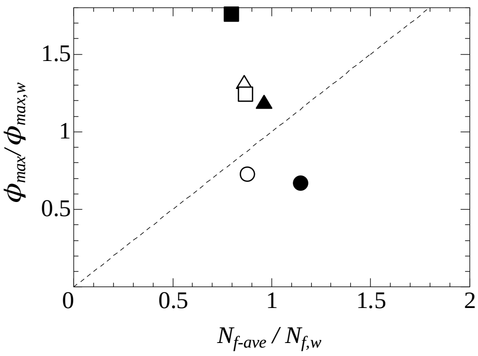

○ 2.0A1-U-Y1 △ 2.0A1-U-Y2 □ 2.0A2-U-Y3 ● 2.0A1-L-Y1 ▲ 2.0A1-L-Y2 ■ 2.0A2-L-Y3

The ratio of M_{max} and $N_{f\text{-}ave}$ in Part A

The ratio of ϕ_{max} and $N_{f\text{-}ave}$ in Part A

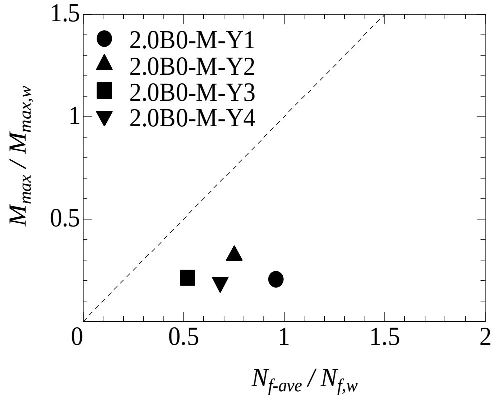

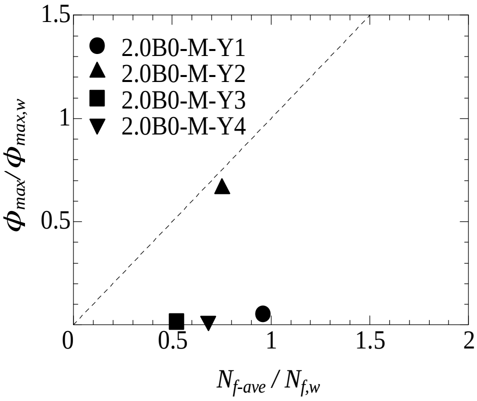

The ratio of M_{max} and $N_{f\text{-}ave}$ in Part B

The ratio of ϕ_{max} and $N_{f\text{-}ave}$ in Part B

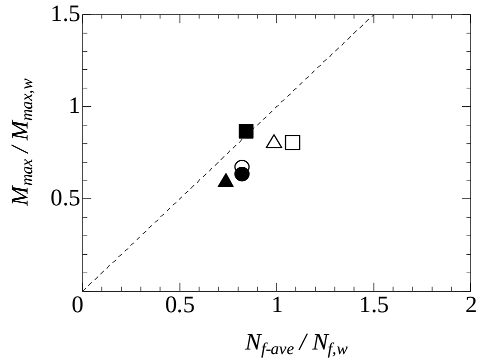

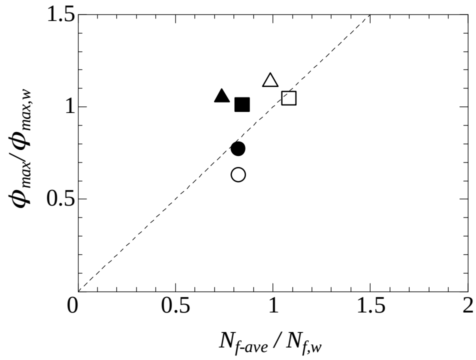

○ 2.0C1-U-Y1 △ 2.0C1-U-Y2 □ 2.0C2-U-Y3 ● 2.0C1-L-Y1 ▲ 2.0C1-L-Y2 ■ 2.0C2-L-Y3

The ratio of M_{max} and $N_{f\text{-}ave}$ in Part C

The ratio of ϕ_{max} and $N_{f\text{-}ave}$ in Part C

Figure 3.8 M_{max}, ϕ_{max} and $N_{f\text{-}ave}$ relationships on Y-direction

3.4. Comparison and Discussion

In this chapter 3, the cross section of prepared specimens and coupons are observed to obtain how the fiber will be orientated and distributed by using the mercury lamp.

The rate of the maximum bending moment and curvature at coupons from lower section is higher that those from upper section at same position number. Also, some results show that the ratio of maximum bending moment and curvature is too low. Therefore, the influence of PVA fiber on cast and cutout surface is little than those on mold surface because a PVA fiber is cut by cutting and polishing on the surface.

To comparison between coupon with 1.5% and 2.0% of fiber volume, the number of PVA fiber on prepared specimens with 1.5% volume fraction of fibers is smaller than those with 2.0% volume fraction of fibers, however, the large difference at the number of PVA fiber in coupons is not seen clearly.

In the ratio of the maximum bending moment or curvature and the number of fiber relationships, the difference between upper and lower section at the ratio of the maximum bending moment and curvature on coupon with 1.5% volume fraction of fibers is bigger than those with 2.0% volume fraction of fibers.

In the coupons on Y-direction, the ratio of maximum bending moment and curvature on coupons with 1.5% volume fraction of fibers is lower than those with 2.0% volume fraction of fibers because the deflection hardening behavior is recognized at coupon with 2.0% volume fraction of fibers on Y-direction.

CHAPTER 4 THE INFLUENCE OF SURFACE

4.1. Introduction

In chapter 2, four-point bending test has been examined and achieved the results that the flexural performance of coupons in upper section is lower than those in lower section and coupons at Part B is lower than another parts such as A and C. Moreover, in chapter 3, the ratio of maximum moment and curvature of coupon at upper section is lower than the ratio of number of PVA fiber at lower section in generally.

Cast surface of coupon in upper section is polished by grinder machine before bending test is applied. In addition, whole surface of coupons at Part B are cutout.

In these result, it can be thought that the influence of polishing and cutout is related to the flexural performance closely. Therefore, in this chapter, specimens of HPFRCC, those are polished, are prepared and examined to know how the polishing affects the flexural performance of HPFRCC by the bending test.

4.2. Mix Proportion

The mechanical characteristic of PVA fiber and the mix proportion of HPFRCC are same as in chapter 2. In addition, the manufacturer and brand name of materials of HPFRCC is used as same as described in chapter 2. However, for HPFRCC with 2.0% volume fraction of fibers, the unit quantity of PVA fiber is 26.00 kg/m^3.

4.3. Outline of Specimens

The outline of specimen for HPFRCC is shown in Figure 4.1. Final size of specimen is 60mm in depth, 60mm in width and 350mm in length that is same as coupons in chapter 2. The thickness of polishing is defined as X mm as shown in Figure 4.1 and all X, described in Figure 4.1, are same. Therefore, specimens of HPFRCC are prepared as the cross section of 60mm x 60mm with increase in thickness of 2X mm in depth and width, and then prepared specimens will be polished and resized to the final size by grinder machine.

The list of specimens is shown in Table 4.1. 5 types of specimens, that is 0mm of thickness is assumed as prepared specimens, 1mm is assumed as the polishing on surface only, 7mm is the half of PVA fiber length, 13mm is the length of PVA fiber and 25mm is the length as twice as the fiber length, are prepared as HPFRCC.

6 specimens are prepared as HPFRCC for each size. 3 out of 6 specimens are HPFRCC with 1.5% volume fraction of fibers and the others are with 2.0% volume fraction of fibers. Therefore, each number of specimens with 1.5% and 2.0% volume fraction of fibers is 15 and total number of specimens is 30.

HPFRCC with 1.5% and 2.0% volume fraction of fibers is mixed with a mortar mixer and specimens are left in atmospheric curing with damp towel for 1st week and polished and resized to 60mm x 60mm of cross section after 2nd week, and then the bending test is performed at 4th week.

In addition, an example of mold, which is 3 specimens for 86mm x 86mm x 350mm, is shown in Picture 4.1.

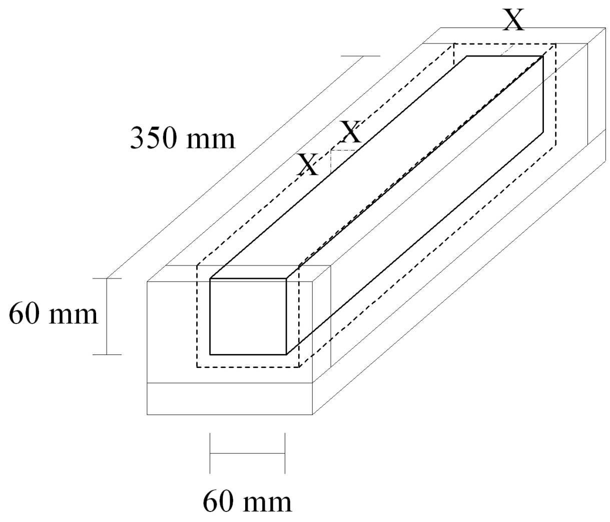

Figure 4.1 Outline of specimen

Table 4.1 The list of specimens

Thickness X (mm)	Size of cross section for cast 60 + 2X (mm)	Working method	Number of specimen
0	60	No polishing	6
1	62	Surface polishing	6
7	74	Polishing	6
13	86	Polishing and cutout	6
25	110	Polishing and cutout	6

Picture 4.1 The mold of 3 specimens for 86mm x 86mm x 350mm

4.4. Specimen Identification

The identification of specimens is shown in Figure 4.2.

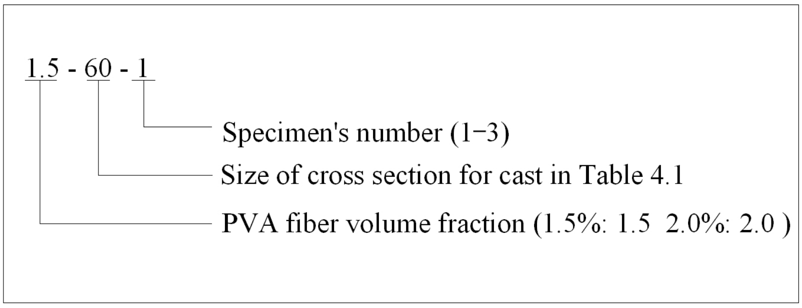

Figure 4.2 Identification of specimens

4.5. Outline of Bending Test

Four-point bending that is same as described in chapter 2 is applied by using 2MN universal testing machine. Machine head is applied the load continuously without shock at a constant rate of 0.5mm per minute.

The bending moment and curvature is calculated by using equation (2.1) and (2.2) to obtain the bending moment - curvature curve.

4.6. Experimental Result

The list of experimental result is shown in Table 4.2. To obtain M_{max}, M_u, ϕ_{max}, ϕ_u, σ_{max}, σ_u, ϕ_{max} and ϕ_u, it is also same calculation as described in chapter 2.

To obtain tensile strain and tensile strength, static modulus of elasticity (E) has been used. For these results, 11.15 GPa is used for specimens with 1.5% volume fraction of fibers and 10.41 GPa for 2.0% volume fraction of fibers.

In addition, the list of averaged experimental result is shown in Table 4.3. $M_{max\text{-}ave}$, $M_{u\text{-}ave}$, $\phi_{max\text{-}ave}$, $\phi_{u\text{-}ave}$, $\sigma_{max\text{-}ave}$, $\sigma_{u\text{-}ave}$, $\phi_{max\text{-}ave}$ and $\phi_{u\text{-}ave}$ are the average at 3 same size specimens of M_{max}, M_u, ϕ_{max}, ϕ_u, σ_{max}, σ_u, ϕ_{max} and ϕ_u, respectively.

In addition, the detailed data of specimens is shown in Appendix: C and the detailed data for compressive test is shown in Appendix: B.

Table 4.2 The list of experimental result

ID	M_{max} (kN・m)	M_u (kN・m)	ϕ_{max} (1/m)	ϕ_u (1/m)	σ_{max} (N/mm^2)	σ_u (N/mm^2)	ε_{max} (%)	ε_u (%)
1.5-60-1	0.328	0.304	0.327	0.439	3.299	2.990	1.676	2.321
1.5-60-2	0.313	0.293	0.551	0.669	3.032	2.806	2.955	3.646
1.5-60-3	0.338	0.329	0.634	0.664	3.399	3.297	3.358	3.533
1.5-62-1	0.351	0.324	1.095	1.443	3.644	3.324	5.863	7.858
1.5-62-2	0.210	0.180	0.205	0.505	2.401	1.941	0.996	2.660
1.5-62-3	0.187	0.100	0.129	0.312	2.211	1.078	0.597	1.638
1.5-74-1	0.241	0.241	0.060	0.060	2.880	2.880	0.251	0.251
1.5-74-2	0.264	0.216	0.416	0.803	2.826	2.228	2.095	4.261
1.5-74-3	0.292	0.290	0.446	0.502	2.946	2.907	2.330	2.646
1.5-86-1	0.207	0.157	0.233	0.238	2.141	1.596	1.187	1.242
1.5-86-2	0.182	0.143	0.107	0.309	2.195	1.571	0.484	1.584
1.5-86-3	0.184	0.156	0.174	0.337	2.082	1.680	0.841	1.742
1.5-110-1	0.284	0.284	0.338	0.338	3.105	3.105	1.678	1.678
1.5-110-2	0.280	0.257	0.374	0.529	2.995	2.687	1.885	2.752
1.5-110-3	0.270	0.237	0.321	0.371	2.882	2.489	1.612	1.905
2.0-60-1	0.350	0.346	0.711	0.803	3.373	3.315	3.825	4.355
2.0-60-2	0.324	0.309	0.675	0.874	3.099	2.918	3.626	4.779
2.0-60-3	0.324	0.324	0.695	0.715	3.199	3.195	3.694	3.807
2.0-62-1	0.271	0.271	0.525	0.525	2.829	2.829	2.758	2.758
2.0-62-2	0.304	0.304	0.686	0.686	3.084	3.084	3.651	3.651
2.0-62-3	0.300	0.299	0.278	0.506	3.361	3.219	1.340	2.576
2.0-74-1	0.321	0.321	1.013	1.013	3.399	3.399	5.384	5.384
2.0-74-2	0.285	0.277	0.498	0.522	2.965	2.871	2.575	2.714
2.0-74-3	0.305	0.291	0.452	0.906	3.384	3.113	2.244	4.732
2.0-86-1	0.361	0.361	1.026	1.026	3.840	3.840	5.382	5.382
2.0-86-2	0.310	0.307	0.412	0.600	3.458	3.349	2.019	3.032
2.0-86-3	0.358	0.356	1.135	1.263	3.744	3.708	6.037	6.758
2.0-110-1	0.368	0.360	1.169	1.202	3.785	3.696	6.169	6.360
2.0-110-2	0.252	0.192	0.412	1.037	2.649	1.925	2.126	5.720
2.0-110-3	0.291	0.261	0.464	1.167	3.207	2.751	2.335	6.252

Table 4.3 The list of the averaged experimental result

ID	$M_{max\text{-}ave}$ (kN・m)	$M_{u\text{-}ave}$ (kN・m)	$\phi_{max\text{-}ave}$ (1/m)	$\phi_{u\text{-}ave}$ (1/m)	$\sigma_{max\text{-}ave}$ (N/mm^2)	$\sigma_{u\text{-}ave}$ (N/mm^2)	$\varepsilon_{max\text{-}ave}$ (%)	$\varepsilon_{u\text{-}ave}$ (%)
1.5-60	0.326	0.309	0.504	0.591	3.243	3.031	2.663	3.167
1.5-62	0.249	0.201	0.476	0.753	2.752	2.114	2.458	4.052
1.5-74	0.266	0.249	0.307	0.455	2.884	2.672	1.559	2.386
1.5-86	0.191	0.152	0.171	0.295	2.139	1.616	0.837	1.523
1.5-110	0.278	0.259	0.344	0.413	2.994	2.760	1.725	2.112
2.0-60	0.333	0.326	0.694	0.797	3.224	3.143	3.715	4.314
2.0-62	0.292	0.291	0.496	0.572	3.091	3.044	2.583	2.995
2.0-74	0.304	0.296	0.654	0.814	3.250	3.128	3.401	4.276
2.0-86	0.343	0.341	0.858	0.963	3.681	3.632	4.480	5.057
2.0-110	0.304	0.271	0.682	1.135	3.214	2.790	3.543	6.111

4.6.1. Bending moment-curvature curve relationships of specimens

(1) Specimens with 1.5% volume fraction of fibers

The result of bending moment - curvature curve relationships of specimens with 1.5% volume fraction of fibers is shown in Figure 4.3.

The deflection hardening behavior is recognized well and the multiple cracks occur in pure bending span in generally so that the bending moment - curvature curve is shown almost same results at same type of specimens.

In other hand, specimens in cross section with 62mm x 62mm, the result of bending moment and curvature curve has vary widely. The reason why only the result of specimens in cross section with 62mm x 62mm has vary widely is that the cracks is occurred with 1 or 2 in pure bending span at specimens of 1.5-62-2 and 1.5-62-3. Therefore, the flexural performance of specimens with a few cracks shows lower ductility than those with multiple cracks.

In specimens, 1.5-74-1, with 74mm x 74mm, the largest crack occurs outside of pure bending span so that the ductility of the specimens is recognized as a little.

(2) Specimens with 2.0% volume fraction of fibers

The result of bending moment – curvature curve relationships of specimens with 2.0% volume fraction of fibers is shown in Figure 4.4.

The deflections hardening behavior is also recognized well and the multiple cracks occur in pure bending span at all specimens so that the bending moment and curvature curve shows almost same results at same type of specimens.

At specimens with 110mm x 110mm, some difference is shown in the result of bending moment – curvature curve relationships. Therefore, it is considered that the influence of the polishing has some to the ductility of specimens because the deflection hardening behavior and multiple cracks are recognized at 3 specimens with 110mm x 110mm.

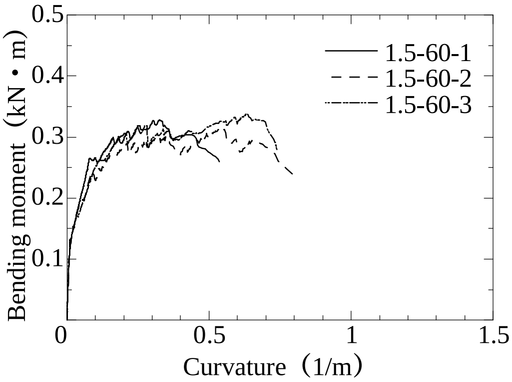

Specimens with 60mm x 60mm

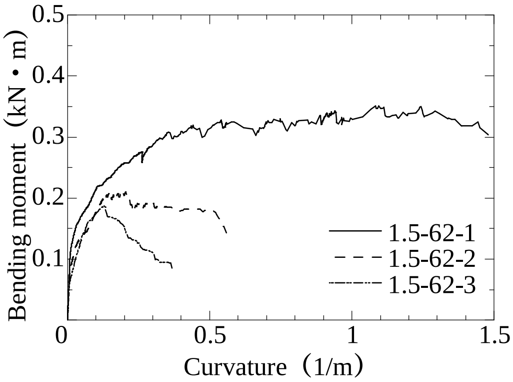

Specimens with 62mm x 62mm

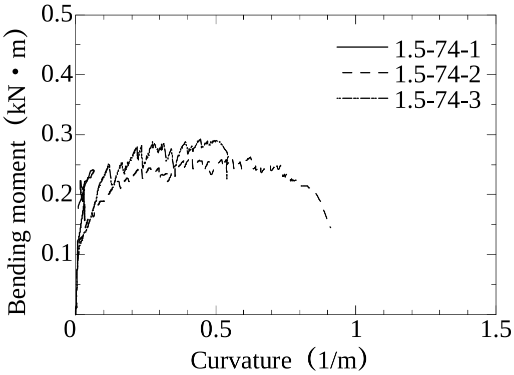

Specimens with 74mm x 74mm

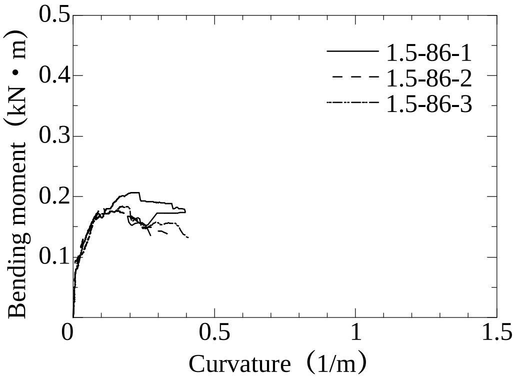

Specimens with 86mm x 86mm

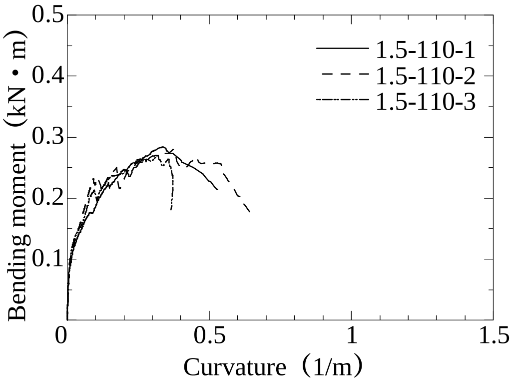

Specimens with 110mm x 110mm

Figure 4.3 Bending moment – curvature curve relationships of specimens with 1.5%

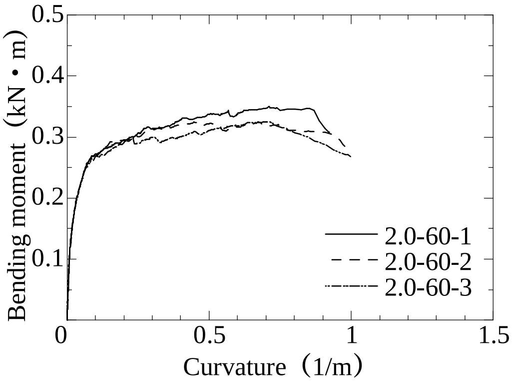

Specimens with 60mm x 60mm

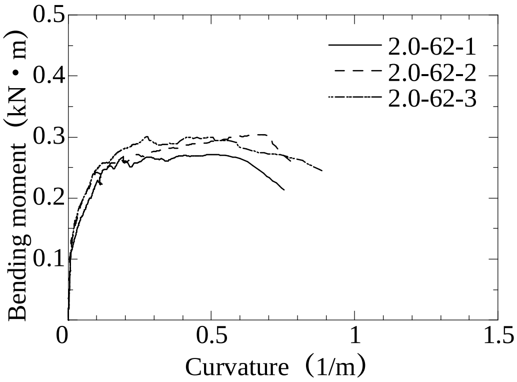

Specimens with 62mm x 62mm

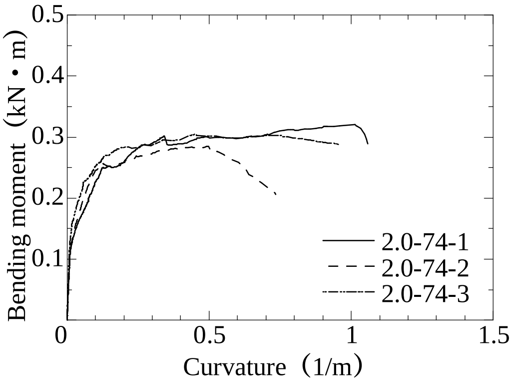

Specimens with 74mm x 74mm

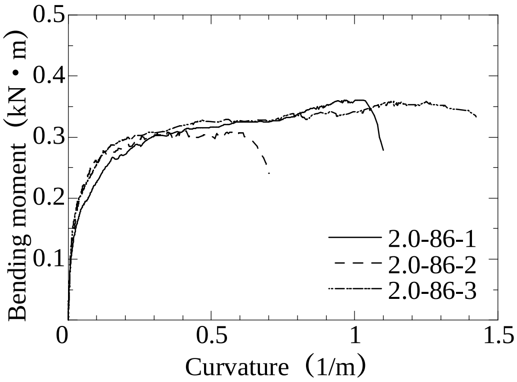

Specimens with 86mm x 86mm

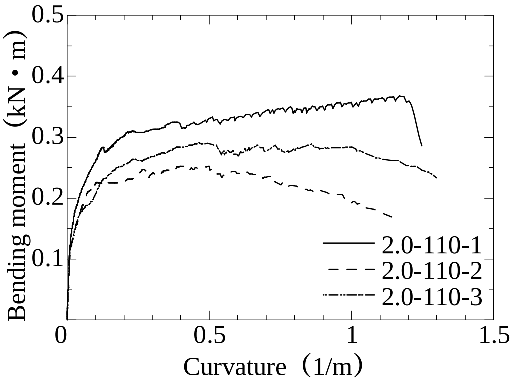

Specimens with 110mm x 110mm

Figure 4.4 Bending moment – curvature curve relationships of specimens with 2.0%

4.6.2. The thickness of polishing and the averaged data relationships

(1) Specimens with 1.5% volume fraction of fibers

The averaged data and the thickness of polishing relationships with 1.5% volume fraction of fibers are shown in Figure 4.5.

The averaged curvature and tensile strain decrease with increase of the thickness of polishing in generally.

For the result of the averaged maximum moment and tensile stress, the maximum bending moment increases at around 25mm of the thickness of polishing, however, the maximum bending moment decreases with increase of thickness of polishing totally. The maximum bending moment decreases up to 50% by compared with the prepared specimens which are 0mm of the thickness polishing.

In these result, the influence of polishing is related to the flexural performance of specimens with 1.5% volume fraction of fibers. Therefore, the influence of cast, mold and cutout surface is related to the flexural performance to specimens with 1.5% volume fraction of fibers also.

(2) Specimens with 2.0% volume fraction of fibers

The averaged data and the thickness of polishing relationships with 2.0% volume fraction of fibers are shown in Figure 4.6.

For the result of the averaged curvature and tensile stain, the curvature decreases around 1mm of the thickness of polishing once, and then, increases with increase of the thickness of polishing.

For the result of the averaged maximum bending moment and tensile stress, the result is almost same at any thickness of polishing in specimens with 2.0% volume fraction of fibers.

In these result, the influence of polishing and cutout is not related to the flexural performance of the specimens with 2.0% volume fraction of fibers directly.

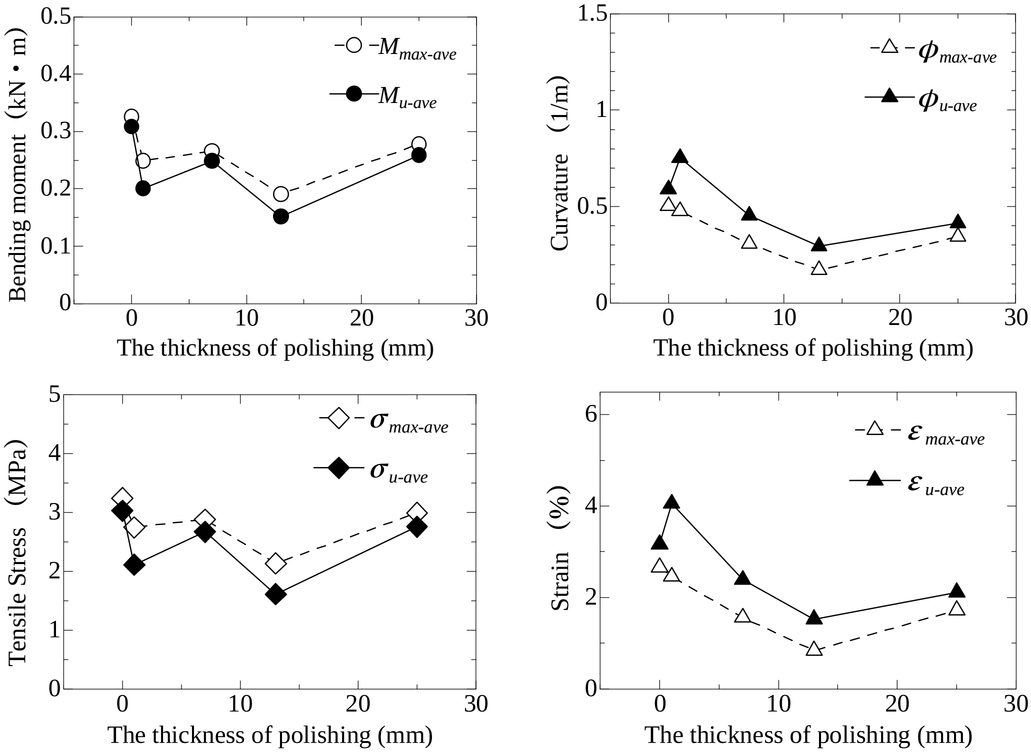

Figure 4.5 The averaged data and the thickness of polishing relationships with 1.5%

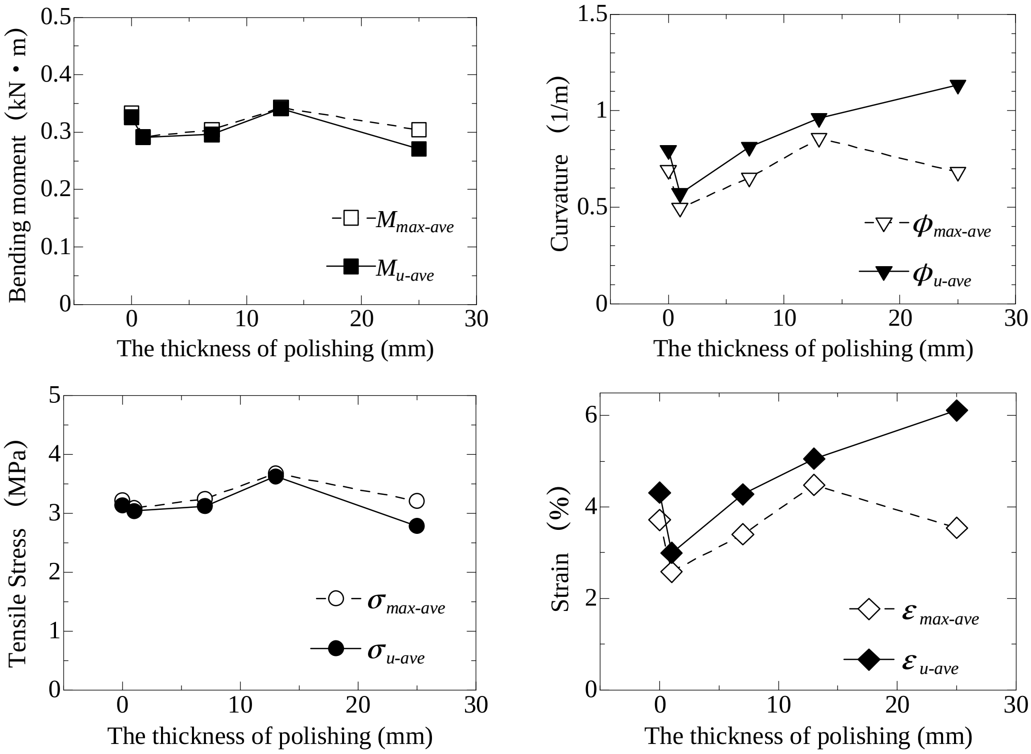

Figure 4.6 The averaged data and the thickness of polishing relationships with 2.0%

4.7. Comparison and Discussion

In this chapter 4, specimens of HPFRCC, those are polished, are prepared and examined to know how the polishing affects the flexural performance of HPFRCC by the bending test.

In this result, the flexural performance of specimens with 1.5% volume fraction of fibers decreases with increase of the thickness of polishing. In other hand, the flexural performance of specimens with 2.0% volume fraction of fibers is not influenced by the thickness of polishing.

To compare the result of coupon between 1.5% and 2.0% volume fraction of fibers, the maximum moment and curvature of specimens with 1.5% volume fraction of fibers is lower than those with 2.0% volume fraction of fibers.

CHAPTER 5 SUMMARY FOR ALL CHPATERS

5.1. Experimental result

Since the flexural performance of HPFRCC in Part A is same as those in Part C at same position number as described in chapter 2, the maximum bending moment and number of fiber is averaged. The list of averaged results of coupons is shown in Table 5.1. Position number is described in chapter 2. The average of coupons on same position number of both upper and lower section in Part A and C is defined as total average, the average of coupons on same position number at upper section in Part A and C is defined as upper section and the average of coupons on same position number at lower section in Part A and C is defined as lower section.

Table 5.1 The list of averaged results of coupons

1.5% volume fraction of fibers								
Position number		X0	X1	X2	X3	Y1	Y2	Y3
M_{max} (kN・m)	Total average	0.203	0.215	0.267	0.364	0.219	0.216	0.248
	Upper section	0.145	0.135	0.202	0.325	0.232	0.180	0.232
	Lower section	0.261	0.296	0.333	0.404	0.206	0.252	0.265
$N_{f\text{-}ave}$	Total average	8936	8010	10204	10065	7076	8519	8728
	Upper section	8715	7271	9072	10096	6390	8111	9135
	Lower section	9157	8750	11335	10034	7763	8928	8321

2.0% volume fraction of fibers								
Position number		X0	X1	X2	X3	Y1	Y2	Y3
M_{max} (kN・m)	Total average	0.194	0.216	0.310	0.334	0.242	0.327	0.361
	Upper section	0.152	0.174	0.310	0.327	0.280	0.347	0.328
	Lower section	0.236	0.257	0.311	0.341	0.204	0.307	0.394
$N_{f\text{-}ave}$	Total average	7659	8745	9448	9292	9786	9468	9591
	Upper section	6473	8415	9208	9180	9068	9860	10425
	Lower section	8845	9075	9688	9404	10504	9077	8757

5.1.1. HPFRCC with 1.5% volume fraction of fibers

The relationship between the averaged maximum bending moment and distance from mold surface to center of each coupon is shown at left side of Figure 5.1 and the relationships between the averaged number of PVA fibers and the distance from mold surface to center of each coupon is shown at right side of Figure 5.1. The distance from mold surface to center is same calculation as in chapter 2.

From Figure 5.1, the result for total average of maximum bending moment around 30mm is same as the average of five prepared specimens, and then decreases with increase of the distance from mold surface to center of each coupon on X-direction. The decreasing rate for coupons between 30mm and 345mm from the mold surface of total average is 40%. The decreasing rate for upper section is 55% and for lower section is 35%. In addition, the maximum moment at lower section is higher than those at upper section. At result of coupon on Y-direction from Table 5.1, the maximum moment increases with increases the number of cast and mold surface.

In these result, it is considered that the influence of mold surface affects larger than the influence of cutout and mold surface to the flexural performance in HPFRCC directly. It is recognized that the reason why the difference of increasing rate at upper section is lower than those at lower section is that the influence of polishing and cutout affects the decrease of the flexural performance since the influence of polishing and cutout to flexural performance is recognized in chapter 3.

For the result of the number of PVA fiber and the distance from mold surface to center of each coupon relationships, the fiber is distributed and orientated at lower section more than at upper section. Moreover, the PVA fiber is more concentrated around 100 mm from the mold surface than around the center line of specimens.

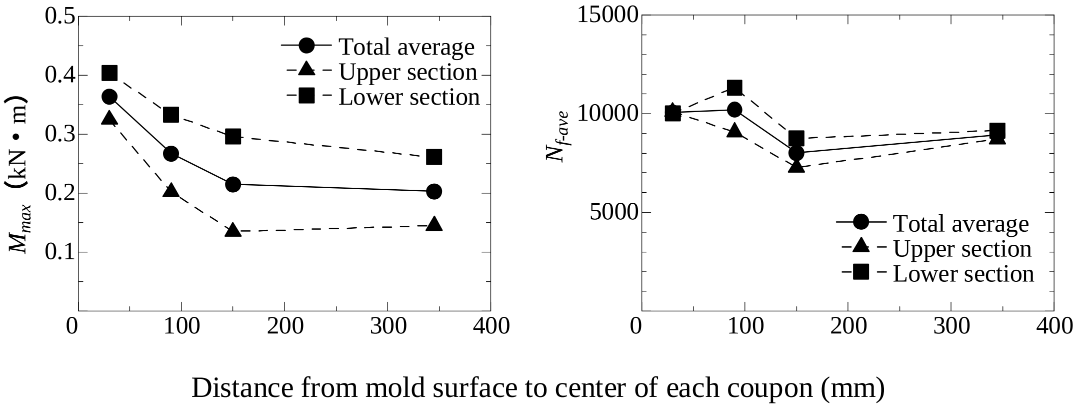

Figure 5.1 The maximum moment or number of PVA fibers and distance relationships

5.1.2. HPFRCC with 2.0% volume fraction of fibers

The relationship between the averaged maximum bending moment and distance from mold surface to center of each coupon is shown at left side of Figure 5.2 and the relationships between the averaged number of PVA fibers and the distance from mold surface to center of each coupon is shown at right side of Figure 5.2. The distance from mold surface to center is same calculation as in chapter 2.

From Figure 5.2, the result for total average of maximum bending moment decreases with increase of the distance from mold surface to center of each coupon on X-direction. The decreasing rate for coupons between 30mm and 345mm from the mold surface of total average is 40%. The decreasing rate for upper section is 50% and for lower section is 30%. In addition, the maximum moment at lower section is higher than those at upper section. In the result of coupon on Y-direction from Table 5.1, the maximum moment increases with increase of the number of cast and mold surface. This tendency is same as in the result of 1.5% volume fraction of fibers. However, the difference of the decreasing rate between upper section and lower section is smaller than those in the result of 1.5% volume fraction of fibers.

From the relationships between the number of fiber and distance from mold surface to center of each coupon, the number of fiber is almost same at any distance from mold surface. In addition, the influence of polishing and cutout does not affect the flexural performance of HPFRCC as described in chapter 3.

In these results, the difference of the decreasing rate between upper and lower section is not related to the influence of polishing and cutout in chapter 3, therefore, it is said that the fiber orientation angle of PVA is related to the influence of flexural performance at specimens with 2.0% volume fraction of fibers.

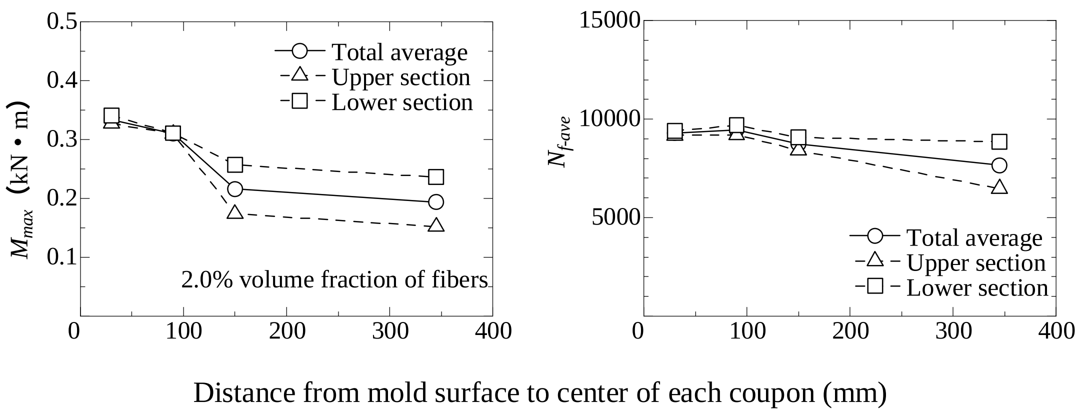

Figure 5.2 The maximum moment or number of PVA fibers and distance relationships

CHAPTER 6 CONCLUSION

In this research, the influence of fiber orientation to flexural performance of HPFRCC has been examined by bending test and cross section observation, and then achieved the results as following below.

6.1. HPFRCC with 1.5% volume fractions of fibers

- The flexural performance of HPFRCC increases with decrease of the distance from mold surface to center of each coupon.
- The flexural performance of HPFRCC at lower section is higher than at upper section at same position number.
- PVA fibers is more distributed and concentrated at lower section than at upper section and more distributed and concentrated at around 100mm from the mold surface than the center of specimens.
- The influence of polishing and cutout on surface to the flexural performance of HPFRCC has been recognized.

6.2. HPFRCC with 2.0% volume fractions of fibers

- The flexural performance of HPFRCC increases with decrease of the distance from mold surface to center of each coupon.
- The flexural performance of HPFRCC at lower section is higher than at upper section at same position number.
- PVA fibers are distributed to equally at any distance from the mold surface.
- The influence of polishing and cutout on surface to the flexural performance of HPFRCC has not been recognized.

6.3. Recommendation

To clarify the result of this research, fiber orientation angle of PVA and the relationships between fiber orientation angle of PVA and the flexural performance has to be cleared.

REFERENCES

[1.1] Inaguma, H., Seki, M., Inaguma, T., and Rokugo, K., “Application of the HPFRCC for the railway RC structure”, Proceedings of the Japan Concrete Institute, Vol. 29, No.1, pp.441-446, 2007. (in Japanese)

[1.2] Li, V. C., “From Micromechanics to Structural Engineering – The Design of Cementitious Composites for Civil Engineering Applications”, Journal of Structural Mechanics and Earthquake Engineering, JSCE, Vol.10, No.2, pp.37-48, 1993.

[1.3] “Recommendations for Design and Construction of High Performance Fiber Reinforced Cement Composite with Multiple Fine Cracks (HPFRCC)”, Japan Society of Civil Engineers, Concrete Library 127, Mar. 2007. (in Japanese)

[1.4] Shimizu, K., “Study on Evaluation of Tensile Properties and Structural Performance of Ductile Fiber Reinforced Cementitious Composites”, Doctor’s Thesis, Doctoral Program in Engineering, University of Tsukuba, Japan, Mar. 2007. (in Japanese)

[1.5] Iiduka, T., Kato, H., Asano, Y., and Rokugo, K., “Influence of mold surface and casting direction on tensile performance of HPFRCC”, Proceedings of the Japan Concrete Institute, Vol.29, No.1, pp.357-362, 2007. (in Japanese)

[2.1] Japan Concrete Institute Standard, “Appendix (Nonmandatory Information): Evaluation method for tensile strength and ultimate tensile strain of Fiber-reinforced cementitious composite”, JCI-S-003-2007, 2007.

[3.1] Torigoe, S., Saito, T., Horikoshi, T., Hamada, T., and Ogawa, A., “Study on Evaluation Method for PVA fiber Distribution in Engineered Cementitious Composite”, JCI International Workshop on Ductile Fiber Reinforced Cementitious Composite, 2002.

APPENDIX

A: Information of Manufacturer and Brand Name of Materials

Material	Manufacturer	Brand Name
Cement	None	Ordinary Portland Cement
Fly ash	Joban Joint Power Co., Ltd.	Type II
Shrinkage-reducing admixture	Taiheiyo Materials Corporation	Tetraguard AS20
High performance AE water reducing agent	BASF Pozzolith Ltd.	SP-8N
Fine aggregate	Toyo Seikan Kaisha, Ltd.	Quartz sand No.7
Expansion agent	Denka Corporation	Denka CSA
Thickening agent	Shin-Etsu Chemical Co., Ltd.	hi Metolose 90SH-4000

B: The test result of compressive test

For Chapter 2:

ID	Secant elastic modulus (GPa)	Compressive strength (MPa)	Strain at compressive strength (%)	Material age (Days)
PVA 1.5% - 1	15.66	39.94	0.44	119
PVA 1.5% - 2	18.49	44.36	0.40	119
ECC - 1	14.89	44.67	0.49	101
ECC - 2	15.49	43.69	0.60	101
ECC - 3	15.63	49.23	0.57	101

For Chapter 4:

Specimens with 1.5% volume fractions of fibers

ID	Secant elastic modulus (GPa)	Compressive strength (MPa)	Strain at compressive strength (%)	Material age (Days)
PVA 1.5% - 1	10.66	21.75	0.46	32
PVA 1.5% - 2	11.34	22.12	0.40	32
PVA 1.5% - 3	10.94	21.34	0.49	32
PVA 1.5% - 4	11.87	23.15	0.44	34
PVA 1.5% - 5	10.92	22.94	0.57	34
PVA 1.5% - 6	11.15	22.74	0.44	34

Specimens with 2.0% volume fractions of fibers

ID	Secant elastic modulus (GPa)	Compressive strength (MPa)	Strain at compressive strength (%)	Material age (Days)
PVA 2.0% - 1	10.37	23.96	0.67	32
PVA 2.0% - 2	10.31	22.88	0.54	32
PVA 2.0% - 3	11.14	23.07	0.49	32
PVA 2.0% - 4	11.09	22.97	0.66	34
PVA 2.0% - 5	10.72	22.84	0.56	34
PVA 2.0% - 6	8.80	24.05	0.62	34

C: The detailed data of specimens

Chapter 2 1.5% volume fraction of fibers

ID	Age	Width	Depth	Fracture	P_{max}
	(Days)	(mm)	(mm)	Position	(kN)
1-1	118	60.8	60.0		7.790
1-2	118	60.2	60.3		8.987
1-3	118	60.8	61.0		8.245
1-4	118	60.2	60.5		8.802
1-5	118	60.2	60.1	×	7.920
A1-U-X0	120	59.5	59.2		2.520
A1-U-X1	120	60.0	59.4		3.175
A1-U-X2	120	60.8	60.1		4.361
A2-U-X3	119	60.0	60.1		7.815
A1-U-Y1	121	56.3	59.2		4.941
A1-U-Y2	120	59.9	59.1		5.520
A2-U-Y3	120	59.2	61.0		3.881
A1-L-X0	118	59.9	60.0		4.991
A1-L-X1	118	59.1	60.0	×	5.974
A1-L-X2	118	60.9	59.1		6.934
A2-L-X3	118	60.1	60.1		7.613
A1-L-Y1	121	56.2	59.1		2.243
A1-L-Y2	119	59.5	61.1		2.847
A2-L-Y3	119	59.1	59.0		4.889
B0-M-X1	120	59.5	59.6		3.229
B0-M-X2	120	60.2	60.0		4.411
B0-M-X3	120	60.2	59.2		6.352
B0-M-X4	120	59.1	60.0		7.562
B1-M-X5	120	59.5	60.0		7.105
B0-M-Y1	120	59.5	60.2		1.460
B0-M-Y2	120	59.9	60.5	×	1.663
B0-M-Y3	120	59.7	59.9		1.436
B0-M-Y4	120	59.5	59.2		1.235
C1-U-X0	121	59.1	59.1		3.278
C1-U-X1	121	59.1	59.1		2.193
C1-U-X2	121	59.8	59.9		3.704
C2-U-X3	121	59.1	59.1		5.168
C1-U-Y1	121	58.2	60.9		4.310
C1-U-Y2	121	59.2	58.1		1.687
C2-U-Y3	121	58.9	59.0		5.396
C1-L-X0	119	59.2	60.0		5.444
C1-L-X1	119	59.0	59.6		5.847
C1-L-X2	119	58.0	59.2		6.377
C2-L-X3	119	60.6	60.0		8.548
C1-L-Y1	119	59.1	60.1		5.976
C1-L-Y2	119	59.2	59.2		7.211
C2-L-Y3	119	60.0	60.0	×	5.672

Chapter 2 2.0% volume fraction of fibers

ID	Age	Width	Depth	Fracture	Crack	P_{max}
	(Days)	(mm)	(mm)	Position	numbers	(kN)
2.0-1	99	60.8	57.0		2	8.918
2.0-2	99	62.1	60.0	×	4	8.135
2.0-3	99	60.8	62.1		5	9.451
2.0-4	99	61.2	60.7		3	7.603
2.0-5	96	62.1	60.2		4	8.133
2.0A1-U-X0	100	59.3	59.9	×	2	3.105
2.0A1-U-X1	100	59.1	58.2		1	3.076
2.0A1-U-X2	100	59.2	60.0	×	4	5.882
2.0A2-U-X3	100	59.1	58.7		6	6.844
2.0A1-U-Y1	100	59.8	60.0		4	5.506
2.0A1-U-Y2	100	59.8	59.5	×	6	7.097
2.0A2-U-Y3	100	59.4	59.5		4	6.315
2.0A1-L-X0	100	58.4	58.8	×	4	4.899
2.0A1-L-X1	100	59.1	58.6		5	5.303
2.0A1-L-X2	100	60.8	59.8		6	6.466
2.0A2-L-X3	100	59.9	59.1		4	6.642
2.0A1-L-Y1	100	59.3	59.8		4	2.802
2.0A1-L-Y2	100	59.2	60.0		6	7.294
2.0A2-L-Y3	100	60.0	60.1		5	8.413
2.0B0-M-X1	99	58.9	59.0		6	5.558
2.0B0-M-X2	99	59.0	58.7		5	5.354
2.0B0-M-X3	99	60.1	59.5		8	7.476
2.0B0-M-X4	99	59.9	59.5		3	7.199
2.0B1-M-X5	99	59.3	59.5		5	7.503
2.0B0-M-Y1	99	55.6	59.5	×	2	1.742
2.0B0-M-Y2	99	60.0	60.0	×	3	2.727
2.0B0-M-Y3	99	59.0	59.3	×	1	1.792
2.0B0-M-Y4	99	58.9	59.1		1	1.591
2.0C1-U-X0	101	59.4	59.8		1	2.955
2.0C1-U-X1	101	58.2	59.9		2	3.888
2.0C1-U-X2	101	60.1	59.1		3	6.516
2.0C2-U-X3	101	60.0	59.4		5	6.215
2.0C1-U-Y1	100	61.5	60.9	×	5	5.684
2.0C1-U-Y2	100	59.9	59.9		6	6.771
2.0C2-U-Y3	100	60.0	59.2		5	6.792
2.0C1-L-X0	101	59.7	58.1		2	4.521
2.0C1-L-X1	101	57.3	57.3		3	4.975
2.0C1-L-X2	101	59.2	59.8		4	5.960
2.0C2-L-X3	101	59.9	59.5	×	4	6.997
2.0C1-L-Y1	100	59.1	59.2		4	5.354
2.0C1-L-Y2	100	58.2	57.2		4	4.976
2.0C2-L-Y3	100	59.5	60.0		3	7.325

		Before Polishing		After Polishing		The thickness of Polishing			
ID	Span	Width	Depth	Width	Depth	Width	Depth	Age	P_{max}
	(mm)	(mm)	(mm)	(mm)	(mm)	(mm)	(mm)	(Days)	(kN)
PVA1.5-60-1	352.1	60.5	60.9	60.5	60.9	0.0	0.0	33	6.561
PVA1.5-60-2	352.0	60.8	60.9	60.8	60.9	0.0	0.0	33	6.259
PVA1.5-60-3	352.0	60.1	60.1	60.1	60.1	0.0	0.0	33	6.764
PVA1.5-62-1	351.9	62.0	62.1	58.9	59.2	1.6	1.5	33	7.017
PVA1.5-62-2	351.8	62.2	62.4	58.0	58.7	2.1	1.9	33	4.207
PVA1.5-62-3	351.2	62.5	62.4	58.8	58.2	1.9	2.1	33	3.735
PVA1.5-74-1	350.5	76.2	75.2	59.4	60.9	8.4	7.2	33	4.821
PVA1.5-74-2	350.5	76.2	75.1	61.0	58.2	7.6	8.5	33	5.273
PVA1.5-74-3	351.0	75.6	75.5	60.5	60.1	7.6	7.7	33	5.838
PVA1.5-86-1	351.0	87.9	88.0	60.1	60.1	13.9	14.0	33	4.138
PVA1.5-86-2	350.8	87.2	87.6	58.8	58.1	14.2	14.8	33	3.633
PVA1.5-86-3	351.1	88.0	86.5	59.1	58.5	14.5	14.0	33	3.683
PVA1.5-110-1	350.0	111.8	110.5	59.7	58.7	26.1	25.9	34	5.676
PVA1.5-110-2	351.5	112.9	111.1	60.1	58.9	26.4	26.1	34	5.601
PVA1.5-110-3	350.1	114.1	111.0	60.0	59.2	27.1	25.9	34	5.402
PVA2.0-60-1	351.9	61.1	60.8	61.1	60.8	0.0	0.0	32	6.990
PVA2.0-60-2	352.0	61.9	60.6	61.9	60.6	0.0	0.0	32	6.484
PVA2.0-60-3	351.5	61.2	60.0	61.2	60.0	0.0	0.0	32	6.488
PVA2.0-62-1	350.0	63.0	62.4	58.5	59.9	2.3	1.3	32	5.424
PVA2.0-62-2	350.1	64.1	62.8	59.5	60.0	2.3	1.4	32	6.082
PVA2.0-62-3	351.5	62.9	62.8	59.4	58.8	1.8	2.0	32	6.007
PVA2.0-74-1	350.0	75.2	76.0	58.3	59.0	8.5	8.5	32	6.411
PVA2.0-74-2	351.0	74.9	75.2	60.0	59.4	7.5	7.9	32	5.705
PVA2.0-74-3	351.0	75.0	75.9	59.6	58.1	7.7	8.9	32	6.105
PVA2.0-86-1	350.8	86.2	87.5	59.1	58.6	13.6	14.5	33	7.216
PVA2.0-86-2	351.1	85.7	85.9	60.1	57.9	12.8	14.0	33	6.209
PVA2.0-86-3	351.0	87.1	86.1	59.0	59.0	14.1	13.6	33	7.165
PVA2.0-110-1	351.0	110.9	111.3	61.0	58.5	25.0	26.4	33	7.360
PVA2.0-110-2	351.1	112.8	111.9	59.2	59.6	26.8	26.2	33	5.047
PVA2.0-110-3	350.8	112.9	110.9	58.9	58.5	27.0	26.2	33	5.827

D: The detailed data of the bending moment and curvature curve relationships

Chapter 2 1.5% volume fraction of fibers

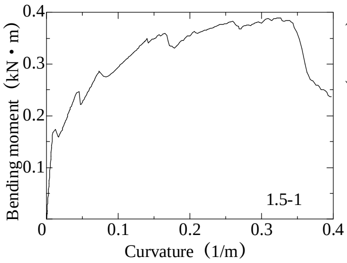

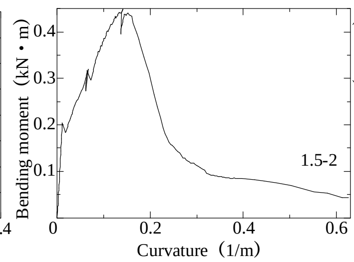

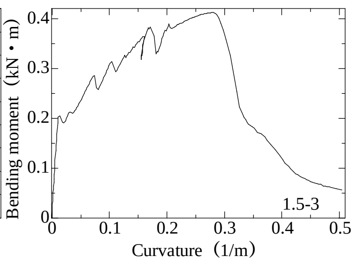

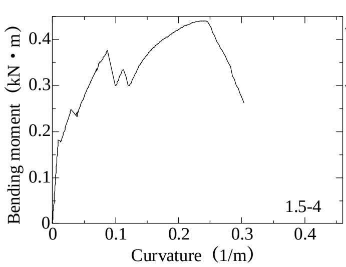

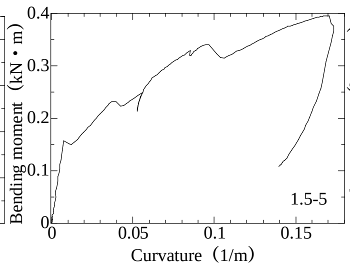

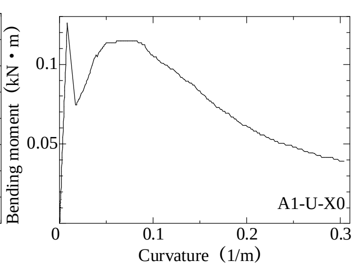

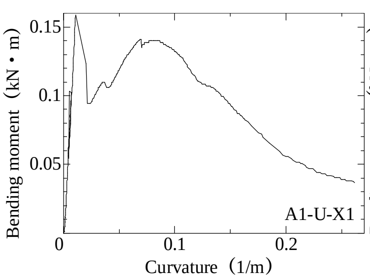

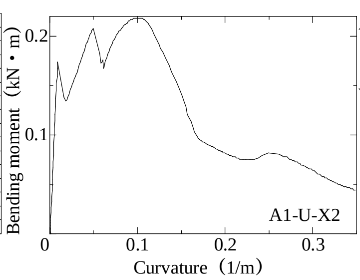

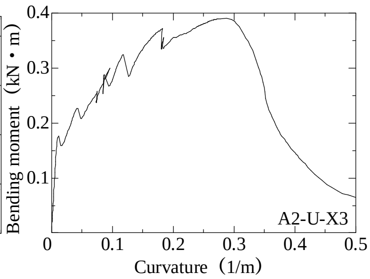

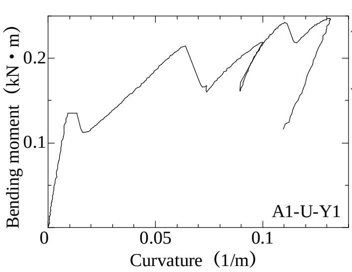

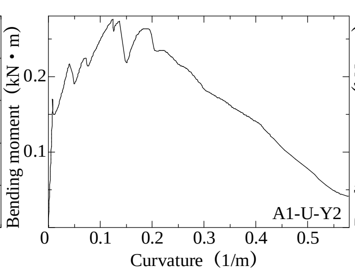

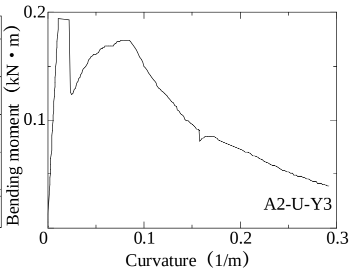

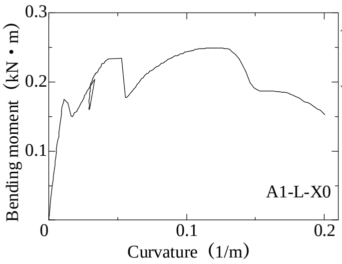
Bending moment（kN・m）
Curvature（1/m）
A1-L-X0

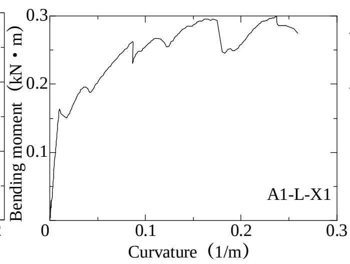
Bending moment（kN・m）
Curvature（1/m）
A1-L-X1

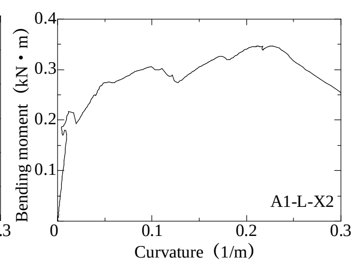
Bending moment（kN・m）
Curvature（1/m）
A1-L-X2

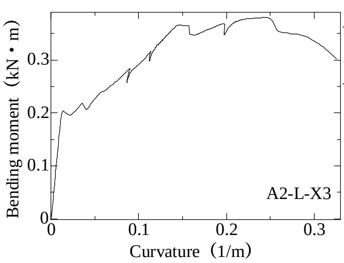
Bending moment（kN・m）
Curvature（1/m）
A2-L-X3

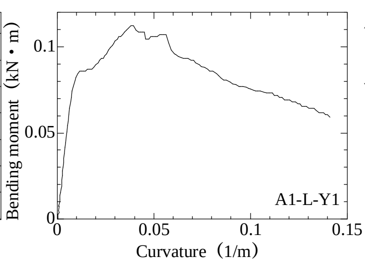
Bending moment（kN・m）
Curvature（1/m）
A1-L-Y1

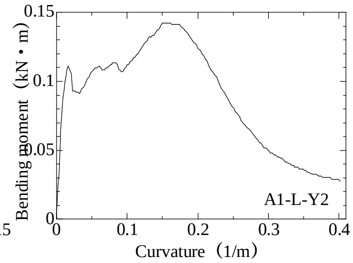
Bending moment（kN・m）
Curvature（1/m）
A1-L-Y2

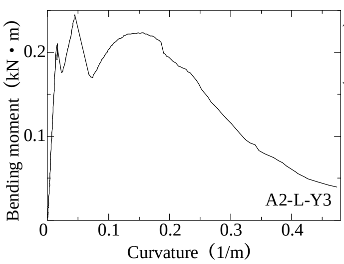
Bending moment（kN・m）
Curvature（1/m）
A2-L-Y3

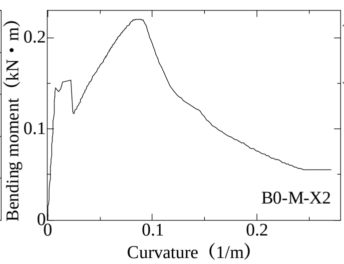
Bending moment（kN・m）
Curvature（1/m）
B0-M-X2

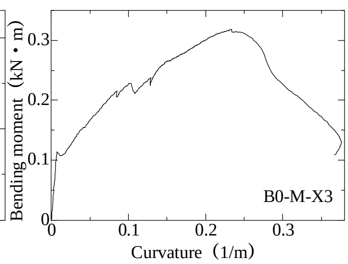
Bending moment（kN・m）
Curvature（1/m）
B0-M-X3

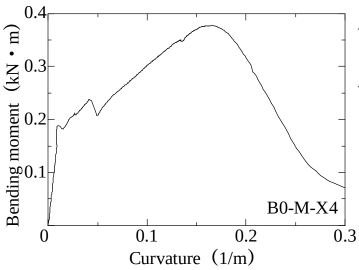
Bending moment（kN・m）
Curvature（1/m）
B0-M-X4

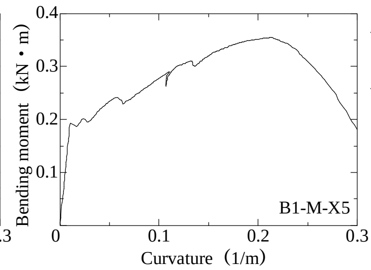
Bending moment（kN・m）
Curvature（1/m）
B1-M-X5

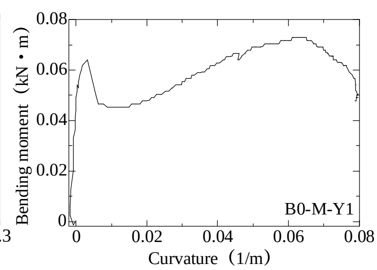
Bending moment（kN・m）
Curvature（1/m）
B0-M-Y1

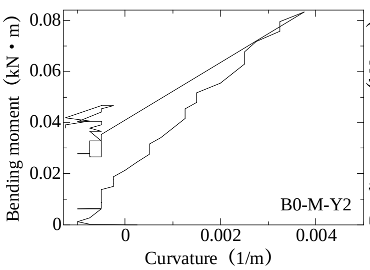
Bending moment（kN・m）
Curvature（1/m）
B0-M-Y2

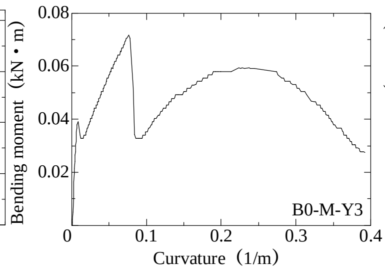
Bending moment（kN・m）
Curvature（1/m）
B0-M-Y3

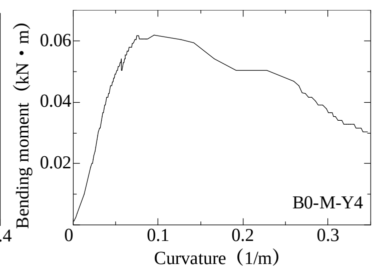
Bending moment（kN・m）
Curvature（1/m）
B0-M-Y4

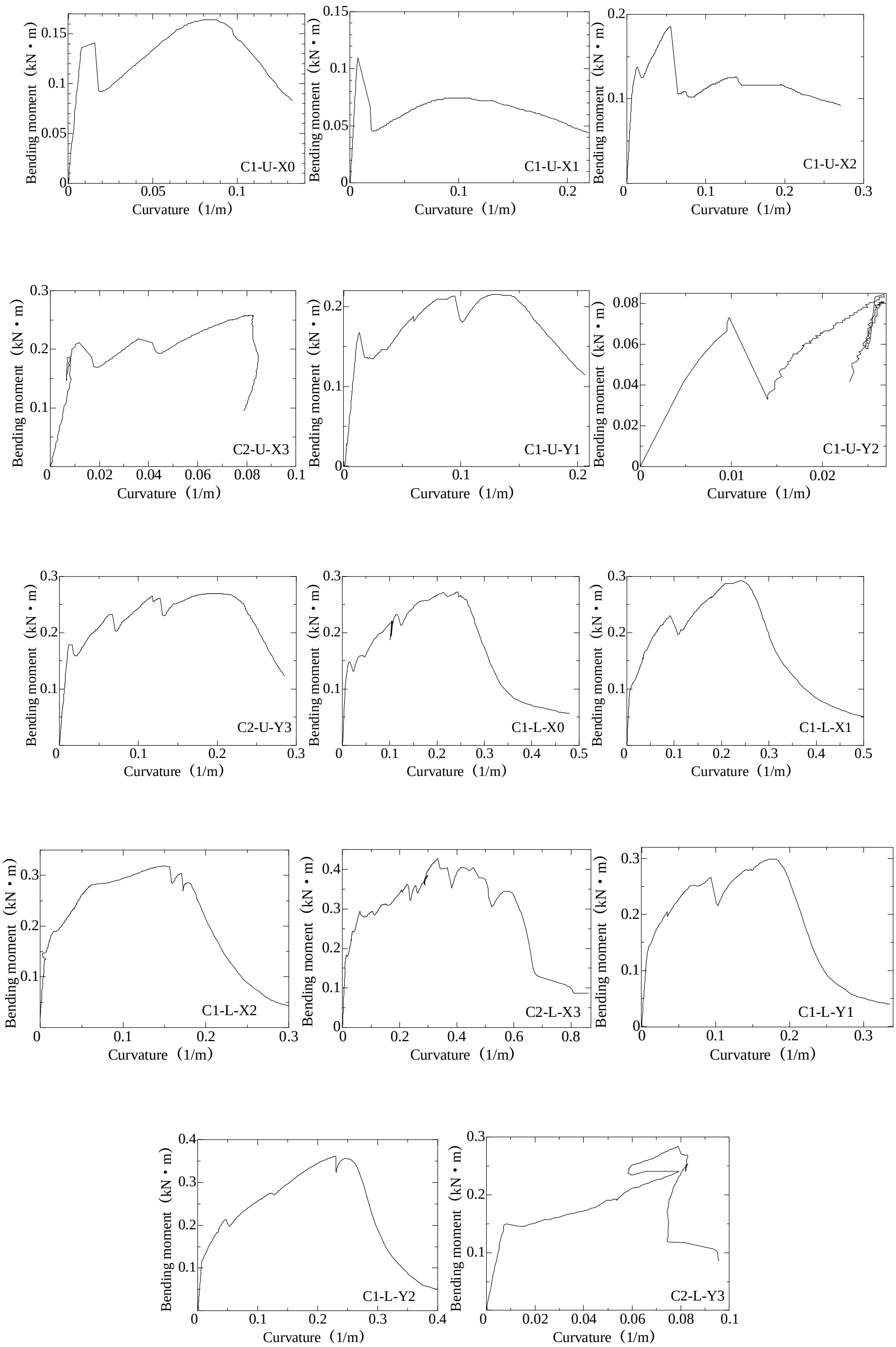
C1-U-X0
C1-U-X1
C1-U-X2
C2-U-X3
C1-U-Y1
C1-U-Y2
C2-U-Y3
C1-L-X0
C1-L-X1
C1-L-X2
C2-L-X3
C1-L-Y1
C1-L-Y2
C2-L-Y3
Bending moment（kN・m）
Curvature（1/m）

Chapter 2 2.0% volume fraction of fibers

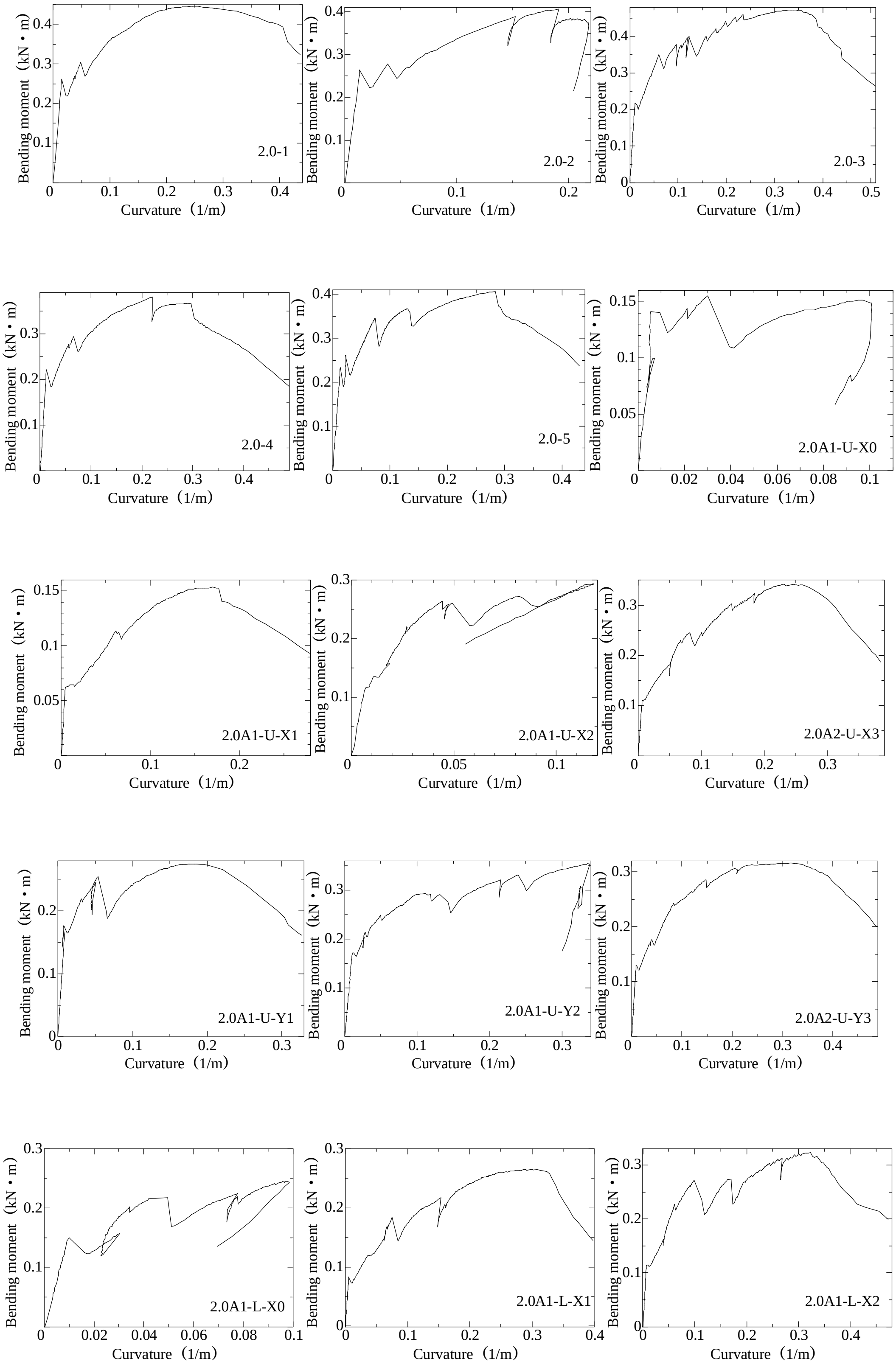

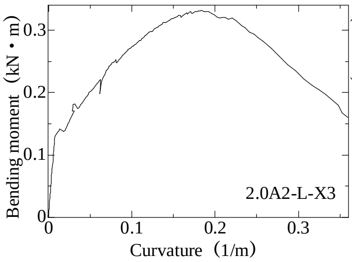
Bending moment (kN • m)
Curvature (1/m)
2.0A2-L-X3

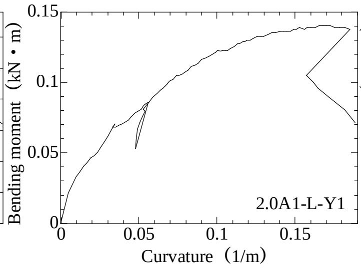
Bending moment (kN • m)
Curvature (1/m)
2.0A1-L-Y1

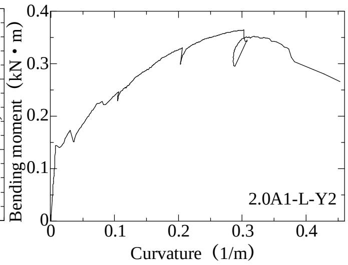
Bending moment (kN • m)
Curvature (1/m)
2.0A1-L-Y2

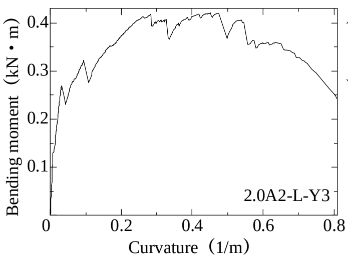
Bending moment (kN • m)
Curvature (1/m)
2.0A2-L-Y3

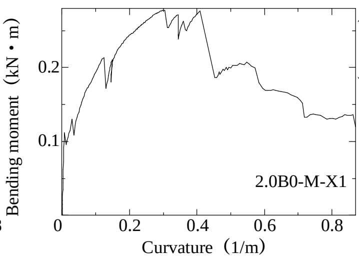
Bending moment (kN • m)
Curvature (1/m)
2.0B0-M-X1

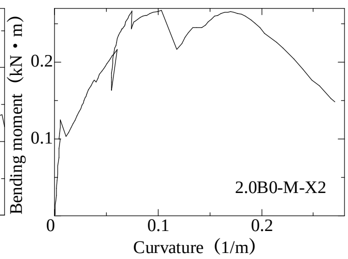
Bending moment (kN • m)
Curvature (1/m)
2.0B0-M-X2

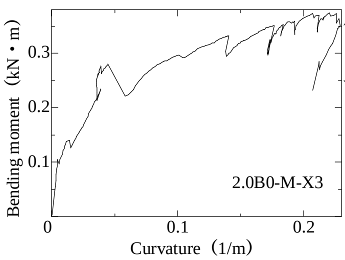
Bending moment (kN • m)
Curvature (1/m)
2.0B0-M-X3

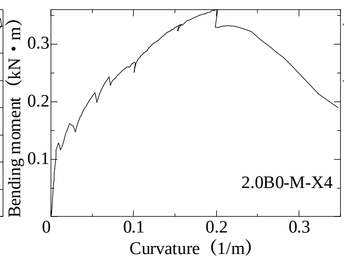
Bending moment (kN • m)
Curvature (1/m)
2.0B0-M-X4

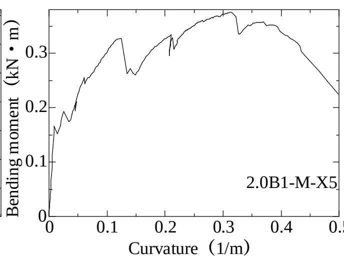
Bending moment (kN • m)
Curvature (1/m)
2.0B1-M-X5

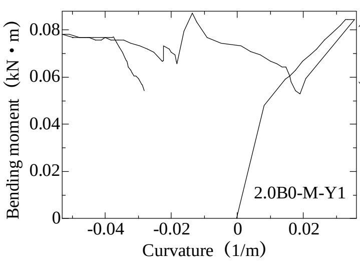
Bending moment (kN • m)
Curvature (1/m)
2.0B0-M-Y1

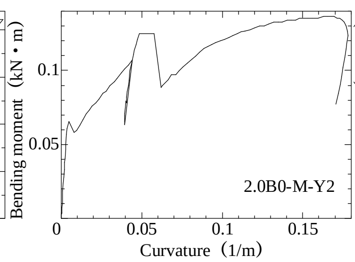
Bending moment (kN • m)
Curvature (1/m)
2.0B0-M-Y2

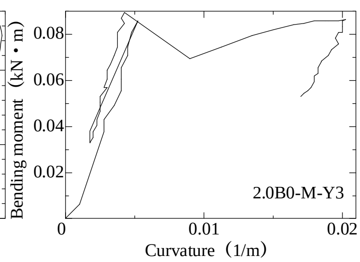
Bending moment (kN • m)
Curvature (1/m)
2.0B0-M-Y3

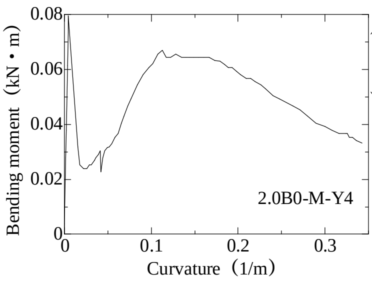
Bending moment (kN • m)
Curvature (1/m)
2.0B0-M-Y4

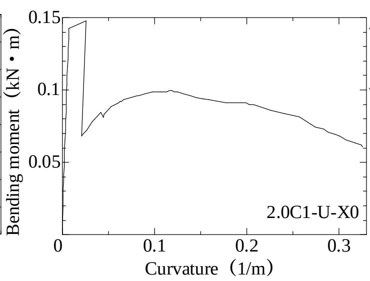
Bending moment (kN • m)
Curvature (1/m)
2.0C1-U-X0

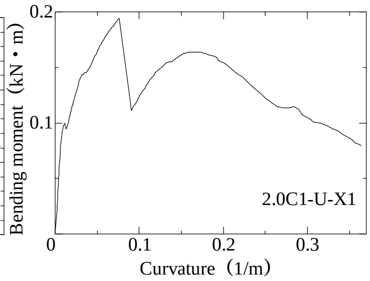
Bending moment (kN • m)
Curvature (1/m)
2.0C1-U-X1

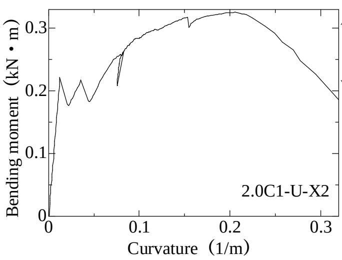
Bending moment（kN・m）
Curvature（1/m）
2.0C1-U-X2

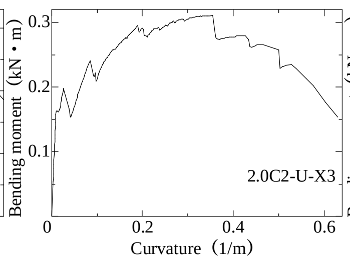
Bending moment（kN・m）
Curvature（1/m）
2.0C2-U-X3

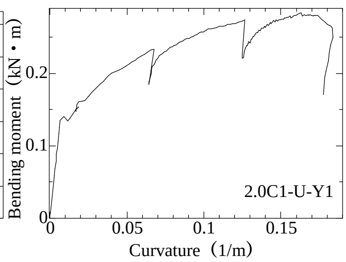
Bending moment（kN・m）
Curvature（1/m）
2.0C1-U-Y1

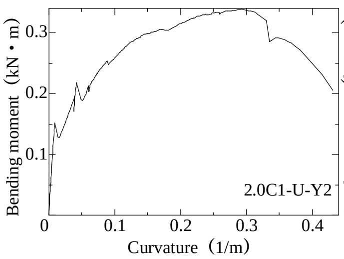
Bending moment（kN・m）
Curvature（1/m）
2.0C1-U-Y2

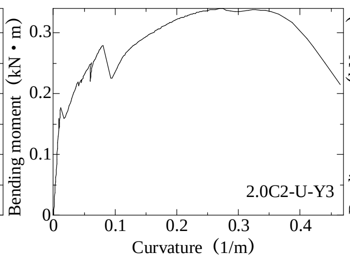
Bending moment（kN・m）
Curvature（1/m）
2.0C2-U-Y3

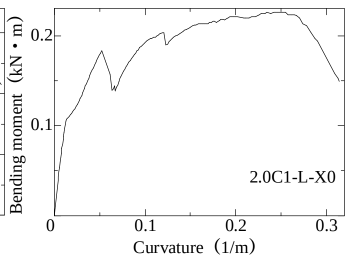
Bending moment（kN・m）
Curvature（1/m）
2.0C1-L-X0

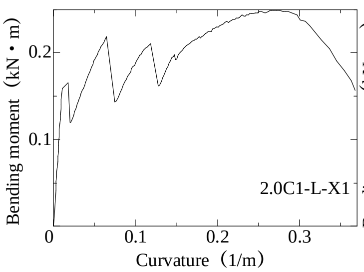
Bending moment（kN・m）
Curvature（1/m）
2.0C1-L-X1

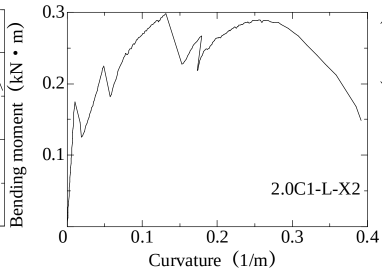
Bending moment（kN・m）
Curvature（1/m）
2.0C1-L-X2

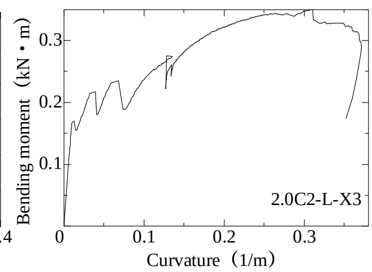
Bending moment（kN・m）
Curvature（1/m）
2.0C2-L-X3

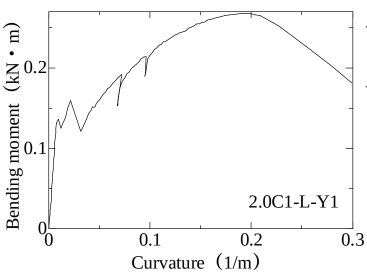
Bending moment（kN・m）
Curvature（1/m）
2.0C1-L-Y1

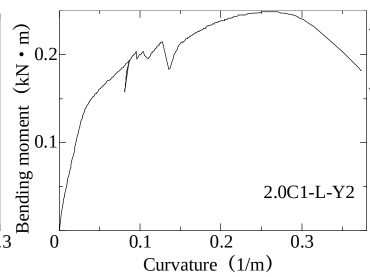
Bending moment（kN・m）
Curvature（1/m）
2.0C1-L-Y2

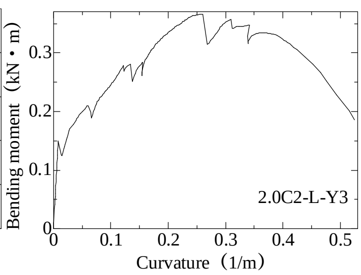
Bending moment（kN・m）
Curvature（1/m）
2.0C2-L-Y3

E: The picture of cross section A

Chapter 3 1.5% volume fraction of fibers

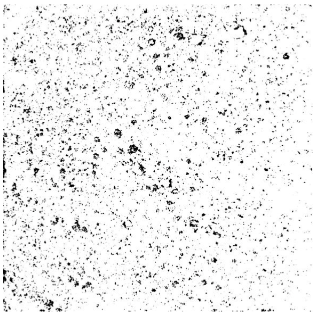
1.5-1

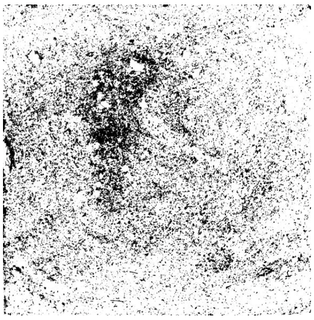
1.5-2

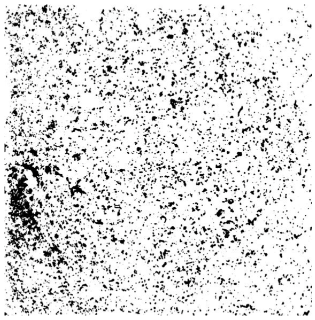
1.5-3

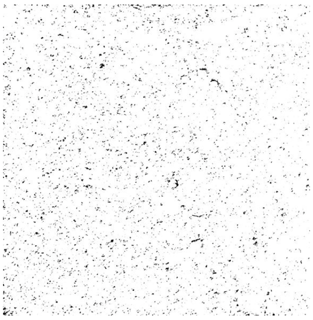
1.5-4

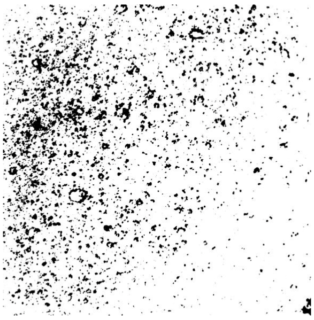
1.5-5

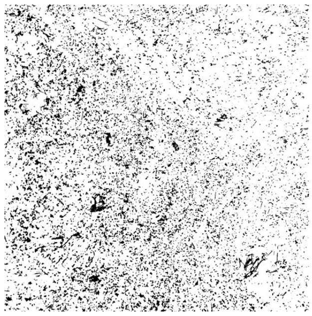
A1-U-X0

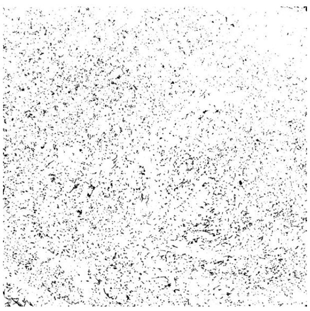
A1-U-X

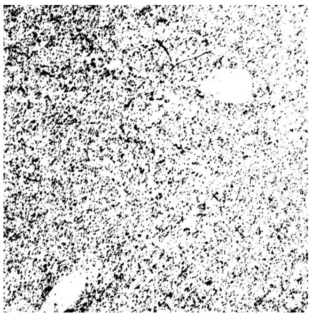
A1-U-X2

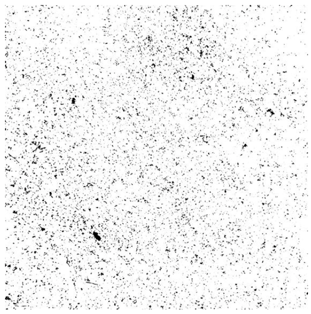
A2-U-X3


A1-U-Y1

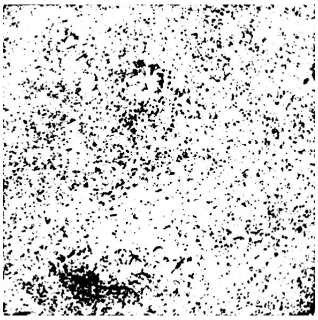
A1-U-Y2

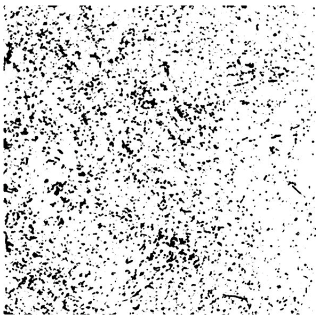
A2-U-Y3

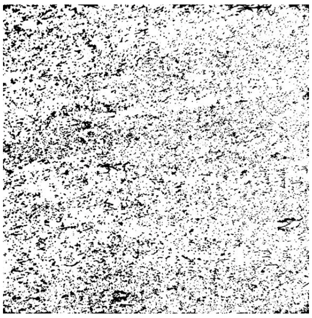

A1-L-X0

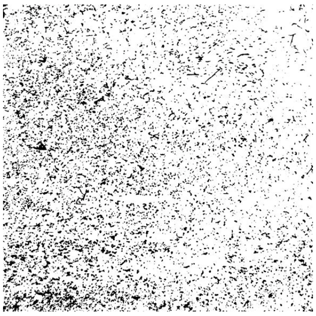

A1-L-X1

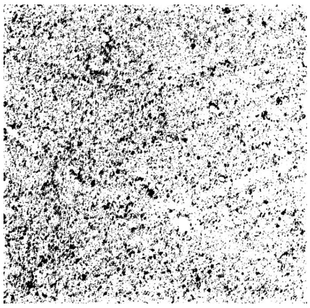

A1-L-X2

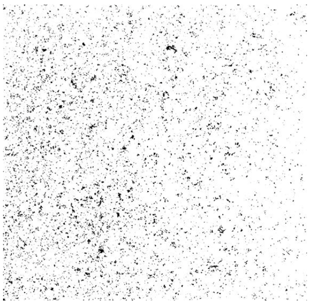

A2-L-X3

A1-L-Y1

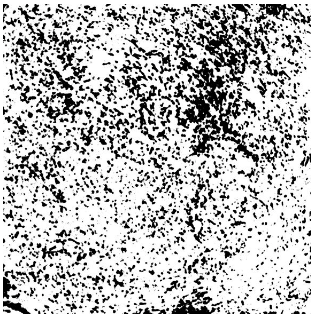

A1-L-Y2

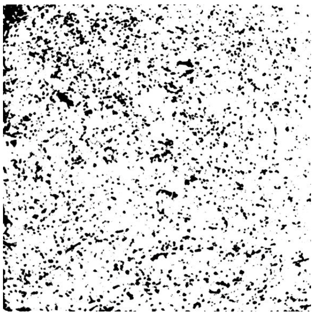

A2-L-Y3

B0-M-X1

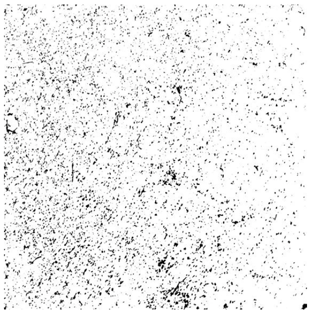

B0-M-X2

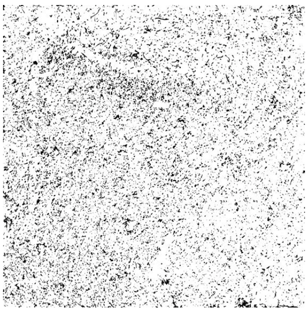

B0-M-X3

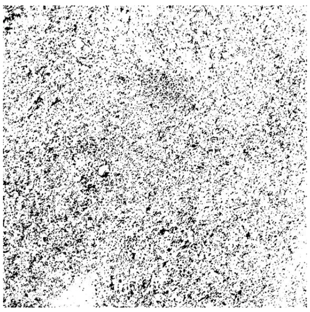

B0-M-X4

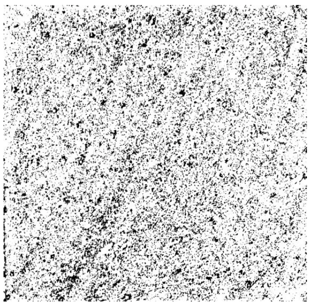

B1-M-X5

B0-M-Y1

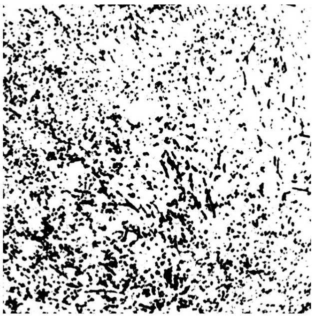

B0-M-Y2

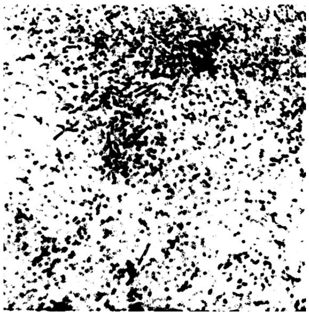

B0-M-Y3

B0-M-Y4

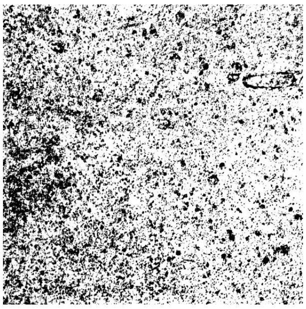

C1-U-X0

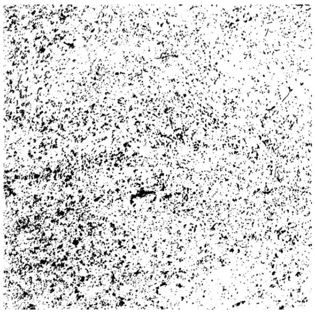

C1-U-X1

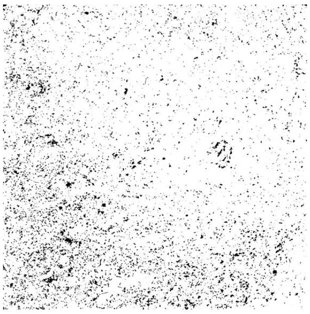

C1-U-X2

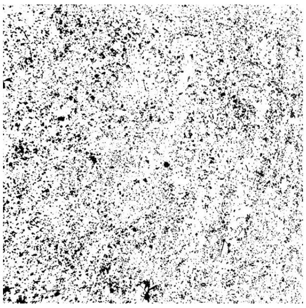

C2-U-X3

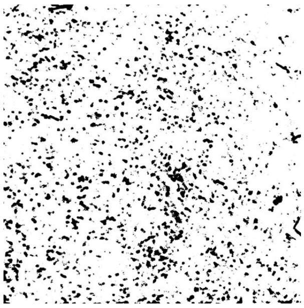

C1-U-Y1

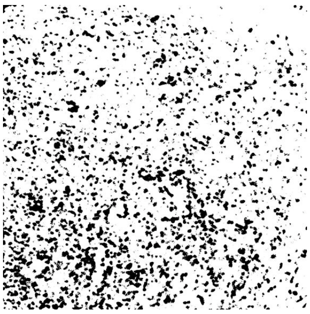

C1-U-Y2

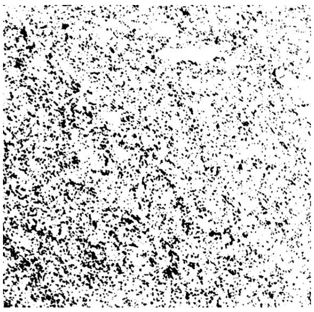

C2-U-Y3

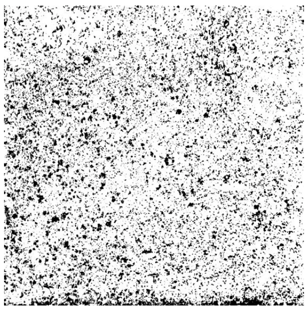

C1-L-X0

C1-L-X1

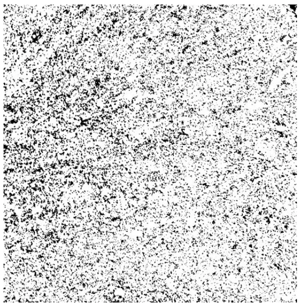

C1-L-X2

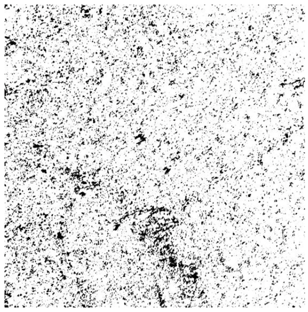

C2-L-X3

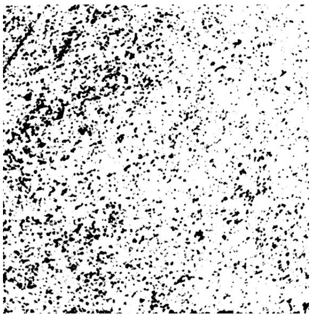

C1-L-Y1

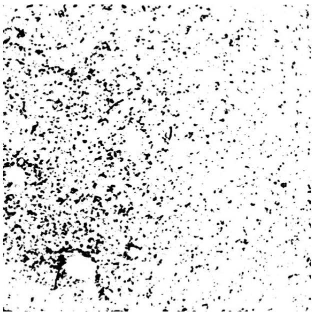

C1-L-Y2

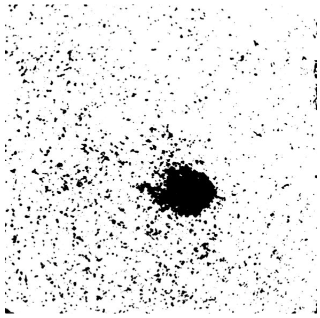

C2-L-Y3

Chapter 3 2.0% volume fraction of fibers

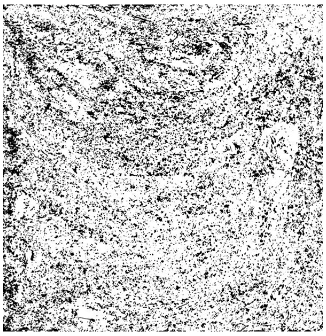
2.0-1

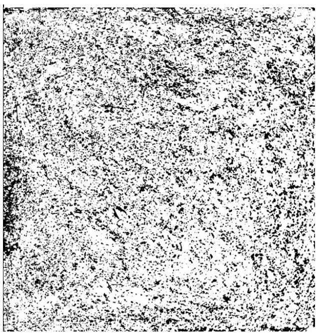
2.0-2

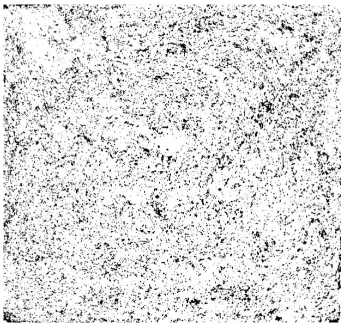
2.0-3

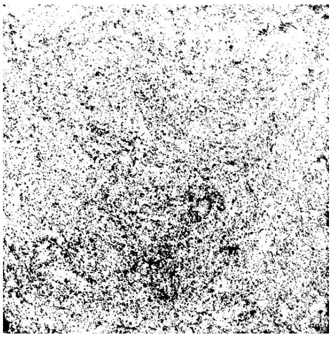
2.0-4

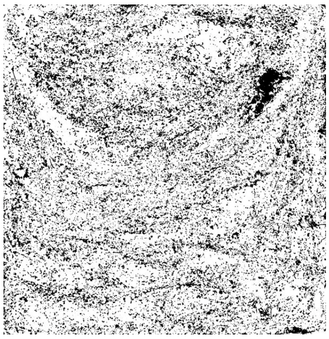
2.0-5

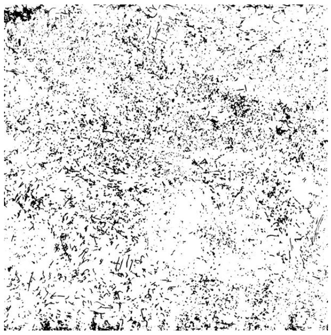
2.0A1-U-X0

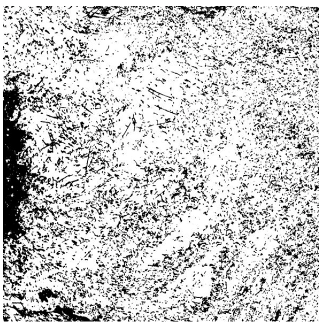
2.0A1-U-X1

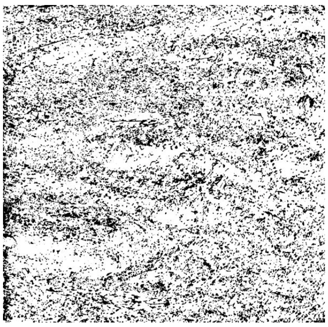
2.0A1-U-X2

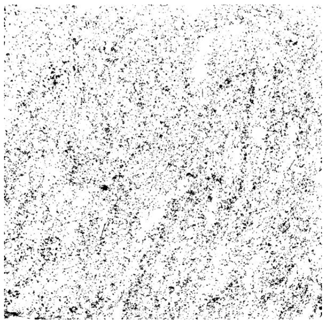
2.0A2-U-X3

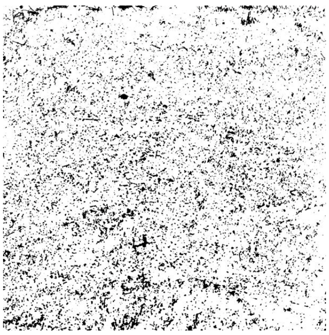
2.0A1-U-Y1


2.0A1-U-Y2

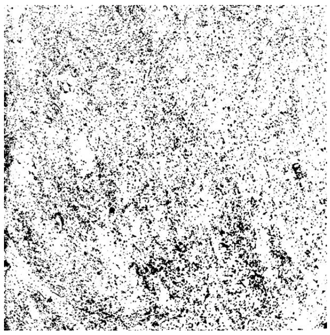
2.0A2-U-Y3

2.0A1-L-X0

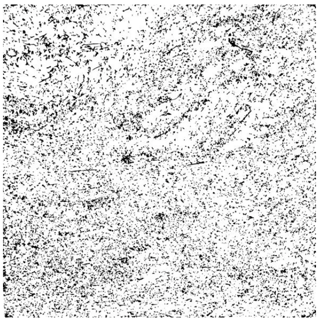

2.0A1-L-X1

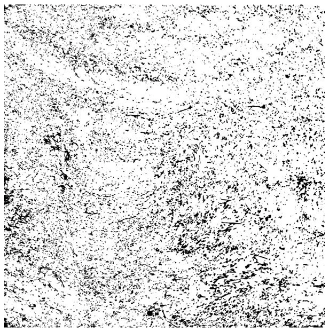

2.0A1-L-X2

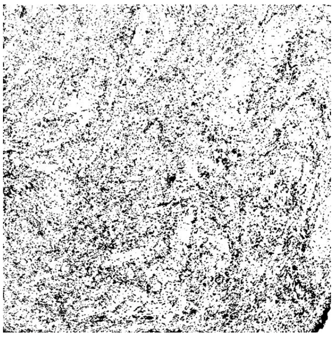

2.0A2-L-X3

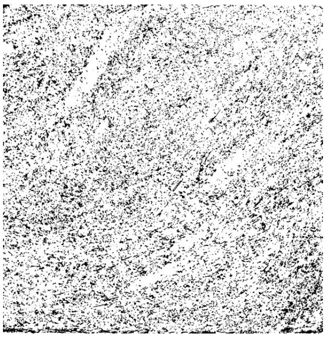

2.0A1-L-Y1

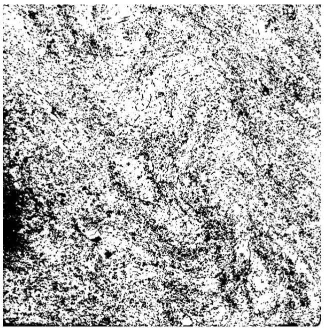

2.0A1-L-Y2

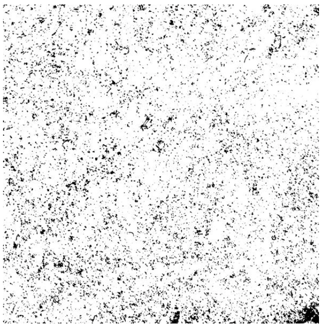

2.0A2-L-Y3

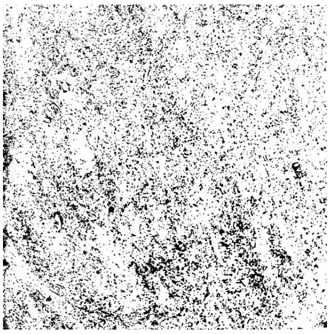

2.0B0-M-X1

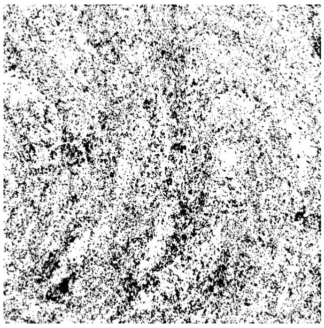

2.0B0-M-X2

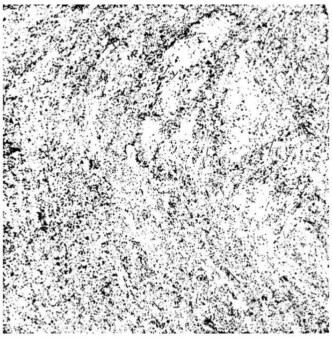

2.0B0-M-X3

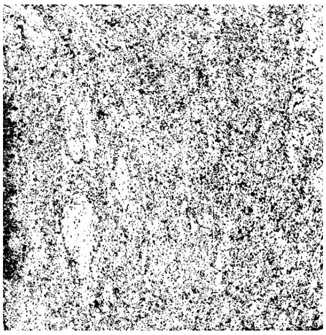

2.0B0-M-X4

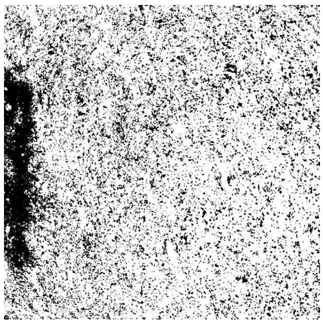

2.0B1-M-X5

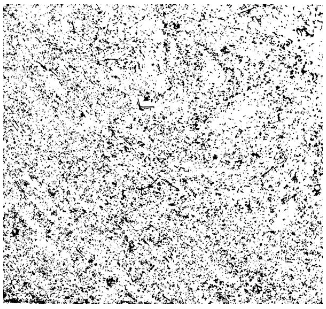

2.0B0-M-Y1

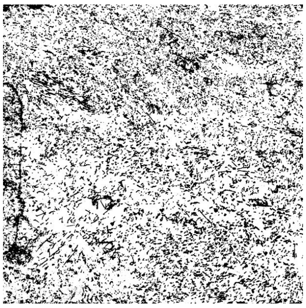

2.0B0-M-Y2

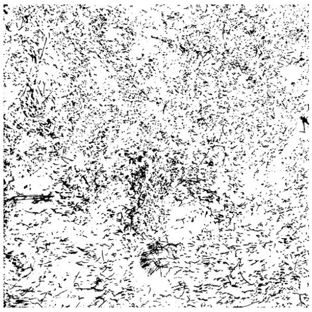

2.0B0-M-Y3

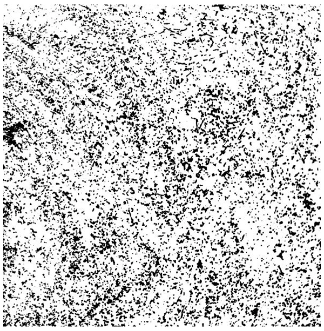

2.0B0-M-Y4

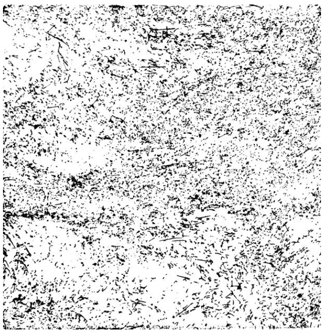

2.0C1-U-X0

2.0C1-U-X1

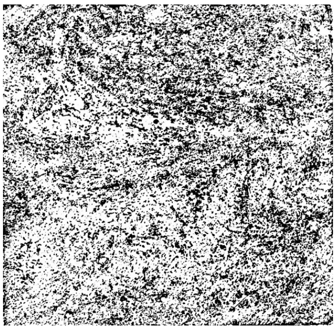

2.0C1-U-X2

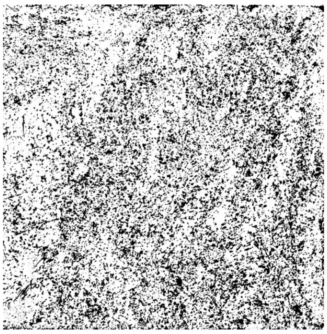

2.0C2-U-X3

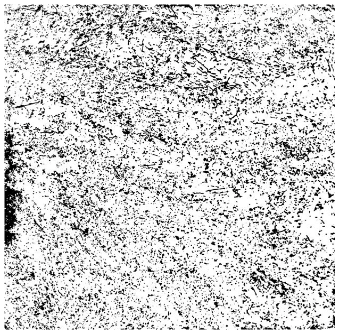

2.0C1-U-Y1

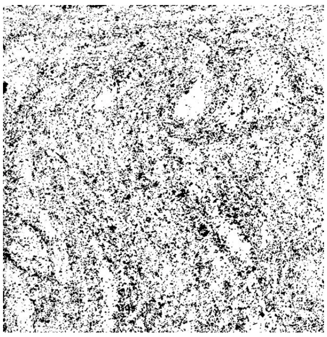

2.0C1-U-Y2

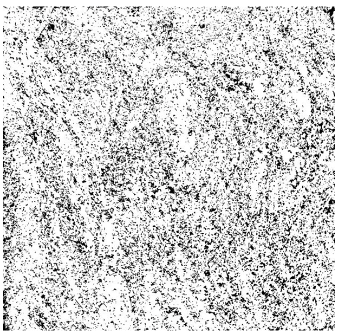

2.0C2-U-Y3

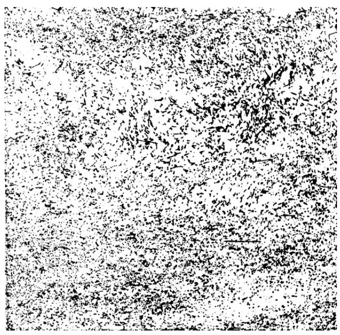

2.0C1-L-X0

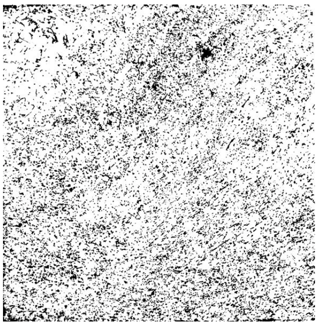

2.0C1-L-X1

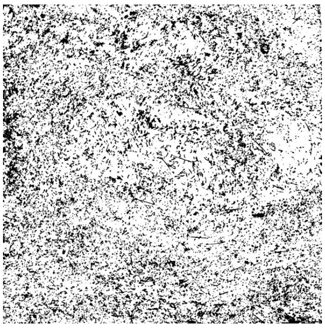

2.0C1-L-X2

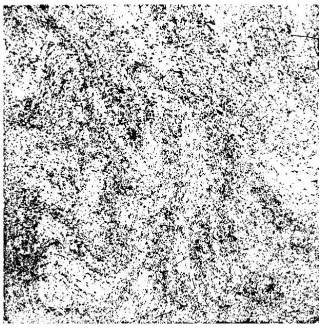

2.0C2-L-X3

2.0C1-L-Y1

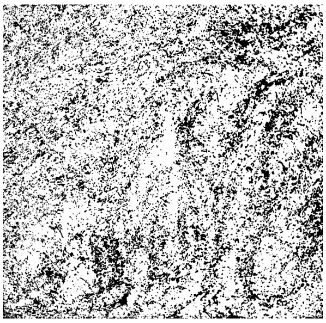

2.0C1-L-Y2

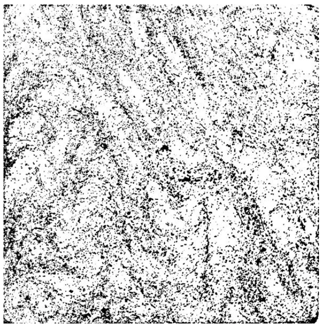

2.0C2-L-Y3

ACKNOWLEDGMENTS

I would like to extend my deepest gratitude to my academic adviser, Prof. Toshiyuki Kanakubo of the Institute of Engineering Mechanics and Systems, for his guidance and supervision during my stay in graduate school, and Mr. Atsuhisa Ogawa in Kuraray Co., LTD., Prof. Hiroshi Imai, Prof. Yuki Sakai and Prof. Gaku Syouzi for comments and suggestions given during the preparation of this dissertation. I would also like to greatly thank Mr. Atsushi Kojima in University of Tsukuba for his technical assistance in the machine shop and BASF Pozzolith Ltd., Denka Corporation, Joban Joint Power Co., Ltd., Koken Sangyo Co., Ltd., Shin-Etsu Chemical Corporation., Ltd., Taiheiyo Materials corporation, Toyo Seikan Kaisha, Ltd. for provide and cast materials.

In addition, I would which to give my sincere appreciation for assistance given by member of the Kanakubo Laboratory (Yuya Saito, Kentaro Matsunaga, Nobuyuki Yamato, Wakae Cho, Yoshiko Hasegawa, Yuka Onizuka, Yuji Nakayama, Takahiro Hirano, Go Hosaka, Kouhei Asano, Takayuki Aso, Norihiro Shigemizu, Wei Zhang, Junlei Zhang). Also, I would like to give my heartfelt acknowledgment to my fiancée, Ikuyo Maeda, and her parents.

Lastly, I want most of all to thank my parents and sister for their support, patience and understanding.

Tetsuo Fukuhara
January 21, 2009